JYU DISSERTATIONS 217

Amir Houshang Adibi Larijani

Oxidative Reactions of Cellulose under Alkaline Conditions

UNIVERSITY OF JYVÄSKYLÄ
FACULTY OF MATHEMATICS
AND SCIENCE

JYU DISSERTATIONS 217

Amir Houshang Adibi Larijani

Oxidative Reactions of Cellulose under Alkaline Conditions

Esitetään Jyväskylän yliopiston matemaattis-luonnontieteellisen tiedekunnan suostumuksella
julkisesti tarkastettavaksi toukokuun 19. päivänä 2020 kello 12.

Academic dissertation to be publicly discussed, by permission of
the Faculty of Mathematics and Science of the University of Jyväskylä,
on May 19, 2020 at 12 o'clock noon.

JYVÄSKYLÄN YLIOPISTO
UNIVERSITY OF JYVÄSKYLÄ

JYVÄSKYLÄ 2020

Editors
Raimo Alén
Department of Chemistry, University of Jyväskylä
Ville Korkiakangas
Open Science Centre, University of Jyväskylä

Permanent link to this publication: http://urn.fi/URN:ISBN:978-951-39-8157-0

ISBN 978-951-39-8157-0 (PDF)
URN:ISBN:978-951-39-8157-0
ISSN 2489-9003

ABSTRACT

Adibi Larijani, Amir Houshang
Oxidative reactions of cellulose under alkaline conditions
Jyväskylä: University of Jyväskylä, 2020, 102 p.
(JYU Dissertations,
ISSN 2489-9003; 217)
ISBN 978-951-39-8157-0 (PDF)

The purpose of this investigation was to elucidate the influence of oxygen, gas pressure, and temperature on the oxidative degradation of cellulose and the formation of degradation products under alkaline conditions. In order to simplify the reaction system the experiments were carried out with the cellulose model compound cellobiose. Reaction products were determined and identified by GC-FID and GC-MSD as their per(trimethylsilyl)ated derivatives.

About 37 degradation products were qualitatively identified of which 33 degradation products were quantitatively evaluated. The degradation products were divided into oxidative and non-oxidative degradation products. The main degradation products were glucose as well as glycolic, lactic, glyceric, 3,4-dihydroxybutanoic, 3-deoxypentonic, and glucoisosaccharinic acids.

An inhibiting character of oxygen upon cellobiose degradation was observed. At lower temperatures an increase in oxygen pressure caused the formation of non-oxidative degradation products in trace amounts. The formation of oxidative degradation products was kinetically and of non-oxidatives thermodynamically favored.

The kinetic calculations revealed that at room temperature the degradation of cellobiose proceeded four times slower in air than in 1 bar nitrogen. Furthermore, the activation energy for cellobiose degradation in 1 bar nitrogen was 79 kJ/mol and rose to 122 kJ/mol in air.

Based on the obtained results and made observations a new ionic reaction mechanism was postulated.

Keywords: cellulose, cellobiose, alkaline oxidative degradation, degradation products, gas chromatography, mass spectrometry, kinetics, activation energy, reaction mechanism

TIIVISTELMÄ

Adibi Larijani, Amir Houshang
Alkalisissa olosuhteissa tapahtuvat selluloosan hapetusreaktiot
Jyväskylä: University of Jyväskylä, 2020, 102 p.
(JYU Dissertations,
ISSN 2489-9003; 217)
ISBN 978-951-39-8157-0 (PDF)

Työn tarkoituksena oli selvittää hapen ja sen paineen sekä lämpötilan vaikutus selluloosan hajoamiseen ja pilkkoutumistuotteiden muodostumiseen alkalisissa olosuhteissa. Reaktiotapahtuman yksinkertaistamiseksi kokeissa käytettiin selluloosan malliaineena sellobioosia. Reaktiotuotteet määritettiin ja identifioitiin per(trimetyylisilyyli)johdannaisinaan käyttämällä menetelmiä GC-FID ja GC-MSD.

Koetyöskentelyssä identifioitiin kvalitatiivisesti noin 37 pilkkoutumistuotetta ja näistä 33 määritettiin kvantitatiivisesti. Pilkkoutumistuotteet ryhmiteltiin sekä hapettavissa että ei-hapettavissa olosuhteissa muodostuviin yhdisteisiin. Päähajoamistuotteet muodostuivat glukoosista sekä glykoli-, maito-, glyseriini-, 3,4-dihydroksibutaani-, 3-deoksi-pentoni- ja glukoisosakkariinihaposta.

Yleisesti havaittiin hapen sellobioosin hajoamista hidastava vaikutus. Erityisesti alemmissa lämpötiloissa hapen paineen kasvaessa muodostui vähäisessä määrin ei-hapettuneita tuotteita. Ei-hapettuneiden tuotteiden muodostuminen todettiin tapahtuvan ensisijaisesti kinetiikan ja hapettuneiden hajoamistuotteiden termodynamiikan mukaisesti.

Kineettiset tarkastelut osoittivat, että huoneen lämpötilassa sellobioosin hajoaminen tapahtui neljä kertaa hitaammin ilmassa kuin hapettomassa typpi-ilmakehässä aktivointienergioiden ollessa vastaavasti 122 kJ/mol ja 79 kJ/mol.

Saavutettujen tulosten perusteella kehitettiin kokonaisuudelle uusi, ionimekanismiin perustuva teoria.

Avainsanat: Aktivoitumisenergia, alkalinen hapettava hajotus, kaasukromatografia, kinetiikka, massaspektrometria, pilkkoutumistuotteet, reaktiomekanismi, sellobioosi, selluloosa

Author's address
Amir Houshang Adibi Larijani
Department of Chemistry
Applied Chemistry
P.O. Box 35
FI-40014 University of Jyväskylä
Amir.H.Adibi-Larijani@student.jyu.fi

Supervisor
Prof. Raimo Alén
Department of Chemistry
Applied Chemistry
P.O. Box 35
FI-40014 University of Jyväskylä
Raimo.J.Alen@jyu.fi

Reviewers
Prof. Timo Repo
University of Helsinki
Department of Chemistry
P.O. Box 55 (A.I. Virtasen Aukio 1)
FI-00014 University of Helsinki
Timo.Repo@helsinki.fi

Ph.D. (Chem. Eng.), docent Chunlin Xu
Åbo Akademi University
Laboratory of Natural Materials Technology
Research Group of Wood and Paper Chemistry
Chunlin.Xu@abo.fi

Opponent
Prof. Herbert Sixta
Aalto University
School of Chemical Engineering
Department of Bioproducts and Biosystems
P.O. Box 16100
FI-00076 Aalto
Herbert.Sixta@aalto.fi

PREFACE

The studies presented in this thesis were carried out in the Laboratory of Applied Chemistry at the University of Jyväskylä, Finland. I am grateful to my supervisor, Professor Raimo Alén, for his continued guidance concerning my studies and for providing an excellent research environment for this work.

Warm thanks go to all the members of the Laboratory of Applied Chemistry with whom I have had pleasure to work with. The close co-operation with them created a pleasant and educational working environment. In particular, I am thankful to Hannu Pakkanen, Jukka Pekka Isoaho, Maria Salmela, Arja Mäkelä, and Marja Salo for their good care and support in the laboratory.

Jyväskylä 23.04.2020

Amir Houshang Adibi Larijani

FIGURES

TABLES

CONTENTS

LIST OF SYMBOLS AND ACRONYMS

A	Cellobiose concentration at a particular time
A_0	Initial cellobiose concentration
BSTFA	*N,O*-bis(trimethylsilyl)trifluoroacetamide
CI	Crystallinity index
DP	Degree of polymerization
GC	Gas chromatography
GC-FID	Gas chromatography-flame ionization detection
GC-MSD	Gas chromatography-mass selective detection
gt	*Gauche* conformation for O5-C5-C6-O6 and a *trans* conformation of C4-C5-C6-O6
ID	Inner diameter
ISA	Glucoisosaccharinic acid (3-deoxy-2-*C*-(hydroxy-methyl)pentonic acid)
Iα	Cellulose Iα
Iβ	Cellulose Iβ
ISTD	Internal standard
k	Cellobiose degradation rate constant
MCC	Microcrystalline cellulose
MD	Molecular dynamical
MSA	Glucometasaccharinic acid (3-deoxyhexonic acid)
NMR	Nuclear magnetic resonance
r^2	Residual sum of squares
RF	Response factor
R-factor	Also residual factor, reliability factor, R-value, or R_{Work}
RMR	Relative molar response
SAXS	Small-angle X-ray scattering
t	Degradation time
T	Temperature
$t_{1/2}$	Half-life
TEM	Transmission electron microscopy
tg	*Trans* conformation for O5-C5-C6-O6 and a *gauche* conformation of C4-C5-C6-O6
TMCS	Trimethylchlorosilane
TMS	Trimethylsilyl
WAXS	Wide-angle X-ray scattering

1 INTRODUCTION

The degradation of polysaccharides in lignocellulosic materials under alkaline conditions is a well-established phenomenon in many industrial processes. It has been applied in the production of artificial fibers, namely rayon, *via* the formation of cellulose xanthate, oxygen bleaching processes, mercerization or other conventional aging processes in order to enhance strength properties, to reduce the degree of polymerization (DP), to cause fiber swelling, and to increase material solubility.

Even though the alkali-oxidative treatment of cellulose has been in use for a century, its reaction mechanism is rather complicated and has not been fully understood yet. Different reaction mechanisms have been proposed to explain experimental results and observations.

The main purpose of this work was to study the degradation under oxidative and non-oxidative alkaline conditions. For this purpose, cellobiose was treated under varying alkaline conditions (the main parameters were, *e.g.*, pressure, reaction time, and temperature) in oxygen and nitrogen atmosphere. A wide range of reaction products were formed and these substances (mainly aliphatic hydroxy carboxylic acids) were separated after per(methylsilyl)ation by gas chromatography (GC) with flame ionization detection (GC-FID) and the chromatographic peaks were identified by GC with mass selective detection (GC-MSD). The detailed data obtained were also utilized for the calculation of reaction kinetics.

A new reaction mechanism was also aimed at based on the results obtained.

2 NATIVE AND ALKALI-MODIFIED CELLULOSES

2.1 Native cellulose

Native cellulose or cellulose I is a linear biopolymer of β-(1→4)-linked D-glucopyranosyl units that are alternately rotated by 180° along the polymer axis, forming flat ribbon-like chains.[1-4] It is formed by higher plants, algae, fungi, protists, bacteria, blue-green algae, and some marine invertebrate animal species (ascidians and tunicates).[3]

Most cellulose is found in higher plants, serving as reinforcing structural microfibrils.[3] Microfibrils are an entity of parallel arranged cellulose chains, hold together by various weak forces like van der Waals forces and strong hydrogen bonds. Cellulose microfibrils are highly elastic and add great amounts of tensile strength to the cells to resist cell turgor pressure. Nevertheless, cellulose microfibrils bend easily and do not add sufficient rigidity and mechanical strength to form a stable structure and withstand gravitational forces.

Since the beginning of the 20th century, X-ray crystallography has been the method of choice to resolve the crystal structure of cellulose. However, this method was not able to provide clear evidence for the existence of different phases. Rather, high resolution ^{13}C solid-state nuclear magnetic resonance (NMR) investigations in the mid 80's by Van der Hart and Atalla showed cellulose I to be a composite of two crystalline allomorphs, cellulose Iα and cellulose Iβ.[5] Both are metastable and formed by living organisms in varying amounts, depending on the species.[6] Cellulose Iα is mainly found in bacteria and algae, while higher plants and animal species show predominantly the latter allomorph. Cellulose Iα is thermodynamically less stable than Iβ.

2.2 Mercerization and regeneration

2.2.1 Cold and hot mercerization processes

In the early years of the 19th century, the autodidact John Mercer discovered unintentionally that cotton fabric noticeably changes its physical properties when it is soaked with highly concentrated NaOH.[7] After washing out the lye, the cotton fabric became shinier, lustrous, light reflecting, and foremost showed a higher affinity for dyes. The mercerization process is usually conducted under either at 20 °C or at 60-70 °C referred as cold and hot mercerization, respectively.[8]

In cold mercerization, the fabric is driven under tension through an about 20 °C-tempered 30 %-NaOH solution at a speed of 30-40 m/min.[7] The fiber remains steeped in the alkali bath for some minutes. After steeping, the fiber is washed free of alkali, and further neutralized in an acidic solution like acetic acid to remove all traces of NaOH.

Under hot mercerization conditions a lye concentration of 22-24 % is used.[7] Mercerization performed at noticeably lower temperatures like -10 °C resulted in the formation of much stiffer yarns with linen-like properties.[9] The addition of acetic acid might also be used, but this could complicate the recycling runs of washing water.

Interposed treatments like scouring and the utilization of additives, like viscosity reducing agents [10], glycerin, alcohols [11], and NaCl [12] in the lye assist mercerization more effectively and influence the physical properties of the mercerized end product. As waxes and pectin contents in fibers impede lye penetration into the mercerized fiber by forming, for example, thin wax layers upon fiber surfaces and reducing the surface area, fibers can be pretreated by various methods before mercerization in order to reduce the content of hindering components.[9]

2.2.2 Viscose process

Regenerated cellulose fibers are mainly produced by the viscose process.[8,13-15] Introduced in the beginning of the 20th century, it allowed the production of high performance viscose fibers, such as tire cord. Performance upgrades to the viscose process like hot-stretching or the addition of modifiers and cations enhanced the viscose fiber quality even further and permitted the production of more advanced fibers.

In the viscose process, highly refined cellulose sheets (also referred to as dissolving pulp or dissolving cellulose) are steeped in the so-called slurry steeping process into a lye solution of 18 % at 40 °C for a maximum of 1 hour.[14] The solution thoroughly penetrates the cellulose and, due to the high alkalinity of the solution, a cellulosate is formed, namely Na-cellulose (sodium cellulose). The formation of alkoxide groups in the cellulose built is crucial for the formation of cellulose xanthate in one of the following steps. Furthermore, additives, such as

nonionic and anionic surfactants, are added in small quantities into the slurry. Additives enhance the xanthation process or permit more efficient viscose solution filterability.

After steeping, the cellulose is freed from excess lye and shredded into small pieces (white crumb) in order to increase the surface area of cellulose.[14] The white crumbs are aged in ambient air. The purpose of this aging step (pre-aging) is to partially oxidize the cellulose and to reduce the DP for lower viscosities in the spinning solution. In the following xanthation step, the pre-aged white crumbs are treated with CS_2 in a mixing vessel. The gaseous CS_2 reacts with the alkoxide groups of sodium cellulose, preferably at the anhydroglucose C-2 position, forming cellulose xanthate ester polyelectrolytes:

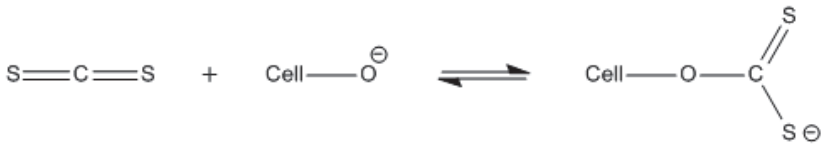

(1)

The crystalline areas of the white crumbs areas are largely inaccessible for CS_2.[14] The end product of the xanthation process is the so-called yellow crumb, *i.e.*, a cellulose-cellulose xanthate copolymer crumb. The yellow crumb is treated with lye in a dissolving tank and, due to the xanthate esterification, the cellulose chains are more effectively separated from one another. Additionally, a sufficient amount of negatively charged dithiocarbonate groups of cellulose xanthate permits their dissolution in the lye solution. However, rather a suspension of dissolved cellulose xanthate and untreated crystalline cellulose is obtained in this step of the process. Due to significant chain stiffening polymer-solvent interactions, the suspension has a high viscosity and for this reason, it has been termed "viscose".

For the regenerated fiber spinning process, only the dissolved cellulose xanthate is of interest.[14] Henceforth, the viscose suspension is filtered to remove the undissolved materials. The filtrate contains parts of crystalline unreacted cellulose. Those crystalline parts are further broken down and converted into cellulose xanthate in a second aging stage, called ripening. Due to the reversibility of the xanthate reaction, the released CS_2 from cellulose xanthate reacts with the unreacted cellulose parts. By the ripening step a higher graded viscose solution is obtained. A part of the reformed CS_2, however, escapes unreacted.

In the following step, the viscose solution is freed from air bubbles in a degassing step that cause casualties during the wet spinning step of regenerated cellulose filaments.[14] During the wet spinning step the viscose solution is pressed through a shower head-like device called spinneret into an acidic solution where cellulose precipitation follows. The acidic solution consists of sulfuric acid, sodium sulfate, and usually Zn^{2+} cations. The zinc cations ensure that the extruded cellulose xanthate jets from a spinneret draw toward one another and, due to the occurring water loss into the acidic solution and the conversion of the xanthate

groups into the instable xantheic acid groups, the viscose jet oversaturates and precipitation takes place under CS_2 gas release.

The obtained viscose filaments are stretched in the following step to ensure parallel chain orientation along the fiber axis.[14] Furthermore, the filament stretching allows the formation of interchain hydrogen bonds and permits the controlled customization of filament properties of the desired textile fiber end product. In the following steps the fibers are cut, washed free from impurities, dried, and finally dispatched for further use, for example, in yarn spinning mills.

Figure 1 illustrates the described viscose process.

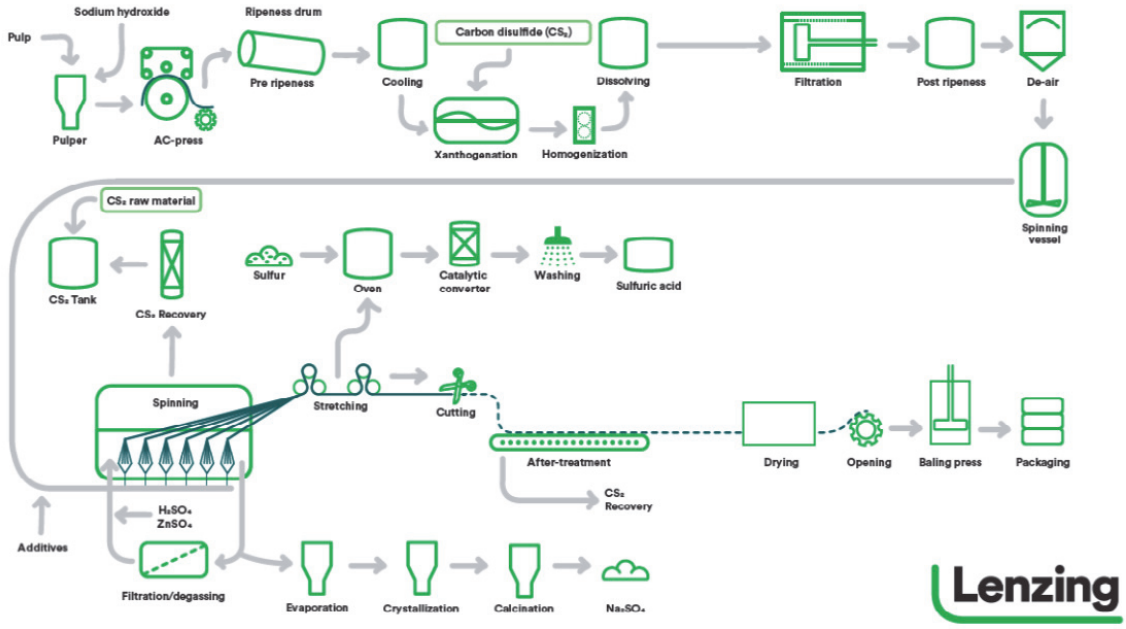

FIGURE 1. Viscose process. Courtesy of Lenzing AG, Austria.

2.3 Na-cellulose I

If native cellulose soaked in NaOH at a concentration range of 12-20 %, then a lattice transformation takes place and intermediate Na-cellulose I is formed.[16] The chemical composition, $NaOH{\cdot}3H_2O{\cdot}C_6H_{10}O_5$, has been determined for Na-cellulose I. From 0-9 % NaOH content, however, Na^+ is absorbed to small extents and the native cellulose structure remains unchanged. In the transition period between native cellulose and Na-cellulose I, the Na^+ uptake rises very rapidly to the Na^+ content of Na-cellulose I. In the Na-cellulose I stage, the NaOH concentration remains constant since no additional NaOH is further absorbed.

Beyond the Na-cellulose I state follows a second transition period at NaOH concentrations of 27 % and a second Na-cellulose intermediate, namely Na-cellulose II with a chemical composition of $NaOH{\cdot}H_2O{\cdot}C_6H_{10}O_5$.[16] Na-cellulose II exists in two forms, Na-cellulose IIA and IIB.[17,18] Na-cellulose IIA is colorless and

formed if fibers are constrained during NaOH treatment.[18] Na-cellulose IIB, however, is bright blue and formed by unconstrained NaOH treatment. The described swelling characteristics of native cellulose fibers have been discovered [16] in the early 20th century and confirmed by multiple researchers. Figure 2 depicts a Vieweg curve.

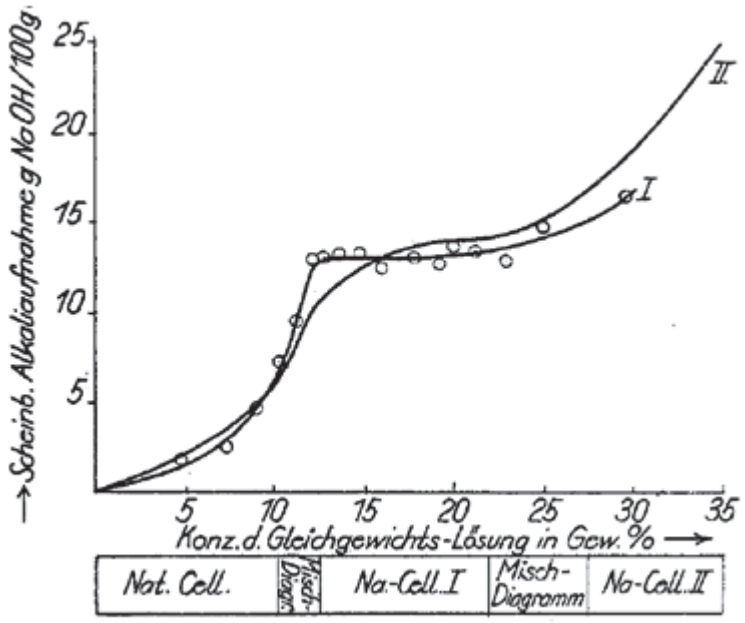

FIGURE 2. Vieweg curves. Formation of Na-cellulose I and Na-cellulose II. Apparent alkali absorption of cellulose, curve I according to Sakurada *et al.* and curve II according to Schramek. Figure reprinted (adapted) with permission from ref. 16. Copyright (1937) Springer Nature Switzerland AG. Part of Springer Nature.

2.4 Chain polarity of Na-cellulose I and cellulose II

It is assumed that Na-cellulose I structure is antiparallel,[19] thus this state being the position where parallel native cellulose is being transformed into the antiparallel cellulose II allomorph. It is widely debated, how the parallel native cellulose form could rearrange in solid state into the antiparallel cellulose II structure. Okano and Sarko [20], Nishimura and Sarko [21], and Revol *et al.* [22] have proposed an interdigitation mechanism. The authors assume that microfibrils that consist of parallel cellulose chains are themselves arranged with opposite polarity and run toward one another. This hypothesis could be confirmed by Revol and Goring.[23] During the swelling process, however, the sheets would gain the necessary mobility freedom to rearrange and form the antiparallel sodium cellulose I intermediate and henceforth, the cellulose II form. The interdigitation mechanism is, however, not generally accepted. Simon *et al.* [24] have suggested that the swelling

process would provide sufficient space for a cellulose chain to leave its straightened state, successively fold together, and result in a single chain that is, once folded and thus being antiparallel (Figure 3).

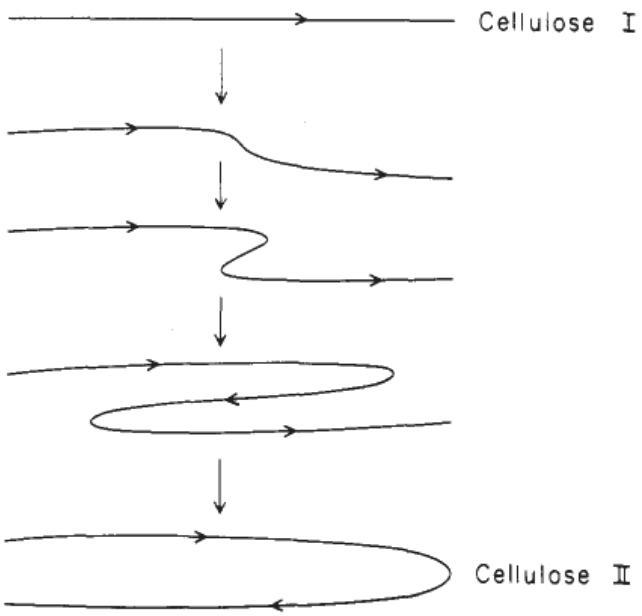

FIGURE 3. Schematic representation of successive stages of the transformation from a parallel to an antiparallel arrangement of cellulose chains during mercerization. Figure reprinted with permission from ref. 24. Copyright (1988) American Chemical Society.

Kroon-Batenburg *et al.* [25] have assumed that mercerized cellulose II is parallel or parallel in parts of the fiber and point out that X-ray crystallography methods would not provide sufficiently clear data to ascertain cellulose chain polarities.[26] Crawshaw *et al.* [27] have suggested a yet unknown intermediate before the formation of Na-cellulose I. They assumed that this intermediate might represent the first stage of the interdigitation mechanism, where the first rearrangements of chains and crystals take place or also possibly be the earliest swelling state of the fiber and thus, not indicating any chain or crystal rearrangements. The proposed Na-cellulose I structure by Nishimura *et al.* [19] from mercerized cellulose is shown in Figure 4.

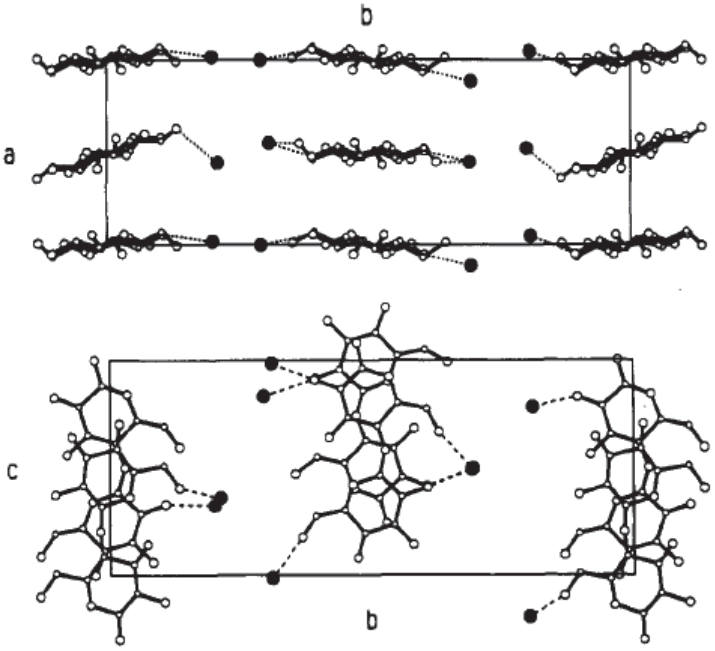

FIGURE 4. *a-b* (top) and *b-c* (bottom) projections of the Na-cellulose I structure. Filled circles denote Na^+ ions and dashed lines denote ionic secondary bonds. Figure reprinted with permission from ref. 19. Copyright (1991) American Chemical Society.

2.5 Swelling and fiber dissolution process

Sodium ions intercalate in between the cellulose sheets and cause fiber swelling and dissolution to occur.[19,28] Crawshaw *et al.* [27] have applied wide-angle X-ray scattering (WAXS) and small-angle X-ray scattering (SAXS) investigations on native ramie cellulose and followed its swelling behavior in water and NaOH. Their investigations could verify a few but large void areas within tightly packed elementary crystallite arrangements.

By steeping native cellulose into water or lowly concentrated NaOH solutions cellulose and solvent form a disequilibrium, the original void gaps collapse while an increased number of smaller gaps in between the elementary microfibrils form.[27] To balance the system and reach an equilibrium state, solvent molecules intercalate in between the elementary microfibrils and cause their separation. The intercalated ions form hydrogen bonds with the elementary microfibrils and alter the existing hydrogen bond network.[28] Equilibrium state is reached when the osmotic pressure is compensated by cohesive forces in the fiber.[8] The described process is referred to as swelling. Even though the fiber swells, the native cellulose structure does not alter. Klemm *et al.* [8] have also suggested that the transition from native cellulose to Na-cellulose I might go through a yet unidentified intermediate, similar to the water-swollen cellulose structure. At NaOH concentrations of 4 M and higher, a well-defined void gap system evolves and

native cellulose transforms entirely to Na-cellulose I. The void gaps are highly ordered and drastically increased in number (Figure 5).

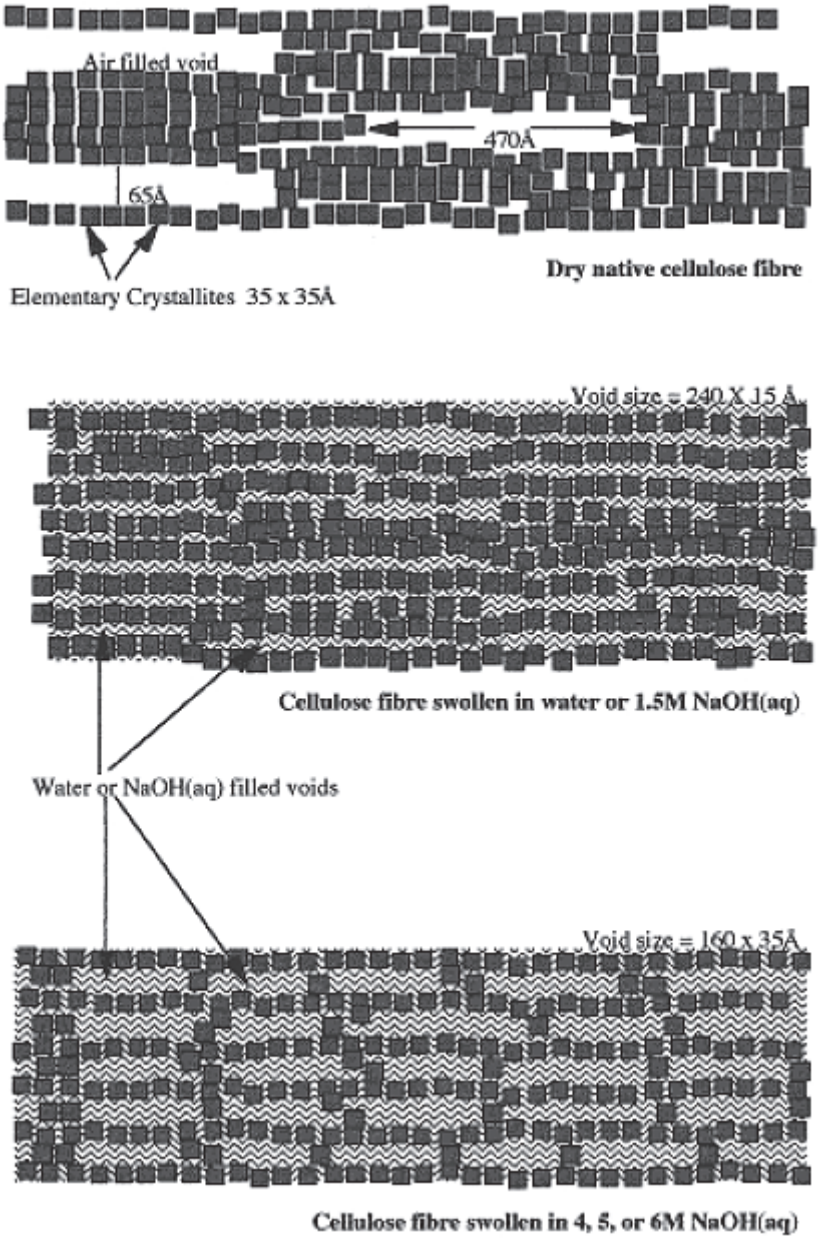

FIGURE 5. Schematic illustration of changes to the voids within native cellulose fibers as during swelling in water, or 1.5 *M* $NaOH_{aq}$, and 4, 5 or 6 *M* $NaOH_{aq}$. View in plane perpendicular to fiber axis. Figure reprinted with permission from ref. 27. Copyright (2002) WILEY-VCH.

Crawshaw *et al.* [27] could also confirm that the conversion from native cellulose to swollen Na-cellulose I proceeds rather rapidly. NaOH molarities above 4 M accelerate the transformation to Na-cellulose I, the swollen fiber structure would, however, remain the same. It has generally been assumed that hydroxyl

anions from the NaOH solution are the interacting agent with the cellulose hydroxyl groups, while the sodium cation is rather responsible for the extensive swelling.[8] During swelling the originally existing hydrogen bonds break and rearrange with intercalation of solvent molecules and ions in between the sheets. During swelling, however, conformational and spatial changes occur to the cellulose chains due to solvent-chain interactions. The swelling reaction of cellulose fibers is diffusion-controlled and shows rather minor temperature influences upon the process. Lowering the temperature increases the swelling efficiency and results in stronger Na^+ binding onto cellulose chains.

Le Moigne and Navard [29] have studied the dissolution mechanisms of wood pulp and microcrystalline cellulose (MCC) at moderate NaOH concentrations and -6 °C solvent temperature, using two different samples (Figure 6). Cellulose samples were stirred for a period of two hours and further fractionated by centrifugation in three steps. Obtained were three insoluble fractions and a clear solution.

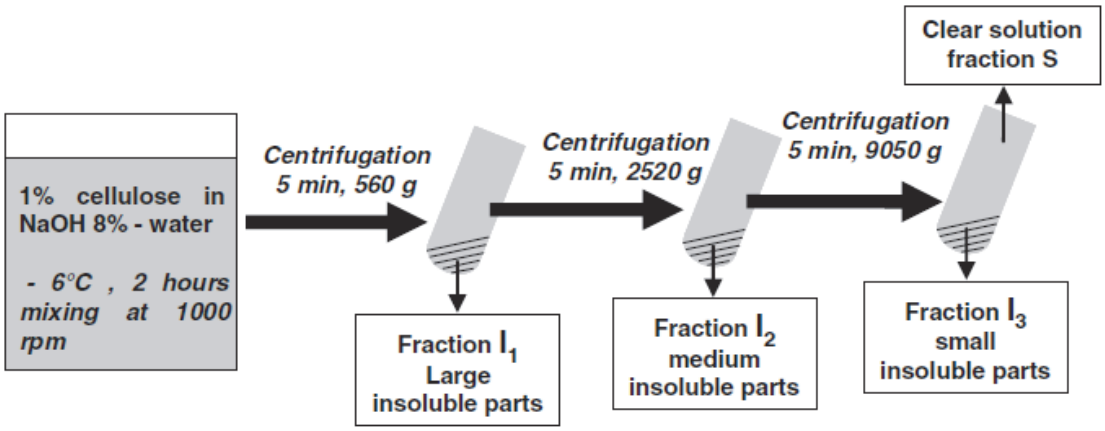

FIGURE 6. Centrifugation protocol in three steps to fractionate the insoluble fractions (I_1, I_2, and I_3) and the clear solution. Figure reprinted with permission from ref. 29. Copyright (2010) Springer Nature Switzerland AG. Part of Springer Nature.

Fraction content was visualized by utilizing the optical and transmission electron microscopy (TEM). The first fraction revealed the presence of undissolved, ballooned, and highly swollen fibers. Fiber ballooning occurs when the secondary wall of the fiber areas swell or dissolve in the solvent and result in the breakdown of the primary wall and the formation of thick helices, while being separated by small sections of unswollen fiber areas. The second fraction revealed large amounts of fragmented and unfragmented sections and flat rings. The last insoluble fraction revealed the existence of little fragments. Insoluble and small unfractionable parts were found in the remaining solution fraction. Figures 7-10 depict the mentioned fractions.

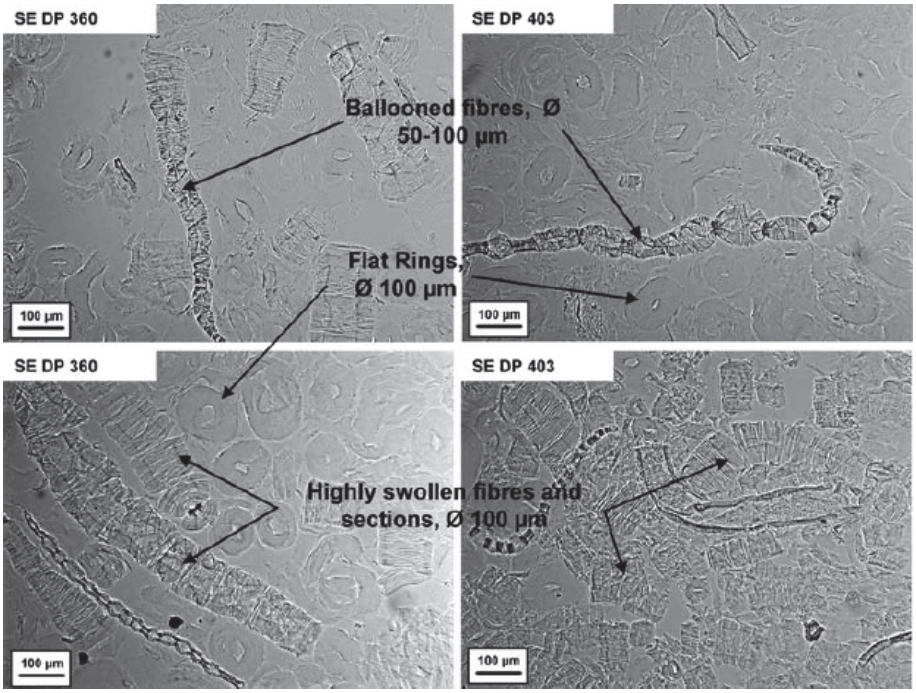

FIGURE 7. Optical microscopy images of the fraction I_1. Ballooned fibers, highly swollen fibers, highly swollen sections, and flat rings are observed. Figure reprinted with permission from ref. 29. Copyright (2010) Springer Nature Switzerland AG. Part of Springer Nature.

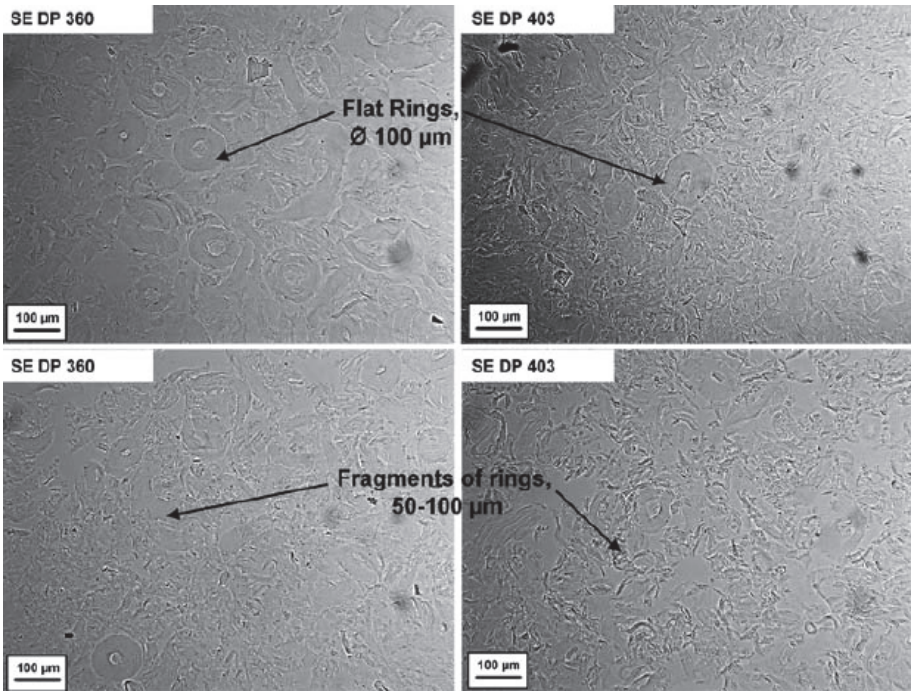

FIGURE 8. Optical microscopy images of the fraction I_2. Flat rings and fragments of rings are observed. Figure reprinted with permission from ref. 29. Copyright (2010) Springer Nature Switzerland AG. Part of Springer Nature.

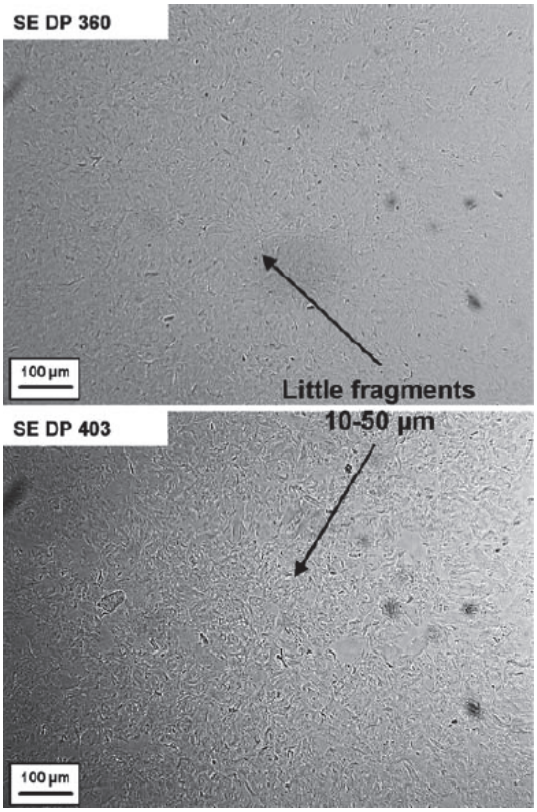

FIGURE 9. Optical microscopy images of the fraction I_3. Only small fragments 10-50 µm are observed. Figure reprinted with permission from ref. 29. Copyright (2010) Springer Nature Switzerland AG. Part of Springer Nature.

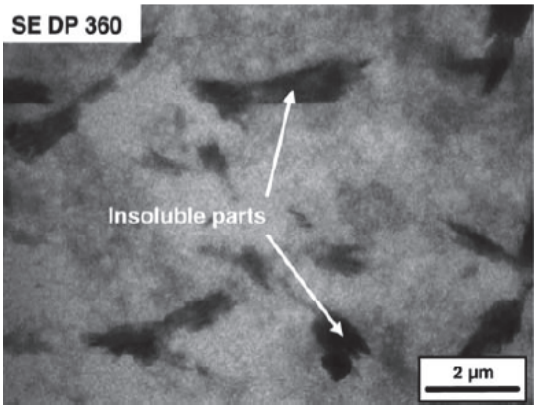

FIGURE 10. TEM image of the clear solution fraction (*S*). Figure reprinted with permission from ref. 29. Copyright (2010) Springer Nature Switzerland AG. Part of Springer Nature.

Based on the observations, Le Moigne and Navard [29] have developed a swelling and dissolution mechanism of wood fibers in a moderately concentrated NaOH-water solution (Figure 11).

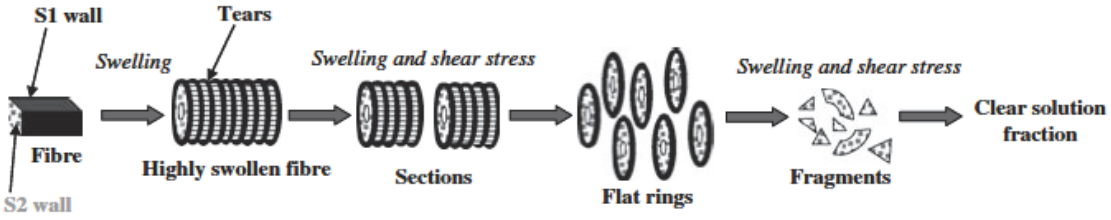

FIGURE 11. Schematic representation of the dissolution steps of wood pulp fibers in NaOH 8 %-water. Figure reprinted with permission from ref. 29. Copyright (2010) Springer Nature Switzerland AG. Part of Springer Nature.

The results of Le Moigne and Navard [29] on the two analyzed steam exploded wood pulps confirmed that the vast amount of hemicelluloses, *i.e.*, mannans and xylans, 72 % and 90 %, respectively, dissolve readily in moderately concentrated NaOH-water solutions, while 28 % and 10 % of mannan and xylan, respectively, remain associated with the cellulose chains. Mannan is more closely bound to cellulose that xylan. The interactions between cellulose fibers and hemicelluloses are supposed to be of physical nature.[30] The associated hemicelluloses might apparently influence the dissolution properties of cellulose fibers [29] by possibly impairing swelling and solvent accessibility to some extent.

2.6 Cellulose I/II reversibility

The cellulose II structure is the thermodynamically most stable cellulose polymorph and it is unlikely that a direct transformation from cellulose II into the metastable cellulose Iα or Iβ would take place. However, both, the existence and the absence of cellulose I/II reversibility have been proposed. Kubo [31,32] has suggested that a thermal treatment of regenerated cellulose fibers (cellulose II) in organic solvents, like glycol and glycerol, can lead to the retransformation into native cellulose.

An interesting observation made by Kroon-Batenburg *et al.* [25] could show in molecular dynamical (MD) simulations that cellulose II with a parallel-down packing arrangement and tg/tg hydroxymethyl conformation readily converts to native cellulose Iβ. Assumed, the cellulose II structure is not static along the entire fiber but rather interchangeable within areas of the fiber, this observation could provide a pattern to explain a possible transformation to native cellulose from cellulose II.

Klemm *et al.* [8] developed based on the work of Philip *et al.* [33] and Hayashi [34] the theory of the existence of two sodium cellulose I modifications, namely sodium cellulose I_1 with a bent $^4C_1$ conformation and sodium cellulose I_2 with a twisted and bent $^4C_1$ conformation. Sodium cellulose I_1 is suggested to be capable of retransforming into the native cellulose I structure while the second structure rather transforms into cellulose II after neutralization and drying. The equation (2) depicts this relation.

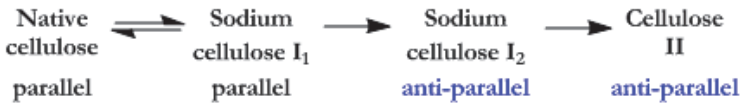

(2)

Independent from Klemm *et al.* [8], the results of Crawshaw *et al.* [27] indicated the existence of a possible Na-cellulose intermediate with a rather water-swollen-like cellulose I structure. The observation of Crawshaw *et al.* [27] could possibly refer to the sodium cellulose I_1 structure and therefore, supporting the theory of the existence of two possible sodium cellulose I forms by Klemm *et al.* [8] Experiments to identify and analyze Na-cellulose I were made in highly concentrated solutions. Observations made by Lee *et al.* [9] supported the earlier assumptions.[8,27]

Lee *et al.* [9] have investigated on enhancing the properties of cotton to a linen-like material through low temperature mercerization. They observed that cotton fibers mercerized with a 10 % NaOH solution remain unaffected in their crystalline structure, even though a temporary mercerization effect is clearly observed. However, after laundering, the fibers loose the property changes that were gained through the low concentration mercerization process and return into their original unmercerized state. Permanent effects were observed if the NaOH concentration was high enough, meaning NaOH concentrations of 15 % and higher. Figure 12 depicts typical curve shapes of the crystallinity index (CI) and cellulose II amount of bamboo fibers at different NaOH concentrations.

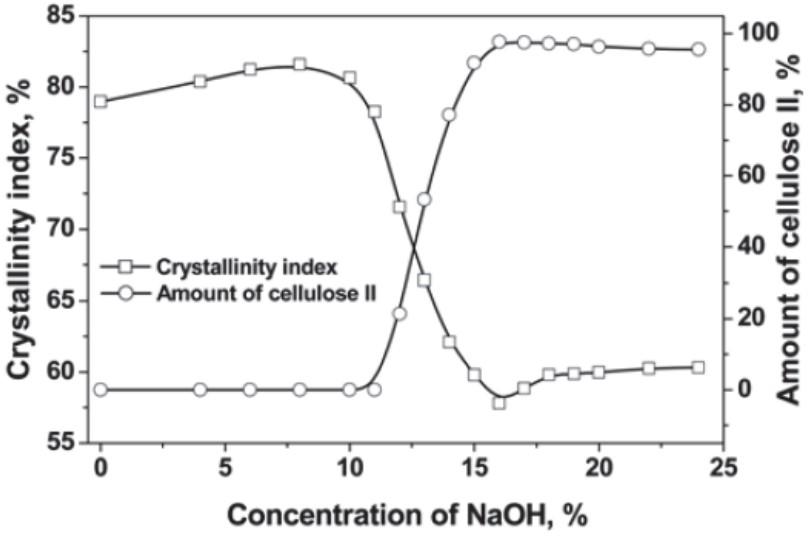

FIGURE 12. Amount of cellulose II and crystallinity index of bamboo fibers *vs.* NaOH concentration (20 °C, 20 min). Figure reprinted with permission from ref. 35. Copyright (2008) Springer Nature Switzerland AG. Part of Springer Nature.

Dinand *et al.* [26] and Schenzel *et al.* [36] came both to similar results. In Figure 12, up to 10 % NaOH concentration, cellulose II remains unformed while the CI rises for about 3 %. With advancing transformation of cellulose II from cellu-

lose I, the CI proportion decreases from about 80 % to 60 %. The reduced proportion of existing crystallites in the cellulose II form explains the superior dyeability of cellulose II compared to cellulose I.

Nishimura *et al.* [19] have used a highly concentrated aqueous NaOH solution (6.3 N NaOH) over a period of about 15 days to achieve a satisfactory transformation of ramie cellulose into Na-cellulose I to obtain clear X-ray diffraction results. According to the observations mentioned above, it is most likely that Nishimura *et al.* [19] analyzed Na-cellulose I_2 with a twisted and bent $^4C_1$ conformation. They could also confirm the antiparallel structure of the Na-cellulose I allomorph. Dinand *et al.* [26] have followed the mercerization process of primary cell wall microfibrils from initial, untreated state up to a NaOH concentration of 20 % by TEM microscopy. The images show clearly the formation of an unordered particulate precipitate, right after swelling occurs at about a transitional NaOH concentration from 8 % to 9 % (Figure 13).

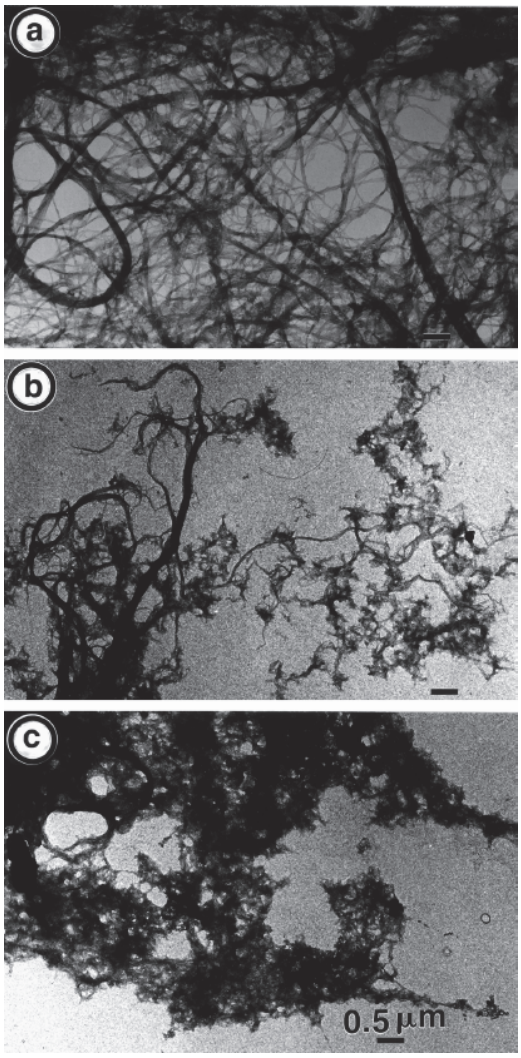

FIGURE 13. TEM micrographs of PCC1 samples. (a) Sample treated with 9 % NaOH, (b) as in (a), but treated with 10 % NaOH, and (c) as in (a), but treated with 12 % NaOH. Figure reprinted with permission from ref. 26. Copyright (2002) Springer Nature Switzerland AG. Part of Springer Nature.

The ordered microfiber structure disintegrates irreversibly and Dinand *et al.* [26] have denied the transformation of cellulose II into cellulose I at either crystallographic or morphological level. Lee *et al.* [9] have assumed that the extent of hydroxide ion hydration is the determining factor whether the transition from cellulose I to cellulose II is permanent or temporary. At lower NaOH concentrations, before the transition state is reached, the large hydrated hydroxide ions do not penetrate sufficiently the fibers to achieve lattice changes, and thus, easily accessible amorphous areas undergo changes. Furthermore, Na^+ intercalate rather unincisively, causing swelling to some minor extent with temporary mercerization effects.

With increasing NaOH concentration, the hydrated hydroxide ion radii decrease and by reaching a critical size the hydrated hydroxide ions start to penetrate the lattice (transition state). The post-transition state would henceforth be a state when the hydrated hydroxide ions would be small enough to penetrate the cellulose lattice quantitatively and lead to Na-cellulose I_2. Liu *et al.* [35] could show that a decrease of mercerization temperature shifts the transition state area in between cellulose I and cellulose II lattice phases toward lower NaOH concentrations. For more details, see Figures 12, 14, and 15.

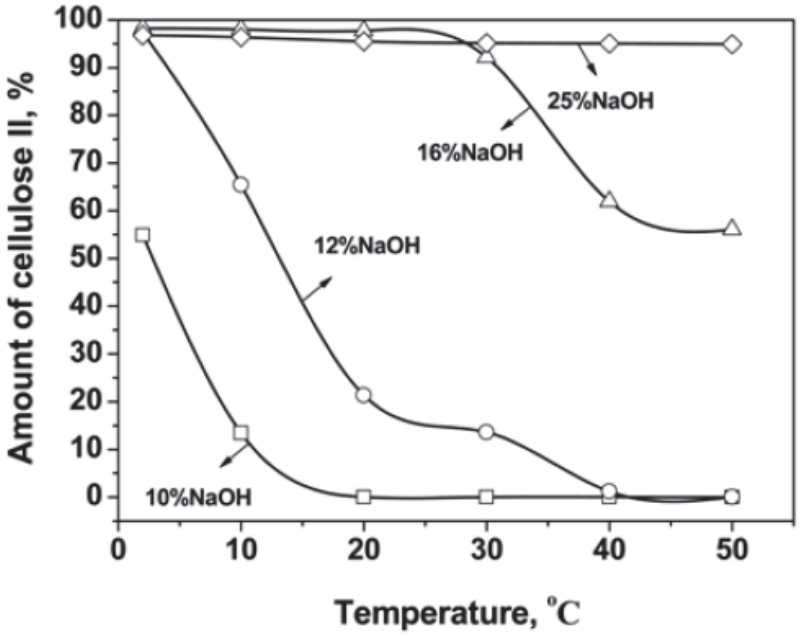

FIGURE 14. Amount of cellulose II of bamboo fibers *vs.* mercerization temperature (20 min). Figure reprinted with permission from ref. 35. Copyright (2008) Springer Nature Switzerland AG. Part of Springer Nature.

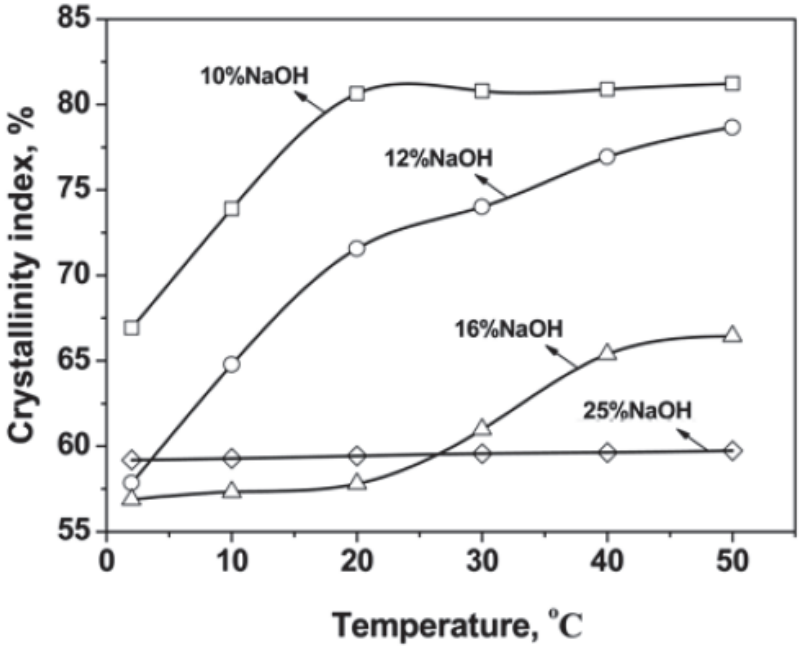

FIGURE 15. Crystallinity index of bamboo fibers *vs.* mercerization temperature (20 min). Figure reprinted with permission from ref. 35. Copyright (2008) Springer Nature Switzerland AG. Part of Springer Nature.

Liu *et al.* [35] have explained that the hydrated hydroxide ion radii decrease when the mercerization temperature is reduced. Depending on the lattice structure and density of the mercerized material, a minimum hydrated hydroxide ion radius is required for an irreversible lattice transformation from cellulose I to cellulose II to occur. Liu *et al.* [35] could also show that an increase of applied tension on fibers during mercerization reduces swelling efficiency. Therefore, this hinders the transformation from cellulose I to cellulose II, so shifting the transition state in between cellulose I and II toward higher NaOH concentrations. In accordance with Crawshaw *et al.* [27] and Klemm *et al.* [8] the observations of Lee *et al.* [9] and Liu *et al.* [35] could confirm the existence of two distinct Na-cellulose I phases. The temporary mercerization effects would therefore have been achieved when Na-cellulose I_1 is formed, the pre-transition state Na-cellulose I form. Permanent mercerization effects are to be expected in the post-transition Na-cellulose I state when Na-cellulose I_2 is formed, and its permanent mercerization effect is due to the irreversibility of the transition from Na-cellulose I_1 with an unchanged cellulose I lattice to Na-cellulose I_2 with an antiparallel cellulose II-like lattice structure.

2.7 Cellulose II structure revision

In the MD simulations of Kroon-Batenburg *et al.*,[25] the two most acceptable cellulose II structures were antiparallel-down cellulose II with gt/gt and gt/tg hydroxymethyl conformations. Even though the gt/tg conformation was preferred energetically, the gt/gt form, even though it has a slightly higher energy, was preferably formed during the simulation process. The gt/gt form sizes well into the cellulose II unit cell and can be overseen in diffraction analysis. It should be pointed out that the focus on searching the lowest-energy structure by computational procedures does not suffice in revealing the exact cellulose structure, for nascent cellulose, emerging out of the terminal complex, does not crystallize in a thermodynamical equilibrium state, making the formation of metastable forms generally inevitable.[25]

Kolpak and Blackwell [37] have determined the cellulose II structure by using regenerated cellulose fibers. It should be pointed out that the production process for regenerated fibers is significantly different than mercerized fibers. The one is formed entirely from dissolved state and precipitates in acid bath while mercerized cellulose is formed in rather solid state where an ideal lowest-energy state of microfiber orientation might not been given. Thus, it could be possible that the cellulose II structure of mercerized cellulose might indeed differ to some extent from regenerated cellulose. Thus, Kroon-Batenburg *et al.* [25] have suggested a parallel-up cellulose II structure with gt/gt hydroxymethyl conformation for mercerized cellulose and a antiparallel-down cellulose II structure with gt/gt hydroxymethyl conformation for regenerated viscose fibers (Figure 16).

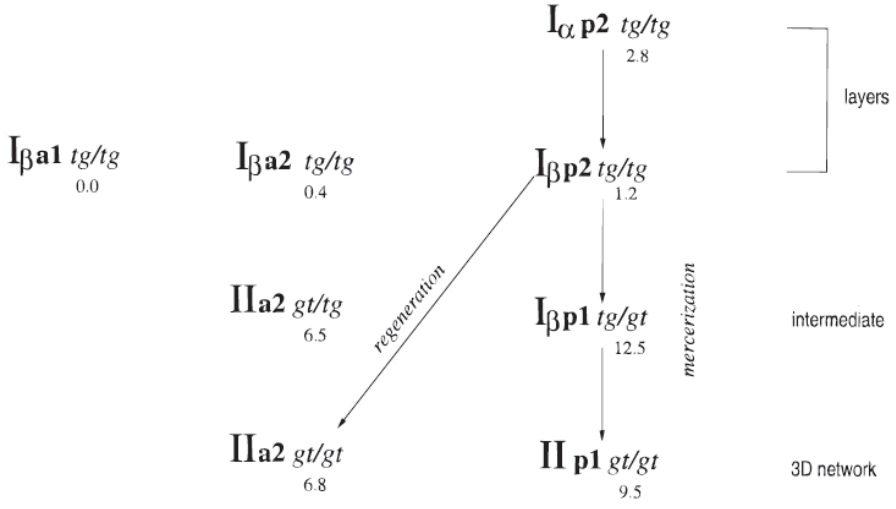

FIGURE 16. Scheme to show the relation between the stable MD structures. The right part represents structures that could occur in the mercerization process. The numbers represent the average relative potential energies in kJ/mol of cellobiose residues in the constant pressure simulations. Figure reproduced with permission from ref. 25. Copyright (1996) American Chemical Society.

Because the cellulose II structure is not static over the entire entity, it is not advisable to base cellulose II structure assumptions, for example, on only the lowest R-values and the maximized hydrogen bonding capabilities. Langan *et al.* [38] could show that hydroxymethyl groups are in both, mercerized and regenerated cellulose, which would to some extent lead to the formation of different intermolecular hydroxymethyl hydrogen bonds. Besides this, it was shown by Raymond *et al.* [39] that the cellulose II center chain is strained, thus allowing higher system energies to be expected than from a supposedly static structure.

3 ALKALINE OXIDATION OF CELLULOSE

3.1 General aspects

3.1.1 Oxygen chemistry

Molecular oxygen in its electronically stable ground state can be described as a diradical.[40] Each oxygen atom has one electron in one of the two antibonding orbitals. The electrons have a parallel spin orientation. Due to this orbital occupancy characteristic, oxygen is renowned for radical reactions; the lack of an unoccupied or fully occupied orbital allows the oxygen molecule to either interact as a Lewis acid in the former or Lewis base in the latter case.

The stepwise reduction of the oxygen molecule to water is illustrated in Figure 17. The transients are hydroperoxyl radicals (HOO·), hydrogen peroxide (HOOH), hydroperoxide anions (HOO^-), and hydroxyl radicals (HO·).

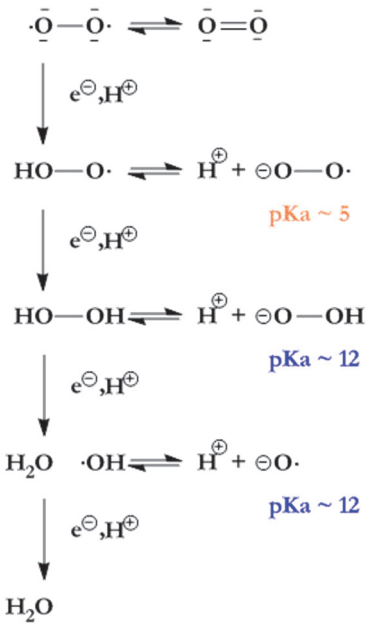

FIGURE 17. Formation of reactive intermediates during the stepwise reduction of oxygen to water. Figure reproduced from ref. 40. Copyright (1993) Elsevier B.V.

3.1.2 Autoxidation in general

Autoxidation [41-45] is defined as a spontaneous radical-chain reaction between molecular oxygen (diradical) and organic compounds at low or moderate temperatures and atmospheric pressure. Autoxidation reactions result in the formation of hydroperoxides:

$$R{-}H + O{=}O \xrightarrow[\text{(slow)}]{\text{initiator}} R{-}O{-}O{-}H \qquad (3)$$

Transition metals are known for their positive catalytic properties, whereas, for example, amines, screened phenols (Figure 18a) or hydroquinone-type compounds (Figure 18b) are utilized as inhibitors (antioxidants).

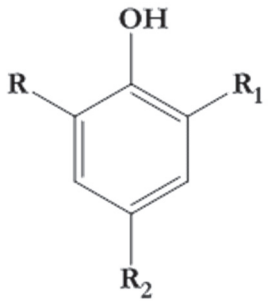

a) R, R_1, R_2 = alkyl and H
b) R, R_1 = alkyl; R_2 = hydroxyl

FIGURE 18. Screened phenol (a) and hydroquinone-type (b) compounds.

The susceptibility for organic substances to autoxidation varies. However, compounds with a high electron density hydrogen atoms (strongly reducing character), like benzaldehyde or cumene, are very susceptible to autoxidation (Figure 19).

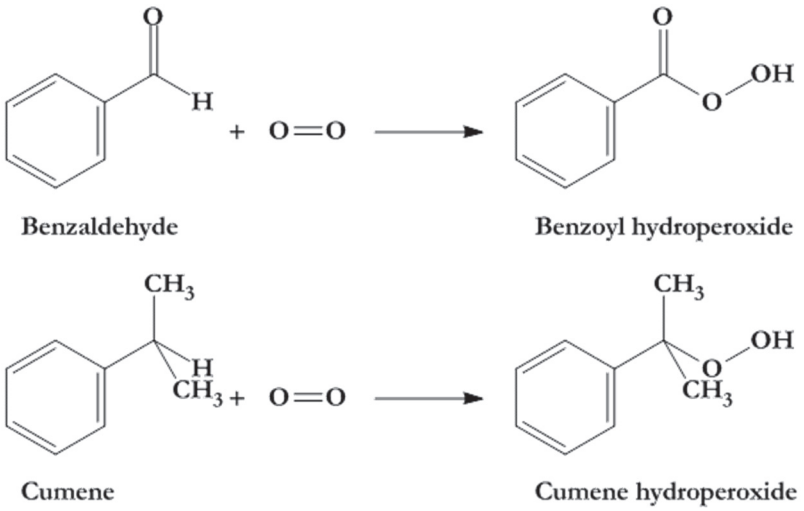

FIGURE 19. Formation of benzoyl hydroperoxide and Cumene hydroperoxide.

A vast variation of different autoxidation reaction mechanisms do indeed exist. However, here the olefinic hydrocarbon autoxidation mechanism is presented. The autoxidation process involves initiation, propagation, and termination steps. The reactions in Figure 20 demonstrate the reaction process. Undesirable autoxidation effects are, for example, the perishing of rubber, petroleum-based products or the rancidification of edible oils.

1. Initiation (a very slow reaction)

$$RH + O_2 \longrightarrow R\cdot + HOO\cdot \quad (a)$$

2. Propagation (a fast reaction)

2.1 $$R\cdot + O_2 \longrightarrow ROO\cdot \quad (b)$$

2.2 $$RH + ROO\cdot \longrightarrow ROOH + R\cdot \quad (c)$$

(Please note that this is a repetitive process.)

3. Termination

$$ROO\cdot + ROO\cdot \longrightarrow \text{Products} \quad (d)$$

4. Autocatalysis

$$ROOH \longrightarrow RO\cdot + HO\cdot \quad (e)$$

$$RO\cdot + RH \longrightarrow ROH + R\cdot \quad (f)$$

$$HO\cdot + RH \longrightarrow HOH + R\cdot \quad (g)$$

FIGURE 20. Olefinic hydrocarbon autoxidation mechanism. Reproduced from Mattor's PhD thesis.[43] Copyright (1963) Georgia Institute of Technology, Institute of Paper Science and Technology, Appleton, WI, USA.

Autoxidation reactions are usually autocatalytic. Due to the weak O—O hydroperoxide ROOH bond, formed hydroperoxide molecules are a subject to dissociate into radicals through occasional thermal fission reactions. Hence, the addition of hydroperoxidic substances accelerates the process noticeably.

Initiation reactions are generally photocatalytic in autoxidative reactions, as demonstrated in Figure 21.

5. Photocatalytic initiation reactions

$$RCHO \xrightarrow{h\nu} R\dot{C}O + H\cdot \quad (h)$$

$$RCHO + R' \longrightarrow R\dot{C}O + R'H \quad (i)$$

$$RCHO + Co^{3+} \longrightarrow R\dot{C}O + Co^{2+} + H^{+} \quad (k)$$

FIGURE 21. Photocatalytic initiation reactions. Reproduced from Mattor's PhD thesis.[43] Copyright (1963) Georgia Institute of Technology, Institute of Paper Science and Technology, Appleton, WI, USA.

3.1.3 Peroxide formation

According to Entwistle *et al.* [41,42], the autoxidation process leads to the formation of peroxides through hydroperoxides in alkaline medium at moderate temperatures. They react as nucleophiles with, for example, electron deficient carbonyl and conjugated carbonyl structures.[46]

Hydrogen peroxide and hydroperoxides have weak O—O bonds (≤ 50 kcal/mol bond energy) which readily dissociate homolytically, notably under light and heat influence.[46] They decompose readily under alkaline conditions *via* disproportionation. An increase of pH and hydroxide ion concentration has rate increasing effects (equation (l) and (m)). Oxygen formed *via* disproportionation as shown in equation (m) appears predominantly in its triplet ground state $^3O_2$. However, to some extent oxygen is also formed in an excited singlet state $^1O_2$.[43]

$$HOOH + HOO^{-} \longrightarrow HO\cdot + HOO\cdot + HO^{-} \quad (l)$$

$$HOOH + HOO^{-} \longrightarrow HO^{-} + {}^3O_2({}^1O_2) + H_2O \quad (m)$$

Bamford and Collins [47] have conducted the degradation of glucose in NaOH and could not detect any presence of radicals at room temperature. Benzene diazonium hydroxide, benzoyl peroxide, sulfur, hydroquinone, and picric acid are used to confirm the presence of radicals. Furthermore, Ag^0, Cu^+, Fe^{2+}, Mn^{2+}, and Ce^{3+} do not show any effect on the overall reaction procedure, while Pt^0 and Co^{2+} do have influence on the reaction rate, but in different ways. No traces of organic peroxides were detected but hydrogen peroxides were found in trace amounts. Sinkey [48] could affirm the results of Bamford and Collins [47] about peroxides under similar reaction conditions. Green *et al.* [49] could not detect organic peroxides at room temperature.

Green *et al.* [49] have followed the hydrogen peroxide concentration formed during the degradation of methyl α-D-glucopyranoside with transition metal stripes under oxygen-alkali pulping conditions. Green *et al.* [49] have conjectured that all the analyzed metals (Pt, Ag, stainless steel, Ni, Zr, Ti, W, and Co) do not have an influence on the hydrogen peroxide formation but rather have either stabilizing or decomposing effects (Figure 22).

It is interesting to note that tungsten or sodium tungstate in NaOH has the same hydrogen peroxide stabilizing effect as magnesium, which reduces the carbohydrate degradation rate.[49] Iron shows the converse effect and hydrogen peroxide molecules degrade more readily according to equations (n) and (o).

$$Me^{n} + H_2O_2 \longrightarrow Me^{n+1} + HO\cdot + HO^- \qquad (n)$$

$$Me^{n+1} + H_2O_2 \longrightarrow Me^{n} + {}^1/_2\,O_2 + H_2O \qquad (o)$$

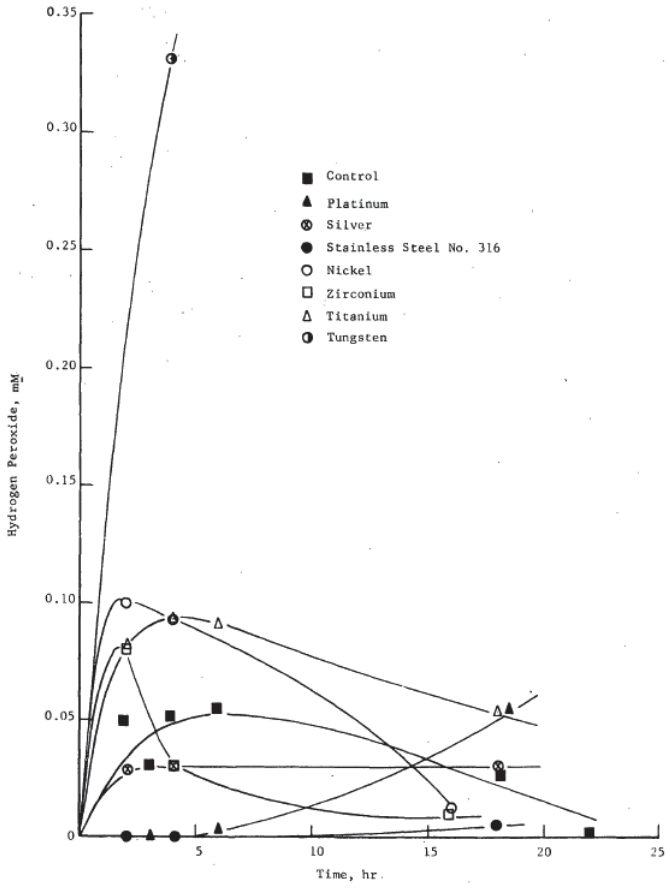

FIGURE 22. The production of hydrogen peroxide from the reaction of methyl α-D-glucopyranoside with oxygen and alkali in the presence of different metals. Photocatalytic initiation reactions. Reproduced from Green *et al.*[49] Copyright (1976) Georgia Institute of Technology, Institute of Paper Science and Technology, Appleton, WI, USA.

Silver, tungsten, cobalt, and stainless steel metal (or their corresponding metal ions) samples showed higher organic peroxide concentrations than the metal free control caustic solution with reagent grade impurities of about 6 ppm iron, 2 ppm aluminium, and 1 ppm copper (Figure 23).

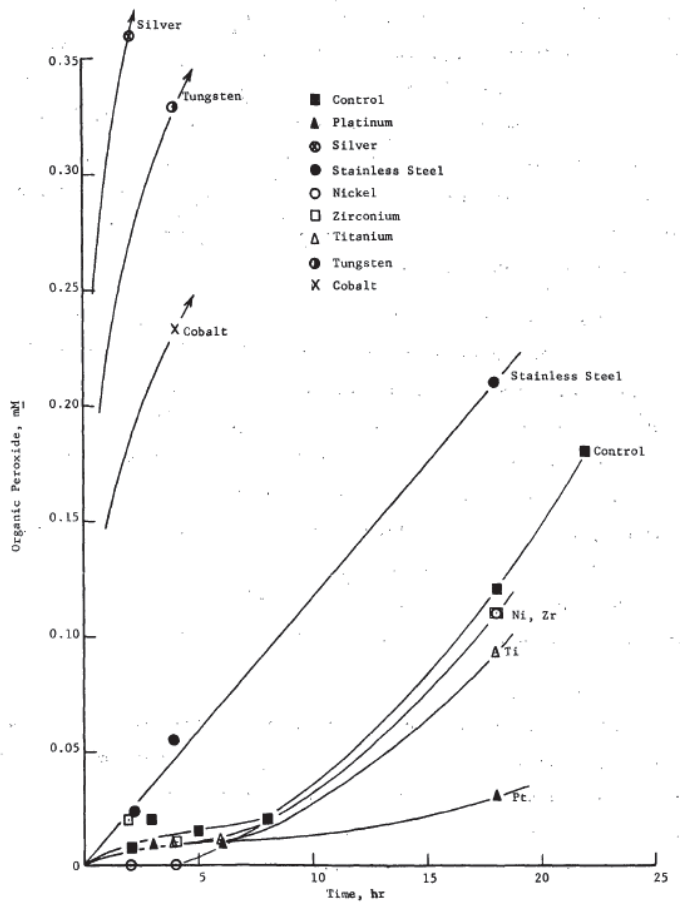

FIGURE 23. Production of organic peroxides from the reaction of methyl α-D-glucopynoside with oxygen and alkali in the presence of different metals. Reproduced from Green *et al.*[49] Copyright (1976) Georgia Institute of Technology, Institute of Paper Science and Technology, Appleton, WI, USA.

Green *et al.* [49] have suggested that the above named metals catalyze a Karasch and Fono [50] type dialkyl peroxide synthesis or termination reaction (p).

$$ROO\cdot + R'\cdot \xrightarrow{Me^n} ROOR' \qquad (p)$$

3.2 Reaction mechanisms

3.2.1 Free radical chain reaction

Entwistle *et al.* [41,42] have studied the autoxidation mechanism of uncatalized alkali cellulose and support the theory of a free radical chain mechanism for the degradation process. The theory is based on the general olefinic hydrocarbon autoxidation mechanism. The theory is supported by Kuptsan *et al.* [51]

One indication for the free radical-based autoxidation theory is the observed presence of an induction period, made on unmodified cotton with a very low copper number.[41] Furthermore, a linear proportionality between the copper number and initial autoxidation rate is identified. The authors conclude that cellulose autoxidation is initiated by a direct reaction between the reducing aldehyde groups with molecular oxygen via one-electron transfer. These are observations that are usually expected of olefinic hydrocarbon autoxidation reactions. However, this observation is not a clear proof, for the presence of an inhibitor could also induce such inhibition that is destroyed in time or inactivated.[41]

A further indication for the radical chain mechanism and the author's main evidence is the observed accelerating effect of benzenediazonium hydroxide which decomposes in benzene and hydroxyl radicals and nitrogen gas.[42] The formed hydroxyl radical is believed to be the rate accelerating component during autocatalysis.[43]

Another indication for the radical-assisted alkaline cellulose oxidation mechanism is that a surplus of used catalysts has a rather inhibitory effect on the overall process, like in case with manganese.[42,51]

The addition of complexing agents, like ethylene diamine, proved to be inhibiting the autoxidation, thus indirectly proving the intervention of transition metals in the reaction process.[42]

Mainly an increasing amount of aldehyde groups are formed during autoxidation,[41] which allows the assumption that predominantly ring hydroxyl groups are chemically reacted.

The effectiveness of autoxidation is essentially dependent on applied conditions, such as elevated temperatures of 100-120 °C or especially the presence of moisture that considerably accelerates oxidation.[41] At room temperature, pure and untreated cellulose does not oxidize. However, cellulose shows photosensitivity and degrades, particularly in the presence of dye and moisture.[41] Under elevated temperatures of >100 °C McCloskey,[52] Sinkey,[48] and Weaver [53] were, however, the opinion that radical autoxidation reactions do occur.

Below, the free radical chain reaction mechanism by Entwistle *et al.* [41,42] is presented.

Entwistle free radical chain reaction mechanism

1. Initiation

The initiation reaction is based on the correlation between copper number and initial autoxidation rate.

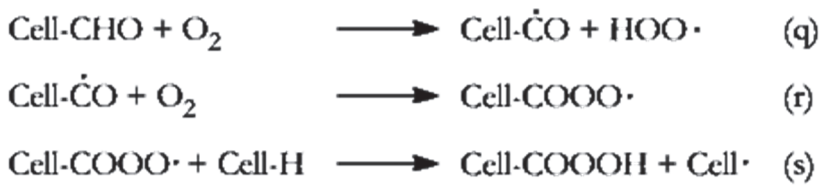

2. Propagation

This sequence is repetitive until some termination occurs.

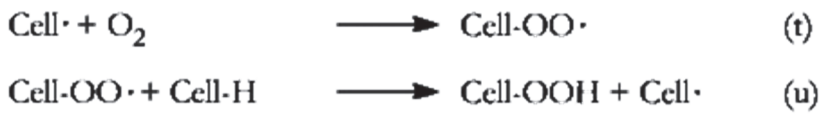

3. Autocatalysis

This is necessary to account for the autocatalytic behavior of the reaction.

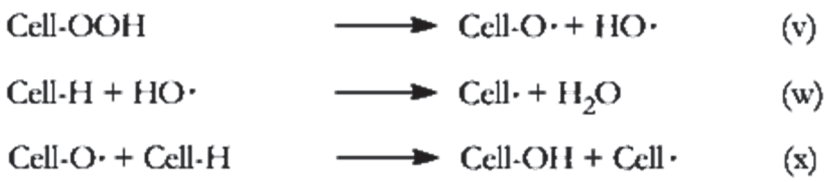

4. Possible termination reactions

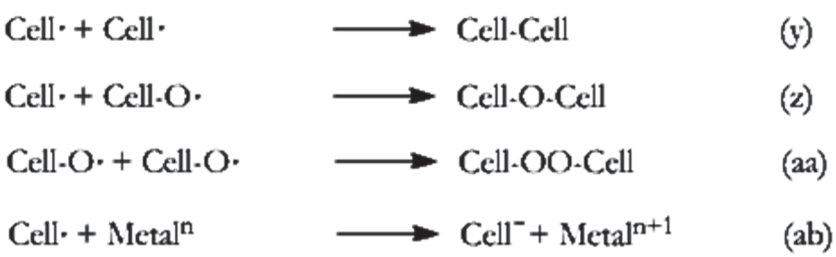

Entwistle *et al.* [41] have investigated the autoxidation rate, depending on various NaOH concentrations. The researchers observed maximum rate at a NaOH concentration of 10 M. At concentrations below 10 M, the autoxidation rate is pressure independent, but shows clear pressure dependence at concentrations

beyond 10 M NaOH (Figure 24). The authors described the observed pressure dependency by postulating the presence of two opposing factors, one factor being the increased cellulose reactivity and the other, the depression of oxygen solubility along with a NaOH concentration increase.

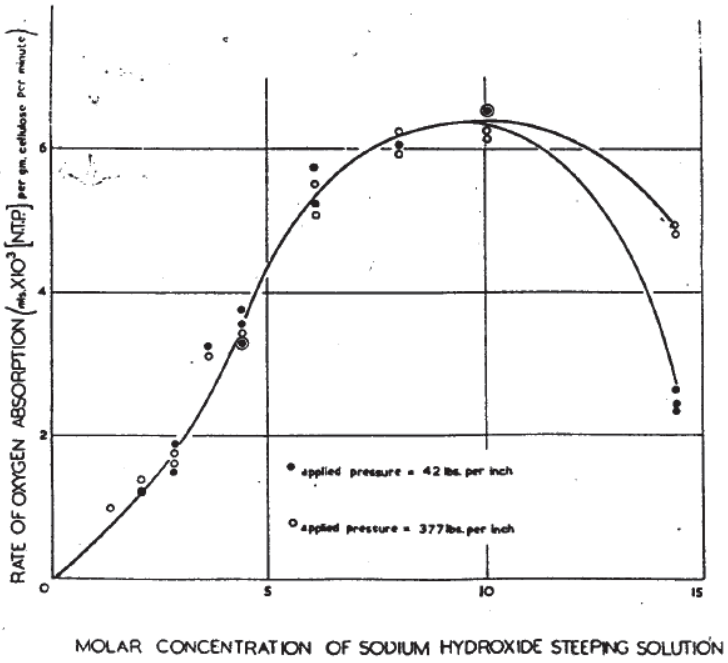

FIGURE 24. Effect of applied pressure and the concentration of sodium hydroxide steeping solution during the manufacture of alkali cellulose on the steady rate of autoxidation at 40 °C and p_{O2} = 500 mm Hg. Figure reprinted with permission from ref. 41. Copyright (1949) SAGE Publications.

Generally, water-swollen oxycelluloses are inert.[41] However, autoxidation can be followed, if they are steeped in alkali.[41] Entwistle *et al.* [41] have traced the alkali initiated cellulose autoxidation back to the enolization of the terminal α-hydroxyaldehyde.

3.2.2 Ionic electron transfer reaction mechanism

The objective of Mattor's experimental work [43] was to detect and prove the existence of hydroxyl radicals in alkaline medium and thus, provide an evidence for the validity of the free radical chain reaction mechanism postulated by Entwistle *et al.* [41,42].

The existence of hydroxyl radicals could not be confirmed and it was concluded that free hydroxyl radicals were not involved in oxidative alkaline reactions of cellulose.[43]

Mattor [43] has postulated an ionic reaction mechanism which was more consistent with observations that were made than the free radical mechanism:

1. Initiation (Peroxide formation)

The ionic autoxidation is initiated by the formation of Cannizzaro intermediates of a cellulosic aldehyde group with a hydroxyl anion in a strongly alkaline medium

In the second step, the Cannizzaro intermediate is oxidized with oxygen *via* two-electron transfer, forming a carboxylic acid end group and a hydrogen peroxide anion.

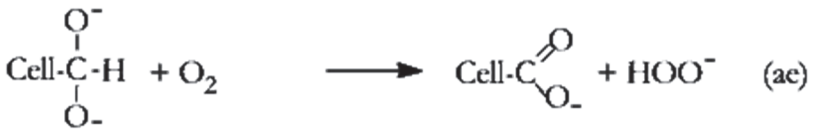

2. Propagation (Peroxide reaction on cellulose)

The *in situ* produced hydrogen peroxide is believed to be involved in three possible reactions. First, the *in situ* produced hydrogen peroxide anion can undergo a nucleophilic substitution reaction at the glycosidic linkage (scission reaction), thus highly adding to cellulose degradation and its rapid fall in DP. Second, the hydroxyl substitution reactions of any of the three hydroxyl groups on the anhydroglucose units are possible. Third, as an oxidation agent, the peroxide oxidizes any hydroxyl groups to a carbonyl group.

3.3 Reaction rates

3.3.1 Catalysts

The addition of transition metals and cations are capable of promoting hydroxyl radical formation,[54,55] while, for example, silver oxide or metallic silver might influence their decomposition in a non-radical way.[41] It is likely that transition metals positively catalyze the secondary process, meaning the decomposition, after the hydroperoxide molecule has been formed (equation (4)).[42,55] Their catalytic effect is based on the acceleration of the secondary process, meaning the propagation step. For the transition metal to be active, it must exist in a suitable valence form.[42] The results of Entwistle *et al.* [42] show that a marginal value of transition

metal presence exists in the solvent, meaning that concentrations beneath the marginal value have no reported influence on the initial rate but rather influence the subsequent rates. Beyond the marginal value, however, further additions have either no noticeable effect or even turn into inhibitors, like in case of manganese.[42]

$$ROOH + Metal^{n} \longrightarrow RO^{-} + Metal^{n+1} + HO\cdot \qquad (4)$$

Also metals with no detectable effects upon the autoxidation process were reported.[42,47,49] Green *et al.* [49] have reported nickel, titanium, and zirconium having no effect on aldose degradation.

The addition of Na_2S noticeably accelerates alkali cellulose autoxidation.[42]

The catalytic effect of transition metals like iron, cobalt, manganese, and copper on hydrogen peroxide and hydroperoxide is described in Figure 25 (Fenton's chemistry), where the peroxide is oxidized in the presence of a transition metal to form both, a hydroxyl radical and organic anion. The reduced transition metal subsequently is oxidized back into its original state by the peroxide to form an organic peroxy radical and a hydrogen ion.[46,49] However, the reactions in Figure 25 are expected to predominate under cellulose aging conditions.

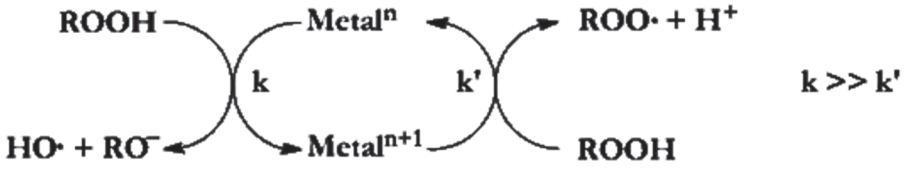

FIGURE 25. Catalytic effect of transition metals – Fenton's chemistry. Reproduced from Kadla *et al.*[46] Copyright (2001) American Chemical Society.

Nickel and titanium ion additives are believed to react under oxygen bleaching conditions according to equation (5) and not in concordance to the reactions shown in Figure 25.[45,46]

$$Metal^{n} \xrightarrow{O_2} Metal^{n+1} \qquad (5)$$

3.3.2 Inhibitors

Metals can also have inhibiting effects, by terminating the chain reaction process according to equations (6) and (7). These inhibitors are strong metallic oxidizing agents, like lead, or the noble metals, like silver and gold.[42] Also cations, like cobaltous ions cause no hydrogen peroxides to be present.[49]

$$RO\cdot + Metal^{n} \longrightarrow RO^{-} + Metal^{n+1} \quad (6)$$

$$HO\cdot + Metal^{n} \longrightarrow HO^{-} + Metal^{n+1} \quad (7)$$

Phenols and $MgSO_4$ are reported to be inhibiting the chain cleavage reaction of the cellulose chain, thus operating as stabilizing agents.[56] $MgSO_4$ has the greater inhibiting potential. As above mentioned, besides magnesium, tungsten additives were reported to share similar stabilizing characteristics.[49] In the following the postulated phenol mechanism by Chen and Lucia [56] is depicted (Figure 26).

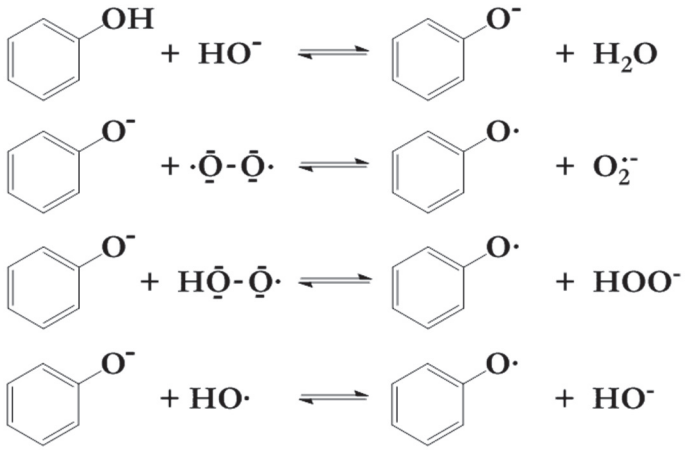

FIGURE 26. Potential mechanism for scavenging reactive free radicals by phenol under alkaline conditions. Reproduced from Chen *et al.* [56]. Copyright (2003) Springer Nature Switzerland AG. Part of Springer Nature.

Carbohydrates and alcohols are known to inhibit the chain reactions.[57] Anthraquinone, however, does not influence the radical initiation process, but rather inhibits the autoxidation process as a scavenger.[42] Borate has been suggested to combine with carbohydrates and inhibiting its reduction capability.[58] Furthermore, it should be pointed out that the combination of additives is more effective than the usage of only one.[56]

4 ALKALINE DEGRADATION OF CARBOHYDRATES

4.1 General aspects

The alkali oxidative degradation of carbohydrates proceeds according to rather complex mechanistic pathways.[49,59] It is generally assumed that carbohydrate degradation with oxygen is initiated through enolization.[58] The first generally accepted theory about alkaline cellulose degradation was made by Nef *et al.* [60] describing the reaction of monosaccharides with hydroxyl ions in two major steps; an isomerization to a α-dicarbonyl intermediate, followed by the formation of acidic degradation products through the benzilic acid type rearrangement.

Almost half a century later, Isbell [61] modified the reaction mechanism by Nef *et al.* [60], which is generally referred to as the Nef-Isbell mechanism for alkaline carbohydrate degradation visualized in Figure 27.

The first step in the Nef-Isbell mechanism is the formation of an enediol [2] from D-glucose [1] (Figure 27) via keto-enol tautomerism (i). The enediol is deprotonated [3] by hydroxide ions (ii), which results in an equilibrium of three possible intermediate anion isomers [3-5] (iii). It is important to note that the chirality at the C-2 position is abolished by the enediol [2] form, which leads to an equilibrium between glucose and mannose. Furthermore, the enolate [4] protonation in the C-2 position leads to the formation of fructose. The transformation between glucose, mannose, and fructose is called the Lobry-de-Bruyn-Alberda-van-Ekenstein transformation and is visualized in Figure 28.

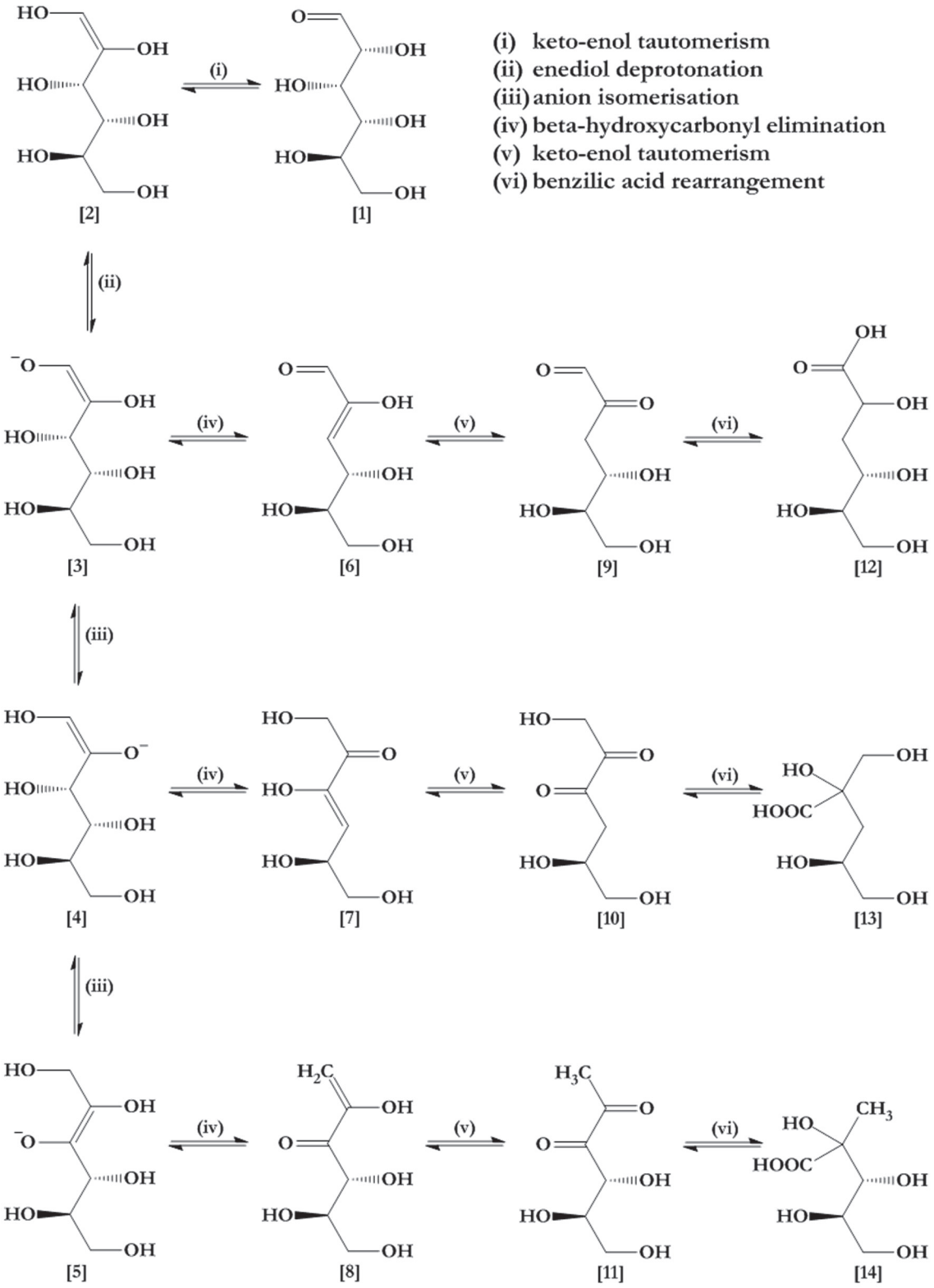

FIGURE 27. Nef-Isbell mechanism for the alkaline degradation of D-glucose. Reproduced from Knill *et al.*[62] Copyright (2003) Elsevier B.V.

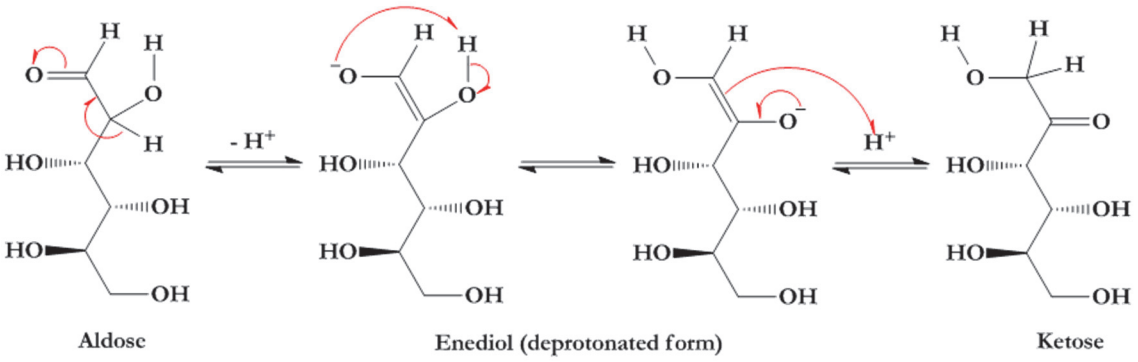

FIGURE 28. Lobry-de-Bruyn-Alberda-van-Ekenstein transformation. Figure reproduced from ref. 40. Copyright (1993) Elsevier B.V.

The enolate [5] is formed at very low rates and is present at considerably lower concentrations than the intermediates [3] and [4]. The intermediates [3-5] undergo β-hydroxycarbonyl elimination (iv) and form the diketodeoxy-glycitols [6-8], which further tautomerize (v) to the corresponding vicinal dicarbonyl compounds [9-11]. In the final stage, the vicinal dicarbonyl compounds undergo benzilic acid rearrangement (vi) to produce deoxyaldonic (saccharinic) acids [12-14], namely D-glucometasaccharinic (3-deoxy-D-*ribo*-/-*arabino*-hexonic acid) [12], D-glucoisosaccharinic (3-deoxy-2-*C*-(hydroxymethyl)-D-*erythro*-/-*threo*-pentonic acid) [13], and D-glucosaccharinic acid (2-*C*-methyl-D-*erythro*-/-*threo*-pentonic acid) [14].

4.2 Peeling reaction

A reduction of molecular mass takes place when cellulose is boiled in lowly concentrated oxygen free NaOH solutions at temperatures below 170 °C, even though the glycosidic (1→4)-linkage does not hydrolyse at such temperatures.[63,64] Purified unbleached cotton, degraded in 95 °C-hot alkali show substantial yield losses of about 20 % after three hours of treatment.[64] To describe this phenomenon, Davidson [65] proposed the so-called peeling reaction, where stepwise detachment of carbohydrate monomer end units under alkaline conditions takes place. The third row in Figure 27 above (*i.e.*, [4], [7], [10], and [13]) illustrates the "classical" alkaline peeling reaction on D-glucose (and 4-*O*-substituted D-glucose, *e.g.*, cellulose).

The alkaline peeling of terminal groups is a very fast reaction and in a up to 0.1 N NaOH solution, the rate is proportional to the NaOH concentration and temperature [49] and remains constant at higher NaOH concentrations.[66] Generally both, peeling and stopping rates are proportional to the concentration of reducing sugar end groups.[64] Furthermore, lesser ordered, amorphous cellulose forms degrade more readily than crystalline cellulose.[67] The ratio between the peeling and the stopping rate is in the rough magnitude of 50-60:1 in average [59,66] or about 90:1 [64], if initial conditions are assumed during the entire reaction period. In fact,

the peeling rate decreases with an increasing time, due to the reduced accessibility and the availability of reducing end group moieties.

4.3 Scission reaction

Alkaline scission of glycosidic linkages, also called secondary peeling, ensues when cellulose is heated above 170 °C.[62,68] An alkali concentration and temperature increase favor alkaline scission.[49] The glycosidic bond cleavage (hydrolysis) can occur on both, either the glycone or the aglycone side of the linkage and randomly, at any accessible chain position. Thus, glucose mono- and oligomers go into solution which can degrade further through peeling. The yield losses are substantially higher than at lower temperatures. Degradation proceeds also favorably at chain centers.

Kaylor *et al.* [68] have investigated cellulose scission reactions of a cellulose model compound under alkaline conditions and illustrate the scission reaction mechanisms of the glycosidic linkage. The authors propose a S_N1 and a $S_N$icB(2)-ro mechanism for the glycon, and a S_N1 and a $S_N$icB(3) mechanism for the aglycon bond scission. Possible S_N2 mechanisms have been rejected for both linkage scission cases. $S_N$icB(2)-ro refers to nucleophilic substitution by an internal nucleophile – the conjugate base of the C2 hydroxyl group involving ring opening. Accordingly, $S_N$icB(3) refers to nucleophilic substitution by an internal nucleophile – the conjugate base of the C3 hydroxyl group involving ring flip. The proposed reaction mechanisms are demonstrated in Figures 29 and 30.

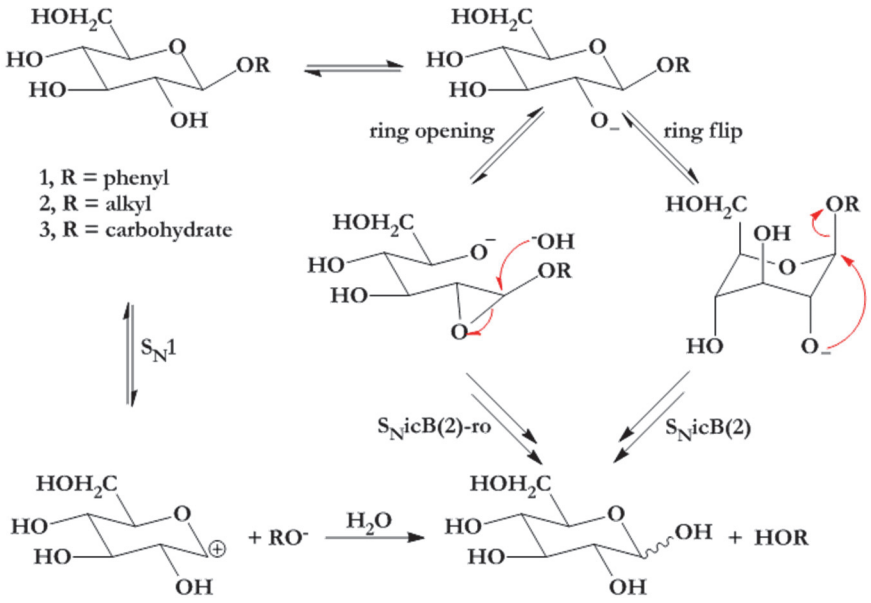

FIGURE 29. Mechanisms for glycosyl-oxygen (G-O) bond cleavage. Reproduced from Kaylor *et al.* [68]. Copyright (1994) Georgia Institute of Technology, Institute of Paper Science and Technology, Appleton, WI, USA.

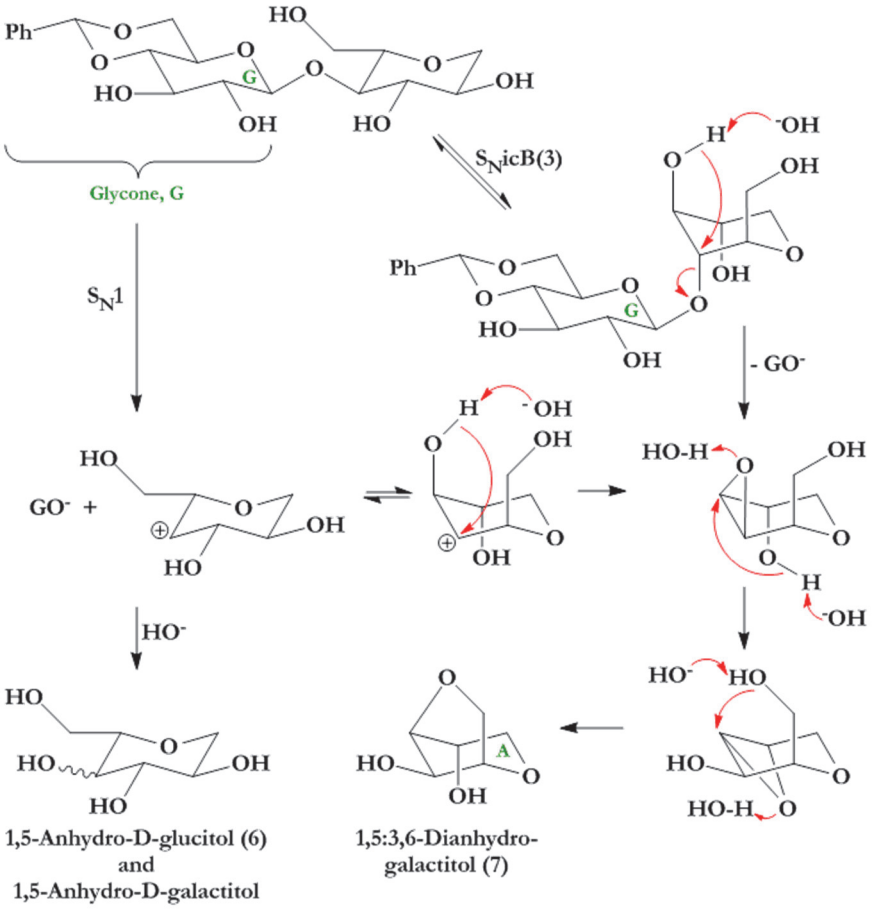

FIGURE 30. Mechanisms for oxygen-aglycone (O-A) Bond cleavage. Reproduced from Kaylor *et al.* [68]. Copyright (1994) Georgia Institute of Technology, Institute of Paper Science and Technology, Appleton, WI, USA.

4.4 Stabilization reactions

The successive peeling degradation of cellulosic molecules in alkaline solvents does not proceed *ad infinitum* unto entire polymer dissolution.[64] The stopping reaction is the competing reaction of the peeling reaction that gives rise to the formation of carboxylic acid end groups that are stable under alkaline conditions.

The formation of 3-deoxyhexonic (metasaccharinic) acid end group is an important stopping mechanism [59,62,64] and is illustrated above on D-glucose (and 4-*O*-substituted D-glucose, *e.g.*, cellulose) in the fourth row in Figure 28 above (*cf.*, [5], [8], [11], and [14]).

The reducing terminal group is also readily oxidized to alkali stable aldonic acids, like mannonic, arabinonic, and erythronic acids.[59] This process is initiated by the formation of an aldos-2-ulose (glycosone) terminal group which rearranges (the benzilic acid rearrangement) to an epimeric pair of aldonic acids. The cleavage of carbon-carbon bonds leads to shorter chained terminal groups like arabinonic, or erythronic acid end groups, as stated above. However, it should

be mentioned that the stability of these acids is drastically minimized in the presence of heavy metals which strongly catalyze their degradation.[66]

Besides the formation of the stabilizing terminal metasaccharinic acid moiety, other moieties were reported, for example, 2-*C*-methylribonic, 2-*C*-methylglyceric, and 2-deoxypentonic acid. The acidic end groups vary in their alkali and temperature stability.[66] Arabinonic acid end groups degrade already at 120 °C under oxygen and oxygen-free conditions. Gluconic and erythronic acid resist degradation up to temperatures around 150 °C.

The stopping reaction is favored by lower temperatures and Ca^{2+}. It is disfavored by Na^{+} cations.[49] Calcium cations catalyze the benzilic acid rearrangement step, and therefore increase the rate of formation of saccharinic acids.[59,69]

The peeling reaction can also be halted when the degrading chain reaches the chemically inaccessible crystalline region of the cellulose molecule and the reducing group remains unattacked.[62,70] This process is referred to as the physical stopping reaction.

4.5 Other reactions

The autoxidation of cellulose under alkaline conditions results in the formation of oxycellulose.[62] In oxycellulose, parts of free hydroxyl groups in pyranose rings (*i.e.*, at C_2, C_3, and C_6, or combinations thereof) are randomly oxidized. The carbonyl groups are labile under alkaline conditions and therefore, the subsequent chain scission can definitely occur.

Multiple chain scission reactions are possible. However, here the most important chain scission reaction is described (Figure 31).[66,71] The reaction is initialized by the oxidation of the C_2 or C_3 hydroxyl group, mainly by a hydroxyl radical (HO·). The C_2 carbonyl group and the C_3 hydroxyl group are stabilized by keto-enol tautomerism. With subsequent deprotonation of one of the hydroxyl groups at C_2 and C_3, the elimination of the alkali labile glycosidic bond at C_4 by β-alkoxy elimination takes place. The cleavage of the alkali labile glycosidic bond is also achieved by oxidation at C_3 and at C_6. The elimination results in the formation of a new reducing end group.

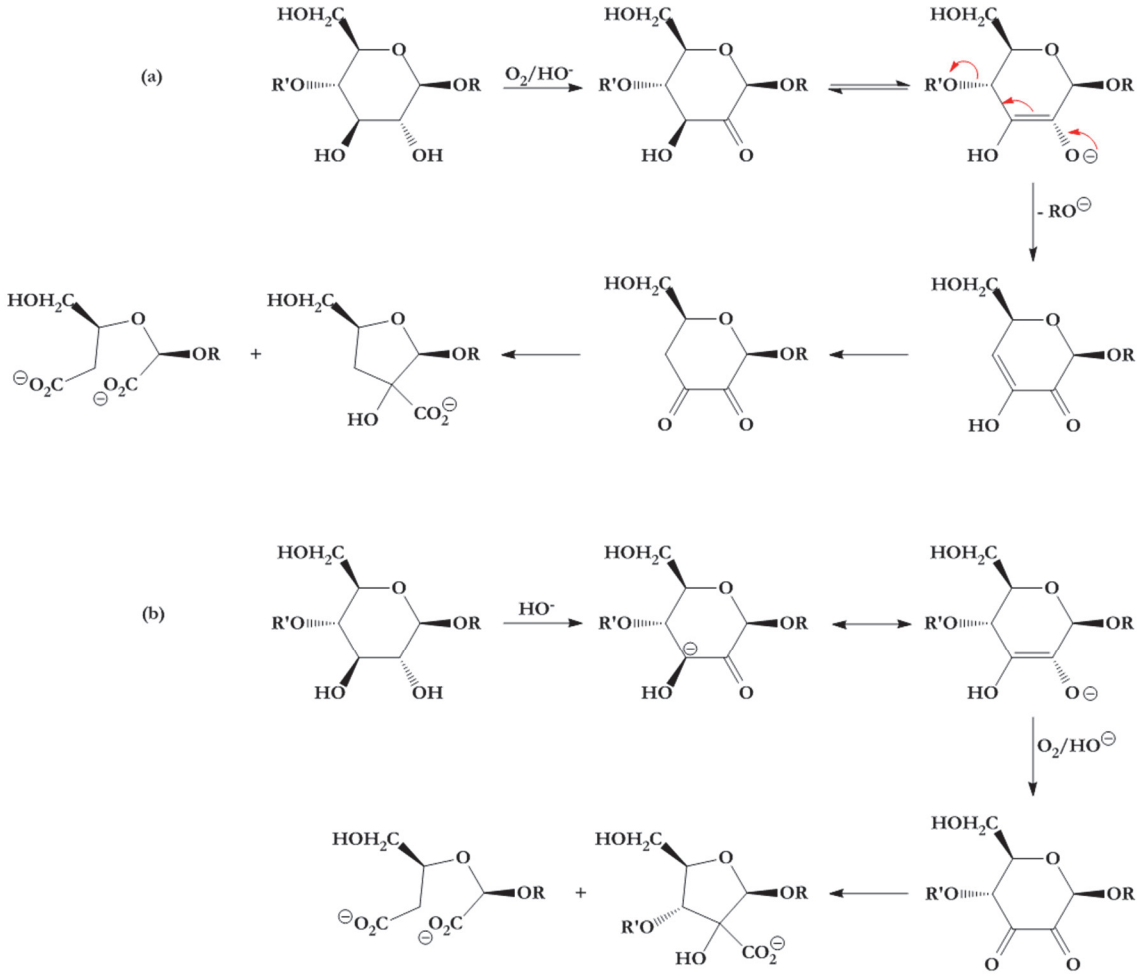

FIGURE 31. Cleavage of glycosidic bonds in polysaccharide chains (a) and oxidation of ketol structures along polysaccharide chains (b) during oxygen delignification. R and R' are part of the polysaccharide (cellulose) chain. Reproduced from Alén. [71] Copyright (2000) Fapet Oy Helsinki, Finland.

A competing reaction is observed when the 2,3-endiolate structure is oxidized into a 2,3-diketo structure (Figure 31). The 2,3-diketo structure can react further to form a furanosidic acid group or an open-chain structure with two carboxylic acid groups.

Alternatively to the benzilic acid rearrangement, the diketodeoxyglycitol intermediates [9-11] in Figure 27 can also easily fragment according to an α-diketo cleavage mechanism, yielding an aldehyde and a carboxylic acid.[59,69] An example of this is illustrated in Figure 32.

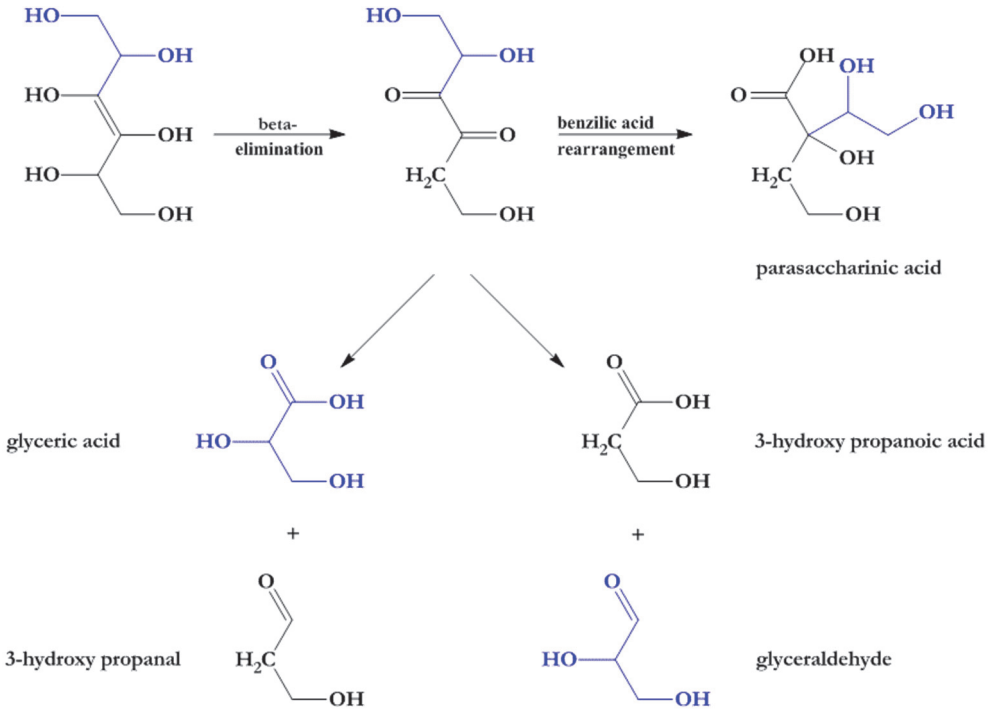

FIGURE 32. Saccharinic acids produced through 3,4-enediol formation of hexose. Reproduced from Yang *et al.*[59] Copyright (1996) Elsevier B.V.

A base-catalyzed aldol reaction occurs between two carbonyl compounds. The deprotonation of a carbonyl molecule at its C,H-acidic position leads to an enolate, which reacts as a nucleophile with a second carbonyl group, resulting in an aldol molecule (Figure 33a). Furthermore, an aldol molecule can be dehydrated, according to an $E1_{cb}$ mechanism, yielding an α,β-unsaturated carbonyl molecule. The reaction is named the base-catalyzed aldol dehydration (Figure 33b).

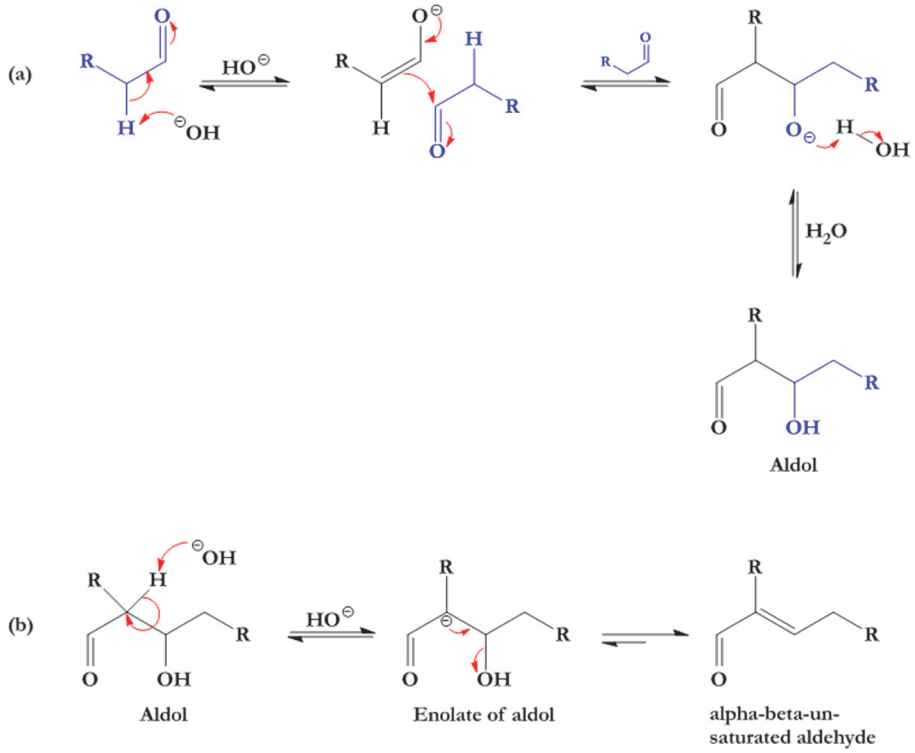

FIGURE 33. (a) Base-catalyzed aldol creation between two carbonyl compounds and (b) aldol dehydration, yielding an α,β-unsaturated carbonyl molecule. Reproduced from Clayden *et al.*[72] Copyright (2009) Oxford University Press.

Another suggested degradation route is the fragmentation of one D-glucose monomer according to the reverse aldol reaction.[66,69] In the first step, D-glucose isomerizes into D-fructose. In the second step, the reverse aldol reaction is initiated through C_4 hydroxyl group deprotonation by a hydroxyl anion, resulting in the formation of glyceraldehyde and dihydroxyacetone, which are subject to further degradation processes. Figure 34 illustrates the described reaction mechanism.

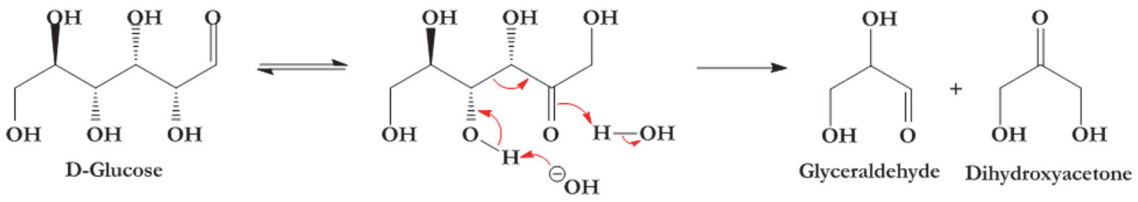

FIGURE 34. Reverse aldol reaction of D-glucose. Reproduced from Malinen *et al.* [66]. Copyright (1972) Paperi ja Puu, Finland.

5 BACKGROUND AND AIMS OF STUDY

The oxidative treatment of cellulose and cellulosic materials under alkaline conditions has been performed for more than a century. It has been applied to oxygen bleaching processes, mercerization or other conventional aging processes in order to enhance strength properties, to reduce the DP, to cause fiber swelling, and to increase material solubility.

Even though the degradation of carbohydrates and related polymeric products under alkaline conditions is widely taken place in the chemical industry, the definite reaction mechanism remains still unsolved to this day. Several reaction mechanisms have been proposed to describe the degradation process.

First systematic investigation of carbohydrate oxidation under alkaline conditions was conducted by Nef.[60] He found that at room temperature and in the presence of oxygen or hydrogen peroxide the carbohydrates, D-glucose, D-fructose, and D-mannose, mainly degraded into formic and D-arabinonic acids. He also assumed that these degradation products were formed through the formation of an 1,2-enediol and the subsequent direct breakage at the double bond. Later, Evans [73] concluded that the theory of Nef [60] explained the observations satisfactorily.

However, Schmidt [74] could show that a direct double bond cleavage would be insufficient and that the bondage split would occur at the bond between the α- and β-carbons.

Warshowsky and Sandstrom [75] investigated the influence of oxygen on glucose in potassium hydroxide and confirmed formic and D-arabinonic acid to be the major degradation products under the applied reaction conditions. The authors concluded that the theories of Nef [60] and of Schmidt [74] did not inevitably exclude one another.

First kinetic studies on carbohydrates under alkaline conditions were conducted by Bamford and Collins [76,77] who confirmed the formation of formic and D-arabinonic acids. The authors could show that carbohydrates did not react directly with oxygen but with intermediates. Furthermore, Bamford and Collins [76,77] suggested that D-glucose and D-fructose degrade by a pseudo-first-order reaction.

Up to the late sixties of the last century the number of kinetic research remained limited. A kinetic investigation is only operable when the concentrations of the carbohydrates and the reaction products are known. The number of research rose drastically during the early seventies of the last century. With the application of gas-liquid chromatography and mass spectrometry (GC-MSD) a deeper understanding about the reaction mechanism and kinetics could be gained since the qualitative and quantitative analysis of degradation products became possible.

Ackman [78] and Verhaar and de Wilt [79] described a method of analyzing acidic degradation products by means of relative molar responses of functional groups by FID.

Carbohydrates degrade into a large amount of acidic mono- to polyhydroxy degradation products. Many oxidized degradation products lactonize into various structures and their GC peaks are depicted in the gas chromatogram. It is desirable that one peak can be assigned to a single degradation product.

Petersson [80] described a method of converting the acidic degradation products into their trimethylsilyl derivatives as sodium salts. Hyppänen *et al.* [81] modified further this method and converted the acids into ammonium salts before silylation.

The aim of this study was to observe the degradation process and formed degradation products of cellobiose in NaOH (18 %) under oxygen and nitrogen atmospheres at varying pressures and degradation temperatures. The degradation of cellobiose was carried out at room temperature (20 °C), 35 °C, and 50 °C. The pressure was set at 1 (atmospheric pressure, *i.e.*, open system with 0.2 % oxygen partial pressure in oxidative degradation), 5, and 10 bar. Samples were taken after 2, 4, 6, 8, and 24 hours. The alkaline degradation was carried out in a stainless steel micro reactor. Samples were analyzed with GC-FID. Degradation products were identified by GC-MSD. The goal was, based on these versatile data, to clarify the reaction mechanisms and to study the reaction kinetics.

6 EXPERIMENTAL

6.1 Chemicals

The following chemicals and materials were used for the alkaline cellobiose degradation reactions and GC-FID and GC-MSD analyses: D-(+)-cellobiose (Sigma-Aldrich), xylitol (Fluka), D-(+)-mannose (Fluka), D-(+)-glucose anhydrous (Fluka), L-(+)-arabinose (Fluka), D-(+)-galactose (Fluka), sodium hydroxide (50 %) (J. T. Baker), potassium hydroxide (Fluka), hydrochloric acid (32 %) (Sigma-Aldrich), ammonium hydroxide (25 %) (Sigma-Aldrich), acetone (Sigma-Aldrich), hexane (Rathburn), Milli-Q water (Millipore), Amberlite IRC-50 (H) ion exchange resin (Alfa Aesar; Fluka), *N,O*-bis(trimethylsilyl)trifluoroacetamide (BSTFA) + 1 % trimethylchlorosilane (TMCS) silylation agent (Regis Technologies), and pyridine (VWR International).

6.2 Laboratory equipment

The following laboratory equipment was used: A Parr Series 4590 micro reactor with a Parr Series 4841 temperature controller (Parr Instrument Company) (Figure 35 depicts the updated 4597 micro reactor with the 4848 temperature controller version), a magnetic hot plate stirrer (VWR International), an adjustable micropipette (200-1000 µL) (Finnpipette), borosilicate glass ion exchange resin columns (50 mL) (Laborexin Oy), pear shaped flasks (100 mL), rotary evaporators (VWR International; Heidolph), a flask shaker (Stuart Scientific Flask Shaker SF1), GC auto sampler vials (2 mL), GC-MSD (a Hewlett Packard Agilent 6890 Series GC System, a 7683 Series Injector, a 5973 *Network* Mass Selective Detector; GC-FID (a Hewlett Packard Agilent 6850 Series GC System, a 6850 Series Auto Sampler.

FIGURE 35. A Parr 4597 micro reactor, update of a 4890 micro reactor with the fixed head, 50 mL volume, and a 4848 reactor controller. Courtesy of Parr Instrument Company, Moline, IL, USA.[82]

6.3 Internal standard stock solution

In the GC analyses, xylitol was used as an internal standard (ISTD). In order to prepare a xylitol internal standard stock solution (1 %), 0.0500 mg xylitol was weighed into a 50 mL volumetric flask, dissolved in Milli-Q water, and filled up to flask marking. The stock solution was stored in a refrigerator.

6.4 Cation exchange resin

An ion exchange column (2000 mL) with a closed valve is filled with new or used cation exchange resin (100 mL). About 300 mL Milli-Q water is added and the column valve was opened, allowing the washing water to drain with a velocity of about 20 drops per minute. During the regeneration process, the drain velocity is retained unchanged. When the water level has reached the upper resin level, 600 mL 1 M HCl is given into the column (in three steps of 200 mL) to charge the resin with H^+ cations. During this procedure the resin volume was decreased. After HCl regeneration, the resin was regenerated with 1200 mL (3 x 400 mL) NH_4OH (4.5 %) to charge the resin with ammonium cations. The resin volume

was increased to its original state. After the regeneration process, excess ammonium content was removed with 900 mL (3 x 300 mL) Milli-Q water. Resin was stored in a reclosable plastic container.

6.5 Cellobiose degradation

About 37 g sodium hydroxide (18 %) was used in the micro reactor for the degradation of cellobiose. For the degradation reactions under nitrogen atmosphere, the solution was purged with helium for about 30 minutes. For oxidative degradation reactions the untreated NaOH solution was utilized. The desired reaction condition was adjusted by setting the water bath temperature and pressure. The reactor was steeped into the water bath and tempered for several minutes. The magnetic stirrer rotated with a velocity of 250 rpm. After setting up the reaction condition, around 0.1100 mg (3000 ppm) cellobiose were given into the reactor and the timer was started. The reactor was tightly screwed up and the valve to the oxygen or nitrogen gas cylinder opened. Reactions under atmospheric pressure were conducted with a closed gas cylinder valve and an open reactor degassing valve. Sampling occurred after 2, 4, 6, 8, and 24 hours by opening the reactor. A sample volume of around 3 mL were taken with a pipette and given into a test tube. After sampling, the reactor was resealed and purged accordingly for a minute with nitrogen or oxygen gas from the gas cylinder. After purging the degassing valve was closed to resume the pressurized reaction.

Into each column, 1 mL of the sample was given, filled with Amberlite IRC-50(NH_4^+) cation ion exchange resin, 5 cm in height, in order to exchange sodium cations with ammonium cations. This procedure avoided the lactonization of hydroxy acids. The eluate was collected in a pear shaped flask (100 mL). The column valves were opened so far to allow the eluent to pass the resin with a velocity of about 20 to 25 drops per minute. When the sample reached the resin level, 1 mL of ISTD (1/10 dilution of stock solution at room temperature) was added into the column. The resin was successively washed three times with 10 mL Milli-Q water when the sample reached resin level.

The flask content was dried with a rotary evaporator to complete dryness. The samples were disposed of water residues by adding about 5 mL of acetone and blow-dried under nitrogen gas stream.

The dried residue was silylated for GC analysis by adding 1 mL of potassium hydroxide-dried pyridine and 500 µL of silylation agent and was shaken vigorously for 45 minutes. The functional groups were derivatized by the silylation agent to decrease polarity and to increase volatility and thermal stability.

The flask content was then transferred into GC auto sampler vials and analyzed on GC-FID. Further, one of the two samples was depicted to be analyzed on GC-MSD for the identification of degradation products.

6.6 Quantitative analysis of cellobiose degradation products

The quantitative analysis of the degradation products of cellobiose was based on the calculated relative molar response (RMR) method by Verhaar and de Wilt.[79] The FID signal intensity varies based on each molecules size and the amount and nature of functional groups. The RMR value expresses the FID signal intensity of a molecule. This method basically explains the relation of FID response and silylated functional groups of polyhydroxy acid compounds. The RMR response depends on the nature and quantity of the functional groups of a molecule passing through the FID. In Table 1 the molar responses for the relevant silylated functional groups are listed. Table 2 indicates the RMR values for the degradation products determined. Based on the response-active fragments that passed through the FID, compared to the FID response of the standard xylitol, a relative response factor (RF) for each degradation product could be determined. For this reason, the RF described the relation of the compound FID response to the xylitol internal standard. By using ISTD, the compound areas could be put in relation to the standard area and based on the known ISTD amount in the sample the amount of the compound could be calculated.

TABLE 1. Relative molar responses of silylated (-OTMS) functional groups. Reproduced from Verhaar *et al.*[79] Copyright (1969) Elsevier B.V.

H_2C-OTMS	HC-OTMS	C-OTMS	CO-OTMS
370	355	340	290

CO-O-C	H_3C-	H_2C-
50	100	100

$$RMR(X) = \frac{(molar\ response\ of\ compound\ X)}{y^{-1}(molar\ response\ of\ a\ normal\ alkaline\ with\ y\ carbon\ atoms)} \cdot 100 \quad (8)$$

$$RF\ (X) = \frac{RMR(ISTD)}{M(ISTD)} \cdot \frac{M(X)}{RMR(X)} \quad (9)$$

$$\frac{RMR(ISTD)}{M(ISTD)} = \frac{1805}{152.1448\ g/mol} = 11.8637\ mol/g \quad (10)$$

$$conc(X) = RF \cdot \left(\frac{Sample\ Area\ [pA{\cdot}s]}{Sample\ Volume\ [mL]} \cdot \frac{ISTD\ [\mu g]}{ISTD\ Area\ [pA{\cdot}s]}\right) \quad (11)$$

TABLE 2. The calculated RMR and RF values of the quantitatively evaluated degradation products (listed according to their appearance in the chromatogram; for chemical structures, see Figures 36-38)

#	Degradation product	RMR	RF
1	Glycolic acid	660	1.37
2	Lactic acid	745	1.43
3	3-Hydroxypropanoic acid	760	1.41
4	Glyceric acid	1015	1.24
5	Methylglyceric acid	1100	1.30
6	2-Hydroxybutanoic acid	845	1.46
7	3,4-Dihydroxybutanoic acid	1115	1.28
8	2,4-Dihydroxybutanoic acid	1115	1.28
9	Erythronic acid	1370	1.18
10	Threonic acid	1370	1.18
11	2,5-Dihydroxypentanoic acid	1215	1.31
12	4,5-Dihydroxypentanoic acid	1215	1.31
13	2-Deoxypentonic acid	1470	1.21
14	3-Deoxy-*erythro*-pentonic acid	1470	1.21
15	3-Deoxy-*threo*-pentonic acid	1470	1.21
16	Arabinonic acid	1725	1.14
17	Anhydroisosaccharinic acid	1160	1.66
18	α-Glucoisosaccharinic acid	1785	1.20
19	α-Glucoisosaccharino-1,4-lactone	1230	1.56
20	β-Glucoisosaccharinic acid	1785	1.20
21	β-Glucoisosaccharino-1,4-lactone	1230	1.56
22	3-Deoxyhexono-1,4-lactone	1230	1.56
23	Gluconic acid	2080	1.12
24	Mannonic acid	2080	1.12
25	Oxalic acid	580	1.84
26	Tartronic acid	935	1.52
27	Methyltartronic acid	1020	1.56
28	Succinic acid	780	1.80
29	Malic acid	1035	1.54
30	2-Hydroxyglutaric acid	1135	1.55
31	3,4-Dideoxy-*erythro*-hexaric acid	1490	1.42
32	3,4-Dideoxy-*threo*-hexaric acid	1490	1.42
33	Glucose	1790	1.18
34	Mannose	1790	1.18
35	Fructose	1805	1.18
36	Cellobiose	3225	1.26

6.7 Degradation product identification

GC-MSD spectra were used to identify the degradation products. The following sources were used to identify the degradation products of cellobiose. The Wiley database that was already available on the GC-MSD device preinstalled. In addition, the mass spectra collection by Niemelä [83] was used.

6.8 GC-FID

The GC column was a Supelco Equity-5 fused silica capillary column (phase: bonded; poly(5 % diphenyl/95 %dimethylsiloxane – 30 m x 0.32 mm ID x 0.25 µm). The injection port temperature was 290 °C and the detector temperature was 280 °C. In this work, the following method was applied. The initial oven temperature was 70 °C with 5 minutes holding time. The temperature was raised to 235 °C at a rate of 2 °C/min without holding time. Subsequently, the oven temperature was raised further to 290 °C at a rate of 70 °C/min with a final holding time of 15 minutes. The total run time was 108 minutes. After the run the oven was cooled down to 50 °C. Between the samples the column was purged with pyridine to remove possible residues attached to the phase. Each analysis series was started and finished with two pyridine purge-runs.

In the following the GC-FID settings are presented that were used during the runs:

Injector. Injection volume, 1.0 µL. Syringe size, 10.0 µL.

	Preinjection	Postinjection
Sample	3	
Acetone	3	5
Hexane	3	5
Pumps	3	

Inlet. EPC-Split-Splitless Inlet. Pulsed Splitless mode. N_2 gas.

ON		Setpoint
☒	Heater, °C	290 °C
☒	Pressure, psi	2.79
☒	Total flow, mL/min	102

Injection pulse pressure, 21.8 psi until 1.00 min. Purge flow to split vent, 98.6 mL/min at 1.00 min.

☒	Gas saver	20.0 mL/min.	2.00 min

Column. N_2 flow, 0.5 mL/min. Average velocity, 11 cm/s. Pressure, 2.79 psi. Mode, constant flow. Source, inlet. Outlet, detector. Outlet psi, ambient.

Oven. Maximum oven temperature, 325 °C. Equilibration min, 0.50 min.

Oven ramp	°C/min	Next °C	Hold min	Runtime
Initial		60	5.00	5.00
Ramp 1	2.00	235	0.00	92.50
Ramp 2	70.00	290	15.00	108.29
Ramp 3	0.00			
Postrun		50	0.00	108.29

Detector. Detector, FID.

ON		Actual Setpoint
☒	Heater, °C	300
☒	H_2 flow, mL/min	40.0
☒	Air flow, mL/min	450
☒	Makeup flow	N_2, 9.5
↳	☒Const. col & makeup, mL/min	10.0

Signal.
Signal: ⦿ Det. Source, detector. Data rate, 20 Hz. Minimum peak width, 0.01 min. ☒ Save data ⦿ all. Start at 0.00 min. Stop at 108.29 min.

The samples 093 to 252 were analyzed with a column nitrogen gas flow velocity of 0.9 mL/min. The subsequent samples, *i.e.*, 253-648, were analyzed with a gas flow velocity of 0.5 mL/min. The velocity reduction was applied in order to achieve a better peak separation in the latter part of the chromatogram where the majority of the degradation products concentrated.

6.9 GC-MSD

A Hewlett Packard Agilent 6890 Series GC System with a 7683 Series Injector, and a 5973*Network* Mass Selective Detector unit was used to carry out the identification of the degradation products. The used column was an Agilent J&W HP-5 ms (19091s-433) with a cross-linked non-polar (5 %-phenyl-)methylpolysiloxane phase (30 m x 0.25 mm ID x 0.25 μm).

The GC-MSD analysis of the samples was carried out after the GC-FID analysis was accomplished. In the beginning of the experimental series, samples with most peaks were analyzed with GC-MSD. However, it was discovered that the different reaction conditions can cause significant variations in the formation amount and the class of degradation products. Therefore, after sample 196, every condition and time was analyzed. One of the two samples of each condition was chosen for the more detailed GC-MSD analysis.

In the following, the GC-FID settings are presented that were used during the runs:

Oven.

Oven ramp	°C/min	Next °C	Hold min	Runtime
Initial		60	5.00	5.00
Ramp 1	2.00	235	0.00	92.50
Ramp 2	70.00	290	15.00	108.29
Ramp 3	0.00	(off)		

Front Inlet. Mode, pulsed splitless. Initial temp. value: 290 °C (on). Pressure, 8.24 psi (on). Pulse pressure, 15.0 psi. Pulse time, 1.00 min. Purge flow, 50.0 mL/min. Purge time, 1.00 min. Total flow, 54.0 mL/min. Gas saver, On. Saver flow, 20.0 mL/min. Saver time, 2.00 min. Gas type, helium.

Column. Capillary column. Model number, HP 19091S-433. Max temperature, 325 °C. Nominal length, 30.0 m. Nominal diameter, 250.00 µm. Nominal film thickness, 0.30 µm. Mode, constant flow. Initial flow, 1.0 mL/min. Nominal initial pressure, 8.25 psi. Average velocity, 37 cm/s. Inlet, front inlet. Outlet, MSD. Outlet pressure, vacuum.

7 DEGRADATION PRODUCTS

7.1 Chemical structures

The degradation of cellobiose resulted in the formation of 37 identified degradation products of which 33 were quantitatively evaluated. Four degradation products were qualitatively identified, *i.e.*, ribose, arabinose, ribonic acid, and galactose. The former three degradation products were rarely formed or appeared in trace amounts. Galactose, however, was formed in noticeable amounts, but its quantitative evaluation was not possible, due to peak overlapping with the β-glucoisosaccharinic acid (3-deoxy-2-*C*-(hydroxymethyl)-D-*erythro*-pentonic acid, β-ISA) peak. Additionally, the unlactonized part of glucometasaccharinic acid (3-deoxyhexonic acid, MSA) overlapped with the β-ISA peak, rendering its quantification impossible. The lactonized ISA fraction was considered in the quantitative result evaluation.

The 33 quantitatively evaluated degradation products are composed of 22 monocarboxylic acids, 8 dicarboxylic acids, as well as glucose, mannose, and fructose. The degradation products are depicted in Figures 36–38.

Monocarboxylic acids

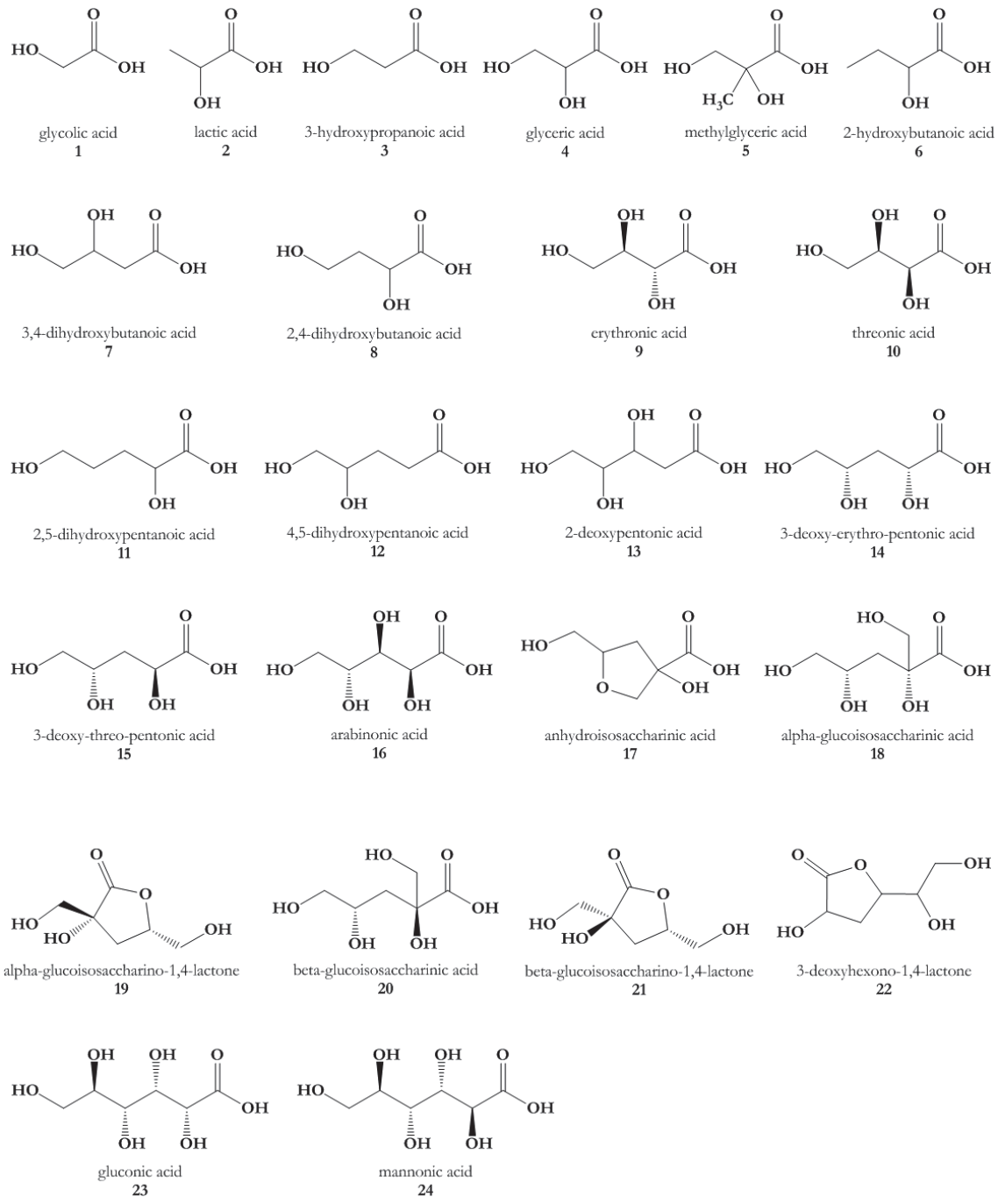

FIGURE 36. Quantitatively evaluated monocarboxylic acids.

Dicarboxylic acids

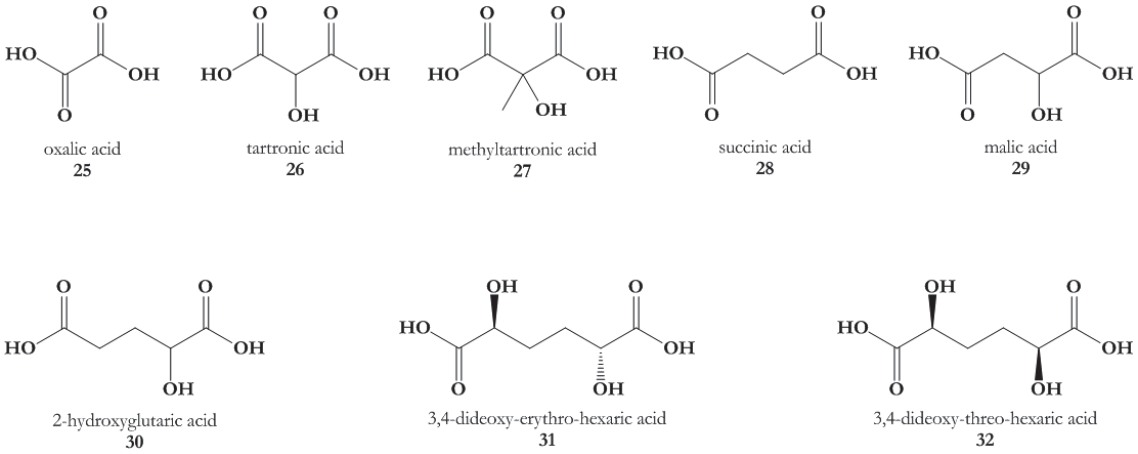

FIGURE 37. Quantitatively evaluated dicarboxylic acids.

Non-acidic degradation products and cellobiose

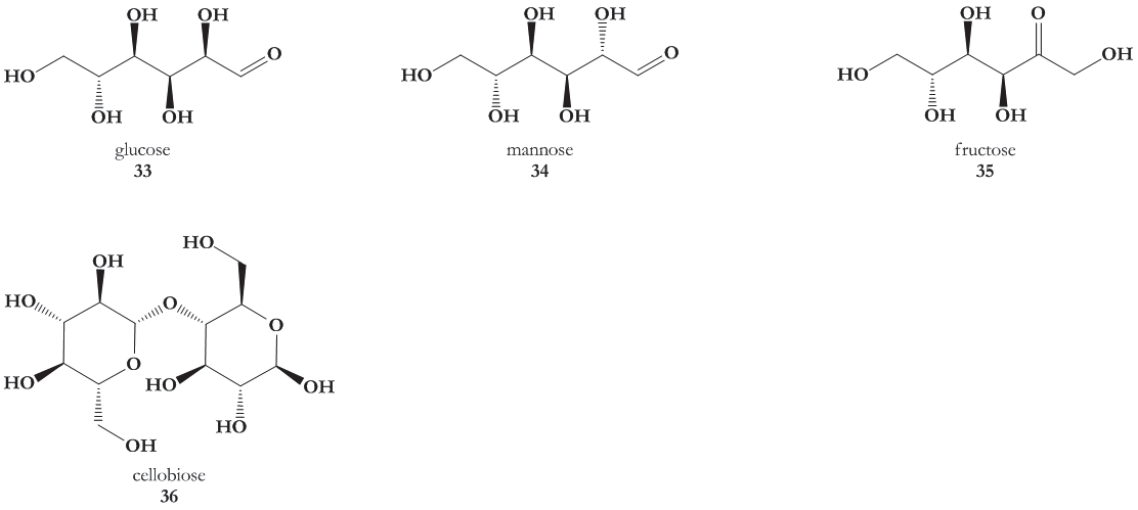

FIGURE 38. Quantitatively evaluated non-acidic degradation products and cellobiose.

7.2 Oxidative and non-oxidative degradation products

Cellobiose was comparatively degraded in both, oxygen and nitrogen atmospheres and at the same temperature and gas pressure conditions in order to obtain detailed understanding about what degradation products were formed in oxygen-free conditions and how increasing pressures of oxygen and rising temperatures would influence the degradation process.

Twelve degradation products were quantitatively evaluated in nitrogen atmosphere (Table 3).

The concentration of non-oxidative degradation products declined in oxygen atmosphere and the formation of 21 further degradation products was favored (Table 4).

The terms "non-oxidative degradation products" or simply "non-oxidatives" refer to degradation products that are formed through the interaction of hydroxyl anions only, without the intervention of oxygen molecules. Correspondingly, "oxidative degradation products" or "oxidatives" are those that are formed with additional influence of oxygen. The main degradation products are in bold font. Degradation products in noticeable but lower concentrations are underlined in Tables 3 and 4.

TABLE 3. Non-oxidative degradation products ("non-oxidatives")

#	Degradation product	#	Degradation product
2	**Lactic acid**	18 & 19	**α-Glucoisosaccharinic acid**
5	Methylglyceric acid	20 & 21	**β-Glucoisosaccharinic acid**
6	2-Hydroxybutanoic acid	22	3-Deoxyhexono-1,4-lactone
8	2,4-Dihydroxybutanoic acid	33	**Glucose**
11	2,5-Dihydroxypentanoic acid	34	Mannose
17	Anhydroisosaccharinic acid	35	Fructose

TABLE 4. Oxidative degradation products ("oxidatives")

#	Degradation product	#	Degradation product
1	**Glycolic acid**	23	Gluconic acid
3	3-Hydroxypropanoic acid	24	Mannonic acid
4	**Glyceric acid**	25	Oxalic acid
7	**3,4-Dihydroxybutanoic acid**	26	Tartronic acid
9	Erythronic acid	27	Methyltartronic acid
10	Threonic acid	28	Succinic acid
12	4,5-Dihydroxypentanoic acid	29	Malic acid
13	2-Deoxypentonic acid	30	2-Hydroxyglutaric acid
14	**3-Deoxy-*erythro*-pentonic acid**	31	3,4-Dideoxy-*erythro*-hexaric acid
15	**3-Deoxy-*threo*-pentonic acid**	32	3,4-Dideoxy-*threo*-hexaric acid
16	Arabinonic acid		

Figures 39 and 40 illustrate the typical behavior of non-oxidative and oxidative degradation products, respectively. Figure 39 shows the concentration of β-glucoisosaccharinic acid at room temperature after 2, 4, 6, 8, and 24 hours, under various gas type and pressure conditions. At all degradation times more β-glucoisosaccharinic acid was formed in nitrogen gas than in the presence of oxygen, indicating its formation rate decrease in favor of other oxidative degradation products like glycolic acid (Figure 40).

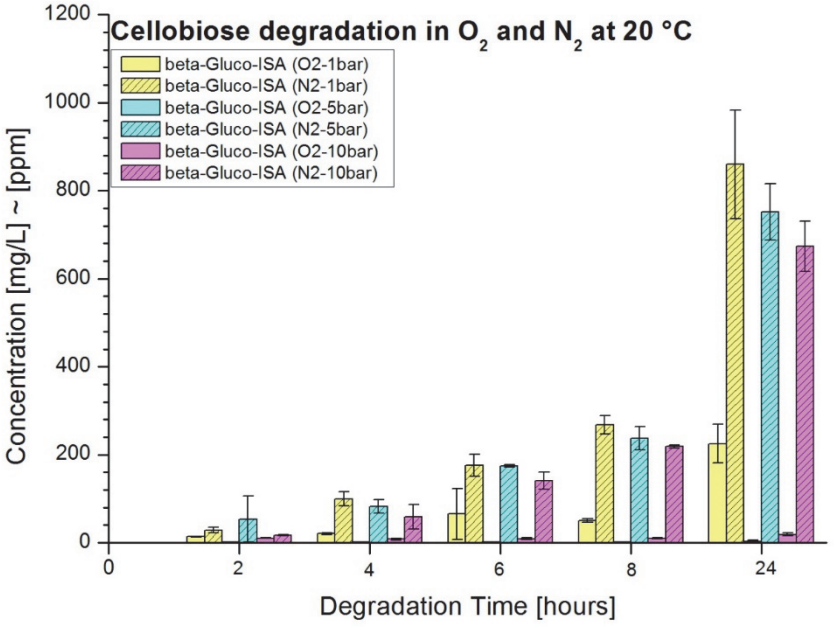

FIGURE 39. Formation of β-glucoisosaccharinic acid at room temperature.

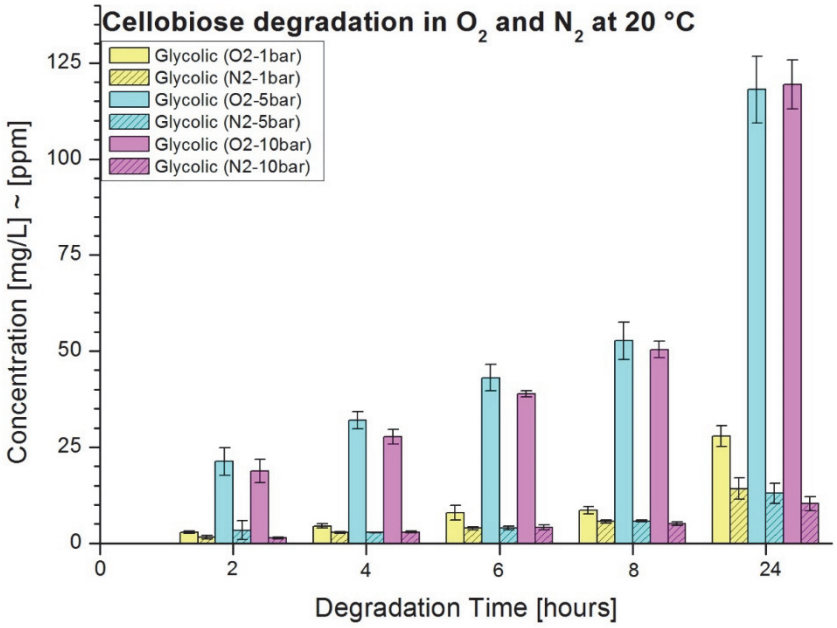

FIGURE 40. Formation of glycolic acid formation at room temperature.

7.3 Product formation

7.3.1 Degradation at 20 °C

Tables 5 and 6 illustrate the amount of non-oxidatives and oxidatives at room temperature (about 20 °C).

TABLE 5. Influence of oxygen and nitrogen pressure on the formation of *non-oxidative* degradation products at room temperature [a, b, c]

	NITROGEN			OXYGEN		
Time [hours]	1 bar	5 bar	10 bar	Air	5 bar	10 bar
0	**0.0** 100.0	**0.0** 100.0	**0.0** 100.0	**0.0** 100.0	**0.0** 100.0	**0.0** 100.0
2	**4.9** 85.7	**7.3** 94.3	**4.3** 83.6	**4.0** 95.2	**5.3** 91.2	**4.7** 92.9
4	**12.2** 77.9	**11.5** 76.4	**9.9** 77.3	**5.0** 94.5	**6.6** 88.4	**5.8** 81.7
6	**19.6** 66.6	**21.5** 76.0	**17.1** 70.5	**8.8** 88.8	**7.9** 86.7	**7.5** 79.0
8	**28.2** 58.8	**26.4** 68.1	**25.3** 64.6	**9.1** 89.3	**9.3** 81.4	**9.2** 76.3
24	**77.9** 16.9	**70.7** 22.8	**65.3** 23.0	**30.6** 65.5	**16.0** 63.0	**16.1** 52.1

[a] The figures are given as per cent of the initial cellobiose amount. .
[b] The figures in bold font illustrate the sum of measured amount of non-oxidative degradation products.
[c] The figures in normal font illustrate the amount of cellobiose.

Nitrogen gas and nitrogen gas pressure had only small to no gas specific effects on cellobiose degradation. The gas pressure increase caused slightly decreasing amounts of non-oxidative degradation products after the degradation time of 24 hours.

The absence of oxygen caused cellobiose to degrade unhindered into non-oxidative degradation products. Therefore, about 80 % of cellobiose was degraded into non-oxidatives after the degradation time of 24 hours.

A surprising observation was that the degradation of cellobiose got noticeably hindered in oxygen atmosphere. Only 35-50 % of the initial cellobiose was degraded after 24 hours.

After a degradation time of 24 hours it was observed that the oxygen content in air and at room temperature caused the formation of rather small amounts of oxidative degradation products. The pressure increase to 5 bar and 10 bar increased the oxidative degradation product content up to 16 % for both pressures. While 30 % non-oxidative degradation products were formed in air, at 5 bar and 10 bar about 16 % were formed.

TABLE 6. Influence of oxygen and nitrogen pressure on the formation of *oxidative* degradation products at room temperature [a, b, c]

	NITROGEN			OXYGEN		
Time [hours]	1 bar	5 bar	10 bar	Air	5 bar	10 bar
0	**0.0** 100.0	**0.0** 100.0	**0.0** 100.0	**0.0** 100.0	**0.0** 100.0	**0.0** 100.0
2	**0.2** 85.7	**0.5** 94.3	**0.2** 83.6	**0.4** 95.2	**2.4** 91.2	**2.5** 92.9
4	**0.5** 77.9	**0.5** 76.4	**0.4** 77.3	**0.7** 94.5	**3.9** 88.4	**3.5** 81.7
6	**0.7** 66.6	**0.9** 76.0	**0.7** 70.5	**1.2** 88.8	**5.3** 86.7	**4.7** 79.0
8	**1.0** 58.8	**1.1** 68.1	**1.1** 64.6	**1.2** 89.3	**6.6** 81.4	**6.2** 76.3
24	**3.5** 16.9	**3.3** 22.8	**2.5** 23.0	**4,2** 65.5	**15.9** 63.0	**15.9** 52.1

[a] The figures are given as per cent of the initial cellobiose amount.
[b] The figures in bold font illustrate the measured amount of oxidative degradation products.
[c] The figures in normal font illustrate the amount of cellobiose.

The presence of oxygen in air noticeably inhibited cellobiose from being degraded at room temperature. While about 30 % non-oxidative degradation products were formed in air, the percentage halved into oxidative and non-oxidative degradation products at 5 bar and 10 bar oxygen pressure, whereas the measured cellobiose content was similar to all three oxygen gas pressures. It could be concluded that if sufficient oxygen was dissolved in NaOH, like at 5 bar and 10 bar oxygen pressure, then oxidative degradation products formed at expense of non-oxidatives. This observation would confirm the observations described by Malinen [84] that both, the main oxidative and the main non-oxidative degradation products except 3-deoxypentonic acid derive from the same intermediate, namely 4-deoxy-D-*glycero*-2,3-hexodiulose:

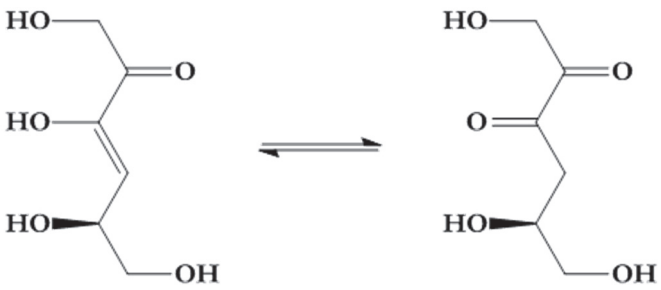

4-Deoxy-D-*glycero*-2,3-hexodiulose

7.3.2 Degradation at 35 °C

Tables 7 and 8 illustrate the amount of non-oxidatives and oxidatives at 35 °C.

TABLE 7. Influence of oxygen and nitrogen pressure on the formation of *non-oxidative* degradation products at 35 °C [a, b, c]

	NITROGEN			OXYGEN		
Time [hours]	1 bar	5 bar	10 bar	Air	5 bar	10 bar
0	**0.0** 100.0	**0.0** 100.0	**0.0** 100.0	**0.0** 100.0	**0.0** 100.0	**0.0** 100.0
2	**34.1** 58.6	**28.6** 62.8	**28.6** 61.7	**21.9** 64.5	**28.4** 67.4	**29.3** 57.6
4	**60.1** 31.2	**51.8** 37.2	**54.0** 36.4	**43.3** 43.3	**46.8** 41.8	**39.9** 35.4
6	**70.7** 16.3	**65.9** 22.2	**67.5** 18.0	**57.9** 26.8	**52.3** 27.4	**35.7** 26.9
8	**78.0** 8.5	**74.5** 13.0	**73.9** 11.5	**66.7** 17.2	**50.2** 20.4	**27.8** 23.5
24	**84.2** 0.5	**83.8** 1.2	**82.6** 0.8	**74.3** 1.4	**23.0** 11.5	**13.4** 15.9

[a] The figures are given as per cent of the initial cellobiose amount.
[b] The figures in bold font illustrate the measured amount of non-oxidative degradation products.
[c] The figures in normal font illustrate the amount of cellobiose.

In nitrogen atmosphere the pressure increase caused the formation of decreased amounts of non-oxidative degradation products. Cellobiose was entirely degraded after 24 hours and about 80 % non-oxidative degradation products were formed. Oxidatives were found in trace amounts.

In contrast to the degradation in 20 °C, the inhibiting effect of oxygen upon cellobiose degradation was observed to a lesser extent at 35 °C, being overshadowed by the increased rate of the formation of non-oxidative degradation products. In air the inhibiting effect of oxygen caused 10 % less non-oxidatives to be formed in comparison to the degradation in nitrogen.

The cellobiose concentrations in oxygen were also 10 % higher than those in nitrogen. Furthermore, oxidative degradation products in air were formed in trace amounts. Their concentrations were in a similar concentration range to the nitrogen atmosphere amounts. This indicated that the oxygen amount in air and at 35 °C did not enhance the formation of oxidative degradation products noticeably.

Oxygen pressures of 5 bar and 10 bar, however, caused lesser amounts of non-oxidatives to be formed. At 5 bar oxygen pressure the non-oxidative concentration increased to an amount of about 50 % and fell to 23 % after 24 hours due to the degradation of glucose.

Furthermore, the formation of lactic acid and glucoisosaccharinic acid was noticeably diminished in favor of oxidatives. The pressure increase to 10 bar oxygen pressure enhanced this effect further and more oxidatives were formed while the amount of non-oxidatives declined.

TABLE 8. Influence of oxygen and nitrogen pressure on the formation of *oxidative* degradation products at 35 °C [a, b, c]

	NITROGEN			OXYGEN		
Time [hours]	1 bar	5 bar	10 bar	Air	5 bar	10 bar
0	**0.0** 100.0	**0.0** 100.0	**0.0** 100.0	**0.0** 100.0	**0.0** 100.0	**0.0** 100.0
2	**1.4** 58.6	**1.4** 62.8	**1.2** 61.7	**1.2** 64.5	**7.2** 67.4	**11.5** 57.6
4	**2.6** 31.2	**2.3** 37.2	**2.3** 36.4	**2.3** 43.3	**15.8** 41.8	**25.3** 35.4
6	**3.2** 16.3	**3.1** 22.2	**3.3** 18.0	**3.5** 26.8	**24.8** 27.4	**37.3** 26.9
8	**3.8** 8.5	**3.7** 13.0	**3.5** 11.5	**4.3** 17.2	**34.6** 20.4	**43.2** 23.5
24	**4.5** 0.5	**4.4** 1.2	**4.1** 0.8	**9.5** 1.4	**52.9** 11.5	**52.9** 15.9

[a] The figures are given as per cent of the initial cellobiose amount.
[b] The figures in bold font illustrate the measured amount of oxidative degradation products.
[c] The figures in normal font illustrate the amount of cellobiose.

7.3.3 Degradation at 50 °C

Tables 9 and 10 illustrate the amount of non-oxidatives and oxidatives at 50 °C.

In both, nitrogen and oxygen atmospheres, cellobiose degraded entirely within the first 2 hours and therefore, it was not possible to observe any inhibiting effect of oxygen upon cellobiose degradation.

In nitrogen, cellobiose degraded entirely into non-oxidative degradation products and oxidatives were formed in trace amounts.

In air the oxidative degradation products were formed in trace amounts (10 %) and the content of non-oxidative degradation products was around 80 %.

By raising the oxygen pressure to 5 bar and 10 bar, the content of non-oxidatives declined from 80 %, as observed in air, to 50-60 %. The oxygen pressure increase reduced the non-oxidative degradation product content and raised the concentration of formed oxidatives to the same amount it was subtracted from the non-oxidatives. At 5 bar oxygen pressure around 25 % oxidatives were measured after 6 hours of degradation time.

TABLE 9. Influence of oxygen and nitrogen pressure on the formation of *non-oxidative* degradation products at 50 °C [a, b, c]

	NITROGEN			OXYGEN		
Time [hours]	1 bar	5 bar	10 bar	Air	5 bar	10 bar
0	**0.0** 100.0	**0.0** 100.0	**0.0** 100.0	**0.0** 100.0	**0.0** 100.0	**0.0** 100.0
2	**81.1** 5.7	**84.0** 0.2	**82.2** 0.7	**73.0** 2.1	**75.9** 6.2	**72.4** 4.5
4	**81.9** 0.8	**79.8** 0.1	**83.3** 0.3	**75.3** 0.9	**69.4** 2.2	**60.0** 2.5
6	**85.2** 0.5	**87.4** 0.1	**84.4** 0.2	**74.9** 0.9	**64.2** 1.3	**56.5** 2.2
8	**89.6** 0.2	**86.0** 0.1	**87.7** 0.2	**75.0** 0.6	**63.3** 1.7	**55.8** 2.3
24	**82.5** 0.1	**91.3** 0,1	**91.8** 0.1	**78.5** 0.4	**63.2** 0.9	**51.2** 1.1

[a] The figures are given as per cent of the initial cellobiose amount.
[b] The figures in bold font illustrate the measured amount of non-oxidative degradation products.
[c] The figures in normal font illustrate the amount of cellobiose.

TABLE 10. Influence of oxygen and nitrogen pressure on the formation of *oxidative* degradation products at 50 °C [a, b, c]

	NITROGEN			OXYGEN		
Time [hours]	1 bar	5 bar	10 bar	Air	5 bar	10 bar
0	**0.0** 100.0	**0.0** 100.0	**0.0** 100.0	**0.0** 100.0	**0.0** 100.0	**0.0** 100.0
2	**4.3** 5.7	**4.6** 0.2	**4.4** 0.7	**5.0** 2.1	**11.5** 6.2	**18.6** 4.5
4	**4.3** 0.8	**3.9** 0.1	**4.1** 0.3	**6.1** 0.9	**20.8** 2.2	**30.8** 2.5
6	**4.2** 0.5	**3.7** 0.1	**3.7** 0.2	**7.2** 0.9	**24.9** 1.3	**32.1** 2.2
8	**4.2** 0.2	**3.4** 0.1	**3.6** 0.2	**7.8** 0.6	**25.9** 1.7	**32.7** 2.3
24	**3.1** 0.1	**3.2** 0.1	**3.3** 0.1	**12.0** 0.4	**27.6** 0.9	**36.4** 1.1

[a] The figures are given as per cent of the initial cellobiose amount.
[b] The figures in bold font illustrate the measured amount of oxidative degradation products.
[c] The figures in normal font illustrate the amount of cellobiose.

7.3.4 Conclusions

In conclusion, the oxygen concentration in air is not sufficient to form noticeable amounts of oxidatives at room temperature and 35 °C. Therefore, non-oxidative degradation products are formed more favorably in air.

Oxygen exercises an inhibiting effect on cellobiose degradation. An oxygen partial pressure of 0.2 bar as observed in air showed the best inhibiting character at room temperature. Higher oxygen pressures reduced the concentration of non-oxidatives to trace amounts but in turn caused the formation of larger amounts of oxidative degradation products, resulting in faster cellobiose degradation rates. At 50 °C the inhibiting effect of oxygen and the formation of oxidative degradation products were weakened in favor of the formation of non-oxidative degradation products.

It could be concluded that the inhibition and oxidation of cellobiose were kinetically favored and the formation of non-oxidative degradation products were thermodynamically favored reaction processes.

7.4 Main degradation products of cellobiose

7.4.1 Non-oxidative degradation

Glucose

Cellobiose degrades to glucose through two major reaction routes. Mainly, it was formed through a direct β-hydroxy elimination in glucosyl-fructose, yielding glucose and 4-deoxy-D-*glycero*-2,3-hexodiulose (Figure 41a).

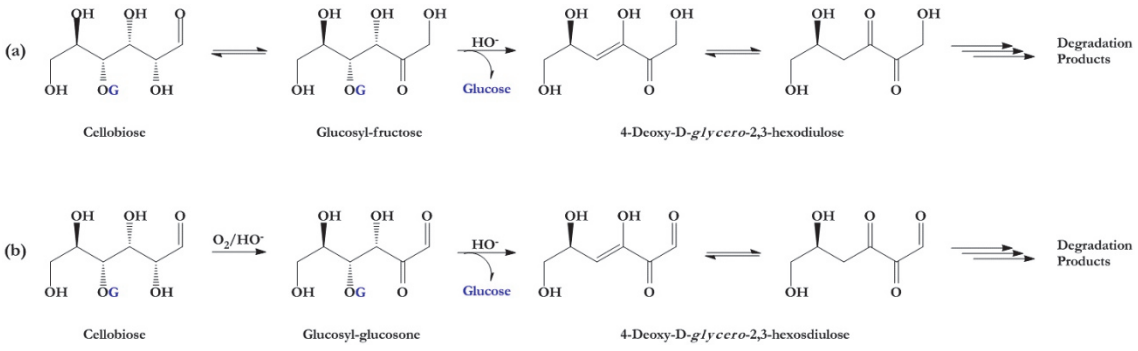

FIGURE 41. Liberation of glucose from glucosyl-fructose (a) and glucosyl-glucosone (b). Reproduced from Malinen.[84] Copyright (1974) Helsinki University of Technology, Laboratory of Wood Chemistry, Otaniemi, Finland.

As glucosyl-glucosone provides a C2 carbonyl group, a direct β-hydroxy elimination yields 4-deoxy-D-*glycero*-2,3-hexosdiulose and glucose (Figure 41b). At room temperature the glucose concentration rose under all the investigated conditions. At all oxygen pressures around 45 % of the degradation products

consisted of glucose after a degradation time of 24 hours. All the main degradation products derived from the two above mentioned intermediates. Henceforth, the glucose content of 45 % indicated that glucose was a stable degradation product at room temperature, as long as cellobiose was still available, and thus, only cellobiose was subject to degradation. In nitrogen atmosphere the approximate glucose content in the degradation products was from 35 % to 40 %, indicating a slight degradation of glucose along with cellobiose.

At 35 °C and in oxygen atmosphere the pressure increase caused successive amounts of glucose to be degraded. After 8 hours of degradation time, in air, at 5 bar, and 10 bar oxygen pressure, respectively, 36 %, 27 %, and 18 % of the degradation products consisted of glucose. This indicated that glucose most likely reacted with oxygen, forming glucosone that either rearranged into either gluconic or mannonic acid or fragmented into various degradation products. Due to the fact that gluconic and mannonic acid were formed in small amounts, it could be concluded that fragmentation was the predominant consecutive reaction.

In nitrogen atmosphere, respectively, 29 % (1 bar), 33 % (5 bar), and 33 % (10 bar) of all the degradation products was glucose. As generally observed, the nitrogen gas pressure increase had almost no effect on the degradation process and the two former mentioned glucose contents were in the same range than the two former glucose contents in oxygen atmosphere. This allowed the assumption to be made that the dissolved oxygen content in air and at 5 bar pressure did not suffice to degrade glucose and therefore rather the more reactive reactant, cellobiose, got degraded by oxygen. At 10 bar oxygen pressure around 15 % less glucose was found than in nitrogen atmosphere. Thus, successive oxygen saturation in NaOH enhanced noticeably the oxidative degradation of glucose.

At 50 °C the overall degradation proceeded rather rapidly and the half-life for all pressure and gas conditions was sooner than an hour. The first sampling showed a glucose content between 10 % and 20 % for all gas and pressure conditions. The second sampling after 4 hours reaction time showed that all glucose had been degraded into degradation products.

Lactic acid

Lactic acid was the smallest non-oxidative degradation product. It was formed through a reverse aldol reaction of the intermediate 4-deoxy-D-*glycero*-2,3-hexodiulose, giving yield to the isomers dihydroxyacetone and glyceraldehyde, which react further to methylglyoxal and eventually lactic acid (Figure 42).

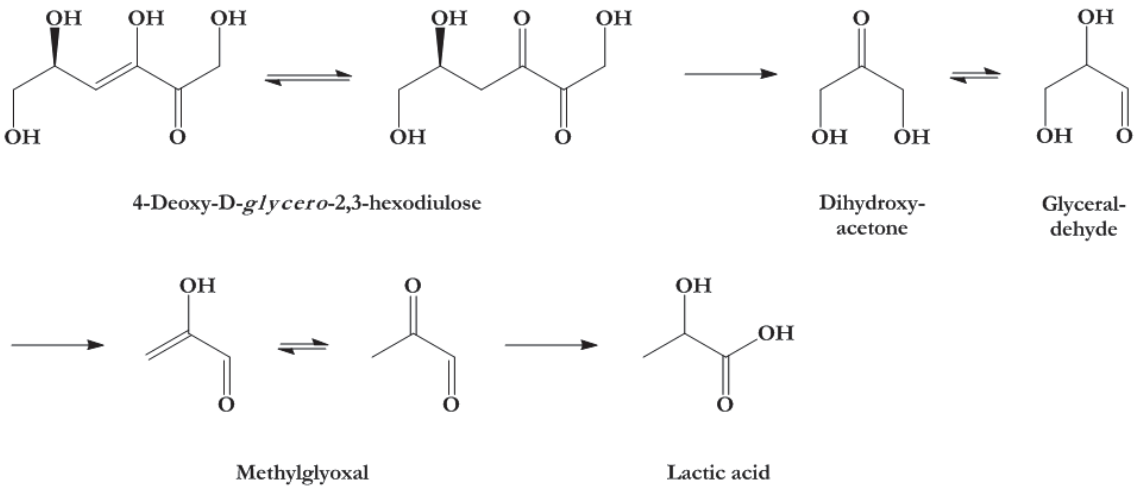

FIGURE 42. Formation of lactic acid. Reproduced from Malinen.[84] Copyright (1974) Helsinki University of Technology, Laboratory of Wood Chemistry, Otaniemi, Finland.

At room temperature lactic acid was formed in trace amounts under oxidative conditions after 24 hours. The lactic acid concentration declined when the oxygen gas pressure was increased. Its percentage rose slightly in nitrogen atmosphere to 5-8 % of the total amount of degradation products. This was a comparatively small value, indicating that the temperature was not high enough to favor the reverse aldol reaction of the 2,3-hexodiulose intermediate to occur.

At 35 °C, air and in all three nitrogen gas pressures, and after 24 hours of degradation time the lactic acid content was found in a range of 30 % of all degradation products. However, when the oxygen gas pressure was increased to 5 bar and 10 bar, the lactic acid content dropped noticeably to a total content of 4 % and 2 %, respectively, indicating a strong inhibition.

At 50 °C, in air and at all three investigated nitrogen gas pressures, and 24 hours of degradation time the lactic acid content was about 30 % to 37 %, which was similar to the values found at 35 °C. At 5 bar and 10 bar oxygen pressure the lactic acid content was elevated and much higher than the corresponding results at 35 °C, being 27 % and 22 %, respectively.

Glucoisosaccharinic acid

At all temperatures, glucoisosaccharinic acid was the main degradation product in nitrogen atmosphere and air. Increased oxygen pressures of 5 bar and 10 bar showed similar concentration reducing effects as evident for lactic acid, described above. Glucoisosaccharinic acid was formed *via* the benzilic acid rearrangement of 4-deoxy-D-*glycero*-2,3-hexodiulose (Figure 43).

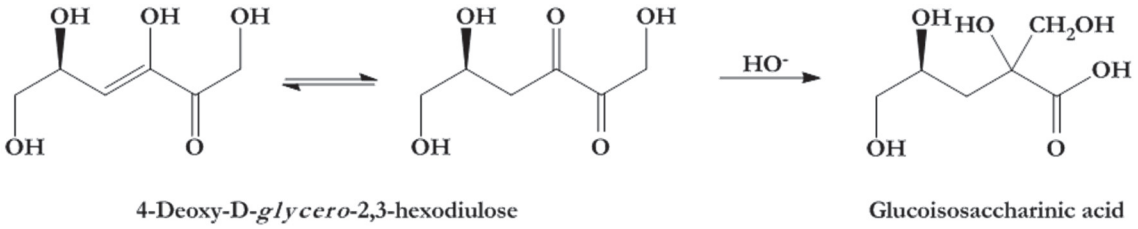

FIGURE 43. Formation of glucoisosaccharinic acid. Reproduced from Malinen.[84] Copyright (1974) Helsinki University of Technology, Laboratory of Wood Chemistry, Otaniemi, Finland.

At room temperature and in nitrogen atmosphere around 40 % of the degradation products consisted of glucoisosaccharinic acid. In air the percentage was 26 % and further oxygen pressure increase caused the acid to be formed in trace amounts, almost fully inhibiting its formation.

The temperature increase to 35 °C greatly increased the glucoisosaccharinic acid content to 58 % and 66 % for nitrogen and air, respectively. At 5 bar and 10 bar oxygen pressure the percentage was 17 % and 10 %, respectively. It should be noted that as mentioned above, glucose seemingly did not degrade at room temperature and the degradation of cellobiose led to a glucoisosaccharinic acid content of around 40 %. In 35 °C, however, the percentage rose to 60 % and glucose was also degraded. The observed increase of 20 % therefore derived mainly from direct glucose degradation.

Similar in pattern to the formation of lactic acid, at 50 °C, either in nitrogen or in air, similar amounts of glucoisosaccharinic acid were formed, *i.e.*, 54 % to 59 % in nitrogen atmosphere and 62 % in air. The temperature rise enhanced the benzilic acid rearrangement reaction and therefore, glucoisosaccharinic acid concentrations of 43 % and 28 % were obtained at 5 bar and 10 bar oxygen pressure, respectively.

Table 11 shows the percentage of glucose, lactic, and glucoisosaccharinic acid in relation to the percentage of the overall degradation product content.

TABLE 11. Relative percentage of the degradation products glucose (33), lactic acid (2), and glucoisosaccharinic acid (18-21)

		20 °C (after 24 h)			35 °C (after 24 h)			50 °C (after 24 h)		
		Air	5 bar	10 bar	Air	5 bar	10 bar	Air	5 bar	10 bar
Oxygen	All products	34.8	31.9	31.9	71.0	84.8	71.0	78.0	87.4	91.0
	Content of (2)	3.5	2.2	1.3	31.3	4.2	2.3	37.0	27.0	22.2
	Content of (18-21)	26.5	0.9	2.3	65.7	17.2	9.8	61.9	42.8	28.2
	Content of (33)	44.7	45.1	43.1	36.0	27.0	18.2	11.6	18.1	12.2
		1 bar	5 bar	10 bar	1 bar	5 bar	10 bar	1 bar	5 bar	10 bar
Nitrogen	All products	81.4	74.0	67.8	81.8	78.2	77.4	85.3	88.5	86.6
	Content of (2)	8.4	5.9	5.5	33.0	31.2	30.4	30.5	31.7	33.9
	Content of (18-21)	38.9	38.2	39.0	57.5	59.1	58.5	54.1	58.9	59.1
	Content of (33)	35.3	39.4	39.4	29.3	32.9	32.8	21.7	10.4	13.2

7.4.2 Oxidative degradation

Glycolic acid

The intermediate 4-deoxy-D-*glycero*-2,3-hexodiulose fragments into dihydroxyacetone and glyceraldehyde through the reverse-aldol reaction, which was oxidized into the C3-intermediate 3-hydroxy-2-oxopropanal. 3-Hydroxy-2-oxopropanal fragments further into glycolic acid and formic acid. Glycolic acid was also formed through the oxidative fragmentation reaction of the first mentioned hexodiulose intermediate that resulted in 3,4-dihydroxybutanoic and glycolic acids (Figure 44).

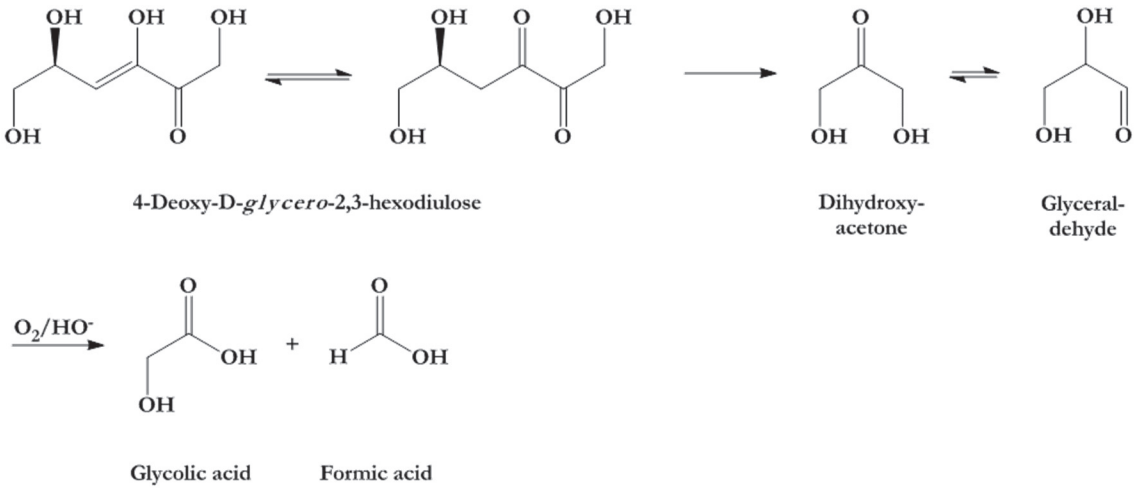

FIGURE 44. Formation of glycolic acid and formic acid. Reproduced from Malinen. [84] Copyright (1974) Helsinki University of Technology, Laboratory of Wood Chemistry, Otaniemi, Finland.

As for all main oxidative degradation products, the percentage of glycolic acid after a degradation period of 24 hours remained below 1 % of the total non-

volatile degradation product concentration. In air the acid was formed in trace amounts (2 % to 3 %) at all temperatures. The oxygen pressure increase noticeably increased the concentration, ranging from 10 % to 16 %. The highest glycolic acid content was observed at 35 °C.

Glyceric acid

Similar to glycolic acid, glyceric acid derived from glyceraldehyde, which was oxidized in the presence of oxygen to the intermediate 3-hydroxy-2-oxopropanal. Through the benzilic acid rearrangement the intermediate rearranges into glyceric acid (Figure 45).

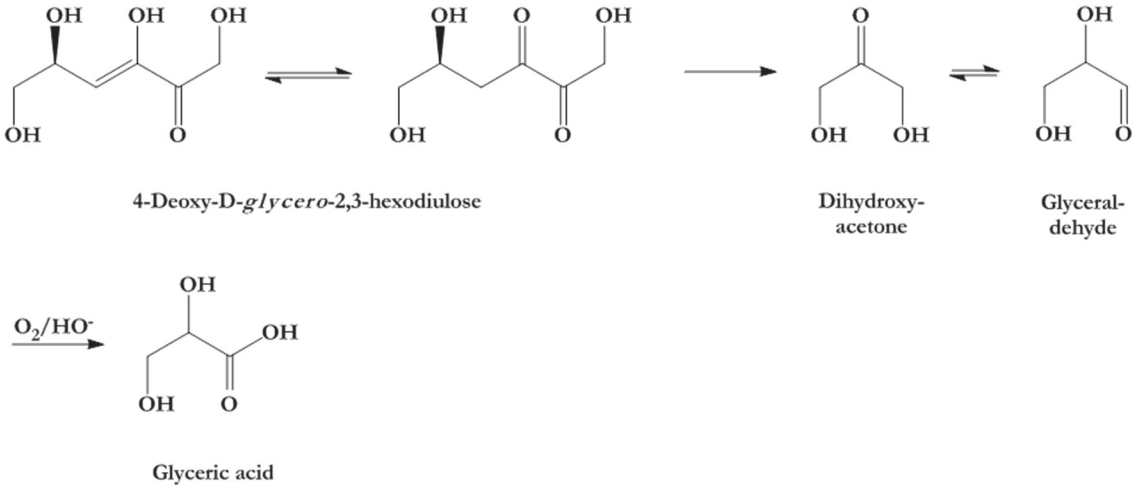

FIGURE 45. Glyceric acid formation. Reproduced from Malinen.[84] Copyright (1974) Helsinki University of Technology, Laboratory of Wood Chemistry, Otaniemi, Finland.

In general, glyceric acid was formed in trace amounts in nitrogen atmosphere and air. At 35 °C, 5 bar and 10 bar oxygen pressure the acid was formed in noticeable concentrations, *i.e.*, 11 % for both pressures. Due to the temperature rise and the favoring of the formation of non-oxidatives, glyceric acid was formed at lower concentrations at 50 °C.

3,4-Dihydroxybutanoic acid

3,4-Dihydroxybutanoic acid along with glycolic acid were both formed directly by an oxidative fragmentation reaction of the 4-deoxy-D-*glycero*-2,3-hexodiulose intermediate. Henceforth, the oxidative fragmentation reaction was directly competing with the benzilic acid rearrangement reaction that leads to the formation of glucoisosaccharinic acid (Figure 46).

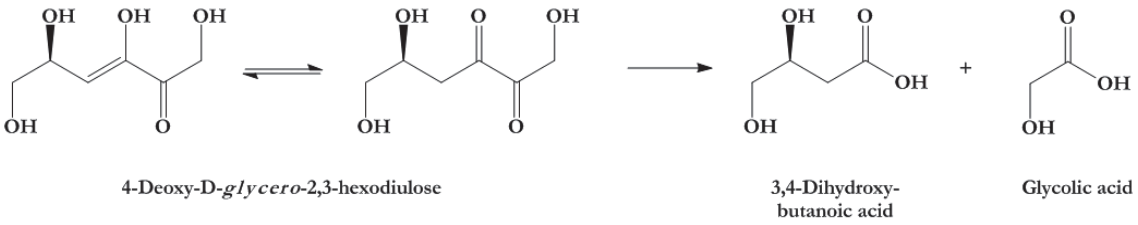

FIGURE 46. Formation of 3,4-dihydroxybutanoic acid and glycolic acid. Reproduced from Malinen.[84] Copyright (1974) Helsinki University of Technology, Laboratory of Wood Chemistry, Otaniemi, Finland.

The highest percentages of 3,4-dihydroxybutanoic acid were measured at room temperature and oxygen gas pressures of 5 bar and 10 bar. The temperature increase enhanced the benzilic acid rearrangement and reverse-aldol reactions, which caused lesser percentages of 3,4-dihydroxybutanoic acid to be formed. At 50 °C 3,4-dihydroxybutanoic acid was formed in trace amounts.

3-Deoxypentonic acid

As illustrated in Figure 47, the two 3-deoxypentonic acid isomers were formed when cellobiose was oxidized into glucosyl-glucosone and further degraded by the β-alkoxy elimination of the glucosyl moiety. After the elimination of the glucosyl moiety, this moiety rearranged into the intermediate 4-deoxy-D-*glycero*-2,3-hexosdiulose. The hexosdiulose intermediate was a 2,3-dioxo-aldehyde. It degraded into 3-deoxy-D-*glycero*-pentosulose after a oxidative fragmentation reaction. The subsequent benzilic acid rearrangement resulted into the two 3-deoxypentonic acid isomers. To some extent also 3,4-dihydroxybutanoic acid derived from 3-deoxy-D-*glycero*-pentosulose.

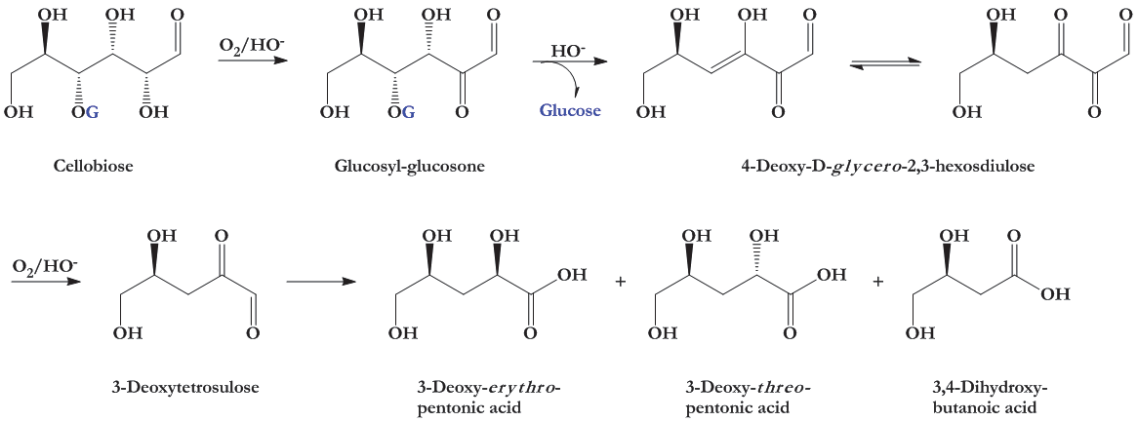

FIGURE 47. Formation of 3-deoxypentonic acid and 3,4-dihydroxybutanoic acid. Reproduced from Malinen.[84] Formation of 3,4-dihydroxybutanoic acid. Reproduced from Malinen.[84] Copyright (1974) Helsinki University of Technology, Laboratory of Wood Chemistry, Otaniemi, Finland.

Similar to the other oxidatives, the two 3-deoxypentonic acid isomers were only formed under 5 bar and 10 bar oxygen gas pressure. The percentages of 3-

deoxypentonic acid were very similar to those of 3,4-dihydroxybutanoic acid under all investigated conditions.

By increasing the temperature the percentage of 3-deoxypentonic acid declined. While 4 %, 15 %, and 15 % of the non-volatile degradation products were formed in air, 5 bar, and 10 bar, respectively, at 35 °C and 50 °C the percentage declined successively until trace amounts were formed at 50 °C. This signified that the formation of glucosyl-glucosone and subsequent formation of 4-deoxy-D-*glycero*-2,3-hexosdiulose is more prominent at lower temperatures.

Table 12 shows the percentage of the main oxidative degradation products in relation to the percentage of the overall degradation product content.

TABLE 12. Relative percentage of the degradation products glycolic acid (1), glyceric acid (4), 3,4-dihydroxybutanoic acid (7), and 3-deoxypentonic acid (14,15)

Oxidatives		20 °C (after 24 h)			35 °C (after 24 h)			50 °C (after 24 h)		
	Pressure	Air	5 bar	10 bar	Air	5 bar	10 bar	Air	5 bar	10 bar
Oxygen	All products	**34.8**	**31.9**	**31.9**	**71.0**	**84.8**	**71.0**	**78.0**	**87.4**	**91.0**
	Content of (1)	2.5	11.1	11.5	2.9	13.0	15.9	2.3	9.8	11.0
	Content of (4)[b]	0.3	1.5	2.0	1.9	10.9	11.4	0.6	5.7	6.0
	Content of (7)	4.0	15.3	14.6	2.6	8.4	11.0	2.5	3.4	4.3
	Content of (14,15)	3.8.	15.1	15.2	2.1	9.3	11.4	1.6	4.0	3.5
Nitrogen	Pressure	1 bar	5 bar	10 bar	1 bar	5 bar	10 bar	1 bar	5 bar	10 bar
	All products	**81.4**	**74.0**	**67.8**	**81.8**	**78.2**	**77.4**	**85.3**	**88.5**	**86.6**
	Content of (1)	0.5	0.5	0.4	0.9	0.8	0.7	0.7	0.6	0.7
	Content of (4)	0.1	0.1	0.1	0.3	0.3	0.3	0.3	0.3	0.3
	Content of (7)	1.2	1.4	1.2	1.3	1.3	1.3	0.6	0.5	0.6
	Content of (14,15)	0.7	0.8	0.6	1.1	1.1	1.0	0.7	0.9	0.9

7.4.3 Conclusions

It has been generally agreed by several investigators [49,84] that oxidation reactions would occur at lower temperatures, and peeling reactions, *i.e.*, the formation of non-oxidative degradation products, would occur at higher temperatures. This research, however, revealed that a steady reduction of degradation temperature did not result in a proportional increase of oxidation reactions. For cellobiose, this research proved the existence of a temperature maximum for oxidation reactions at somewhere between room temperature and 50 °C, possibly around 35 °C.

Furthermore, it could be shown that the benzilic acid rearrangement, fructose transformation, and reverse-aldol reactions were reactions that did not involve the participation of oxygen but only hydroxyl anions. These reactions were thermodynamically favored.

Oxidation reactions were kinetically favored.

As both, glyceric acid and glycolic acid are formed by 3-hydroxy-2-oxopropanal

and glycolic acid being formed at higher concentrations than glyceric acid, it could be assumed that the oxidative fragmentation reaction of 3-hydroxy-2-oxopropanal into two fragments, glycolic acid and formic acid, was energetically more favored than the benzilic acid rearrangement reaction of the C3-intermediate into glyceric acid. This finding supported the assumption that oxidation reactions are faster than rearrangement reactions that do not involve oxygen intervention.

Furthermore, the highest percentages of 3-deoxypentonic acid were measured at room temperature. However, at 35 °C, 3-deoxypentonic acid was formed in the highest concentrations. At 50 °C, 3-deoxypentonic acid was formed in small amounts for the temperature increase rather increased the concentration of thermodynamically favored degradation products.

It should be noticed that glucosyl-glucosone, the intermediate from which 3-deoxypentonic acid derived, could also rearrange *via* the benzilic acid rearrangement into cellobionic acid. Cellobionic acid, however, could never been identified in this research. This was most likely due to the preference of the β-alkoxy elimination of the glucosyl moiety over the benzilic acid rearrangement reaction.

Degradation products with more than six carbon atoms, like glucosyl-arabinose, glucosyl-erythrose, glucosyl-threose, cellobionic acid, and other acids that have been generally proposed in the literature were not found among the degradation products. Henceforth, the existence of these acids could not be confirmed in this work. Surprisingly, important and generally proposed intermediates like ribose, arabinose, glyceraldehyde, and dihydroxyacetone remained undetected or were formed inconsistently in trace amounts. Unexpected was also the detection of galactose in large amounts. Its concentration could not get quantitatively verified due to its peak overlap with the β-glucoisosaccharinic acid peak.

Overall, the error bars of the degradation product concentrations were relatively small even though all reactions were repeated twice or thrice. This could indicate a controlled and predictable reaction mechanism, like an ionic based reaction mechanism. A radical reaction mechanism would most likely cause a much greater variety of degradation products with large concentration error margins.

8 KINETICS

8.1 First order degradation kinetics

The degradation of cellobiose followed the first order decay in nitrogen and could be fairly approximated by pseudo-first order decay kinetics in oxygen according to the equation (5):

$$A = A_0\, e^{-kt} \tag{5}$$

where A is the cellobiose concentration at a particular time,
A_0 the initial cellobiose concentration,
k the cellobiose degradation rate constant, and
t the degradation time.

The half-life $t_{1/2}$ of the first-order or pseudo-first-order reaction was given by:

$$t_{1/2} = \frac{\ln(2)}{k} \tag{6}$$

The initial cellobiose concentration A_0 and the cellobiose degradation rate constant k of each curve were determined by developing a degradation curve through nonlinear interpolation of the exponential equation (5) to the concentration points obtained after 2, 4, 6, 8, and 24 hours.

A nonlinear regression of the first order decay function to the measured cellobiose concentrations was performed with Microsoft Excel Solver.[85]

The Microsoft Excel Solver uses the GRG2 Algorithm [86] for the numerical optimization processes. The fitting of the first order decay function to the actual data points is carried out by minimizing the residual sum of squares, r^2, that occur between the generated and experimental data, under variation of the rate constant k and the initial cellobiose concentration.

$$r^2 = \sum_{i=1}^{n} \left(F(t_i) - f(t_i)\right)^2 \quad (7)$$

In the residual sum of squares equation, n is the number of experimental data to be fitted, y_i is the calculated value at time t_i and $f(t_i)$ is the experimentally observed cellobiose concentration at time t_i.

8.2 Activation energies and half-lives

The degradation of cellobiose at room temperature is depicted in Figure 48. The corresponding rate constants, half-lives, and initial cellobiose concentrations are presented in Table 13.

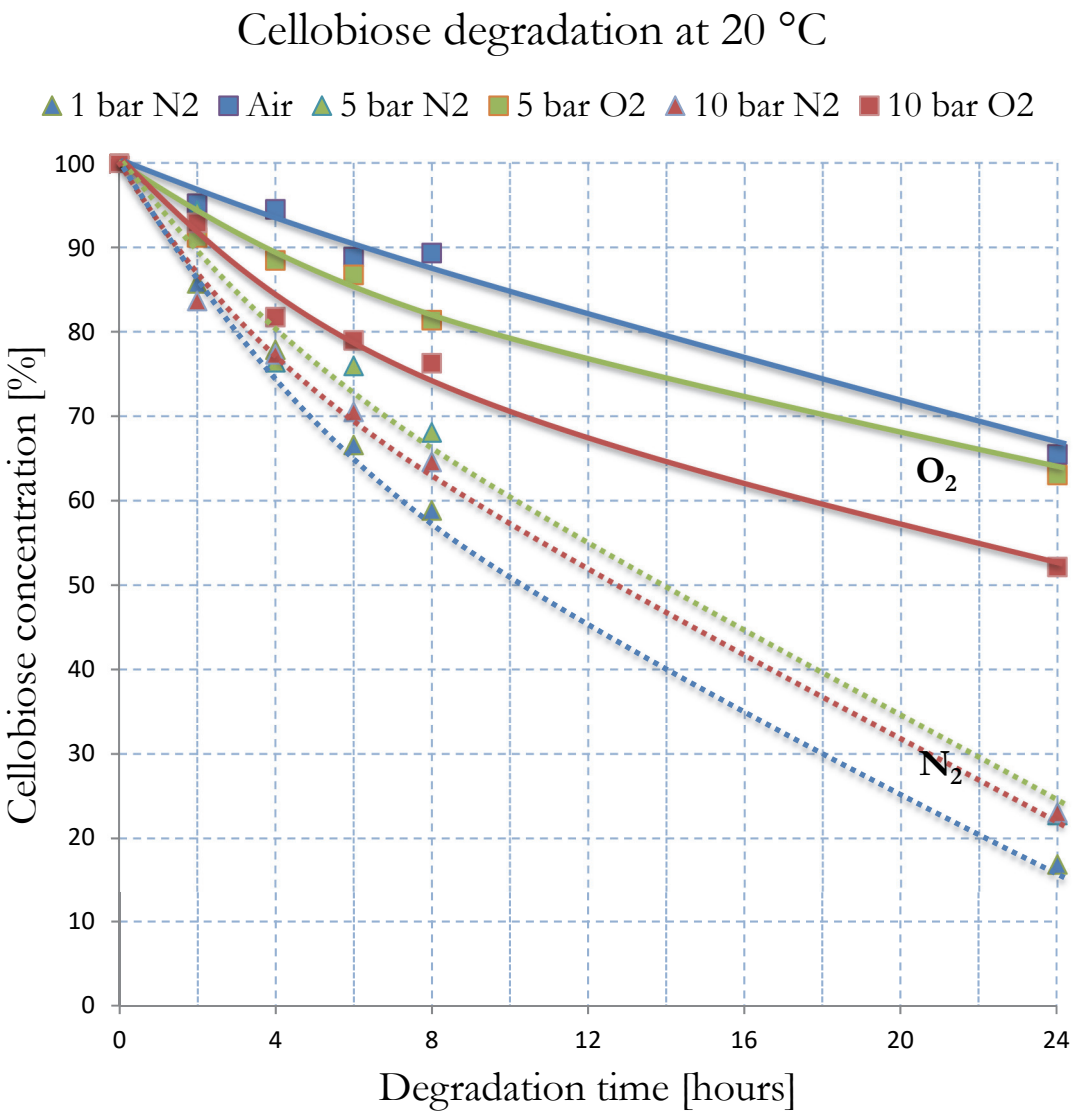

FIGURE 48. Cellobiose degradation at room temperature in nitrogen (dotted lines) and oxygen atmosphere (full lines).

TABLE 13. A_0, k, and $t_{1/2}$ values at room temperature

	Pressure [bar]	A_0 [ppm]	k [h^{-1}]	k/k_{AIR}	$t_{1/2}$
Nitrogen	1	3,573	0.0698	4.0	9 h 56 min
	5	3,470	0.0574	3.3	12 h 5 min
	10	3,458	0.0590	3.4	11 h 45 min
Oxygen	0.2 (air)	3,244	0.0173	1	40 h 10 min
	5	3,347	0.0214	1.2	32 h 19 min
	10	3,250	0.0311	1.8	22 h 17 min

Depending on the reaction conditions, oxygen has the potential of both, accelerating and inhibiting the degradation of cellobiose. At room temperature the degradation of cellobiose in oxygen atmosphere proceeded noticeably slower

than in nitrogen. The values in Table 13 illustrated a 3 to 4 times faster degradation of cellobiose in nitrogen than under atmospheric pressure with an oxygen partial pressure of 0.2 bar. This observation was unexpected and surprising. To our understanding an inhibiting effect of oxygen upon the degradation of cellulose, cellulosic materials or model substances has not been reported in the literature. Furthermore, the oxygen pressure increase accelerated the degradation of cellobiose. An oxygen gas pressure increase to 10 bar almost doubled the degradation rate in comparison to thedegradation rate in air.

The temperature rise to 35 °C significantly enhanced the degradation of cellobiose. In oxygen, however, cellobiose degraded with a slightly slower rate than in nitrogen. The variation in the nitrogen gas pressure from 1 bar to 10 bar had no noticeable influence on the cellobiose degradation rate. Half-lives were around 2 hours and 30 minutes and 3 hours 15 minutes for nitrogen and oxygen, respectively.

Table 14 illustrates A_0, k, and $t_{1/2}$ values of the six degradation curves that are depicted in Figure 49.

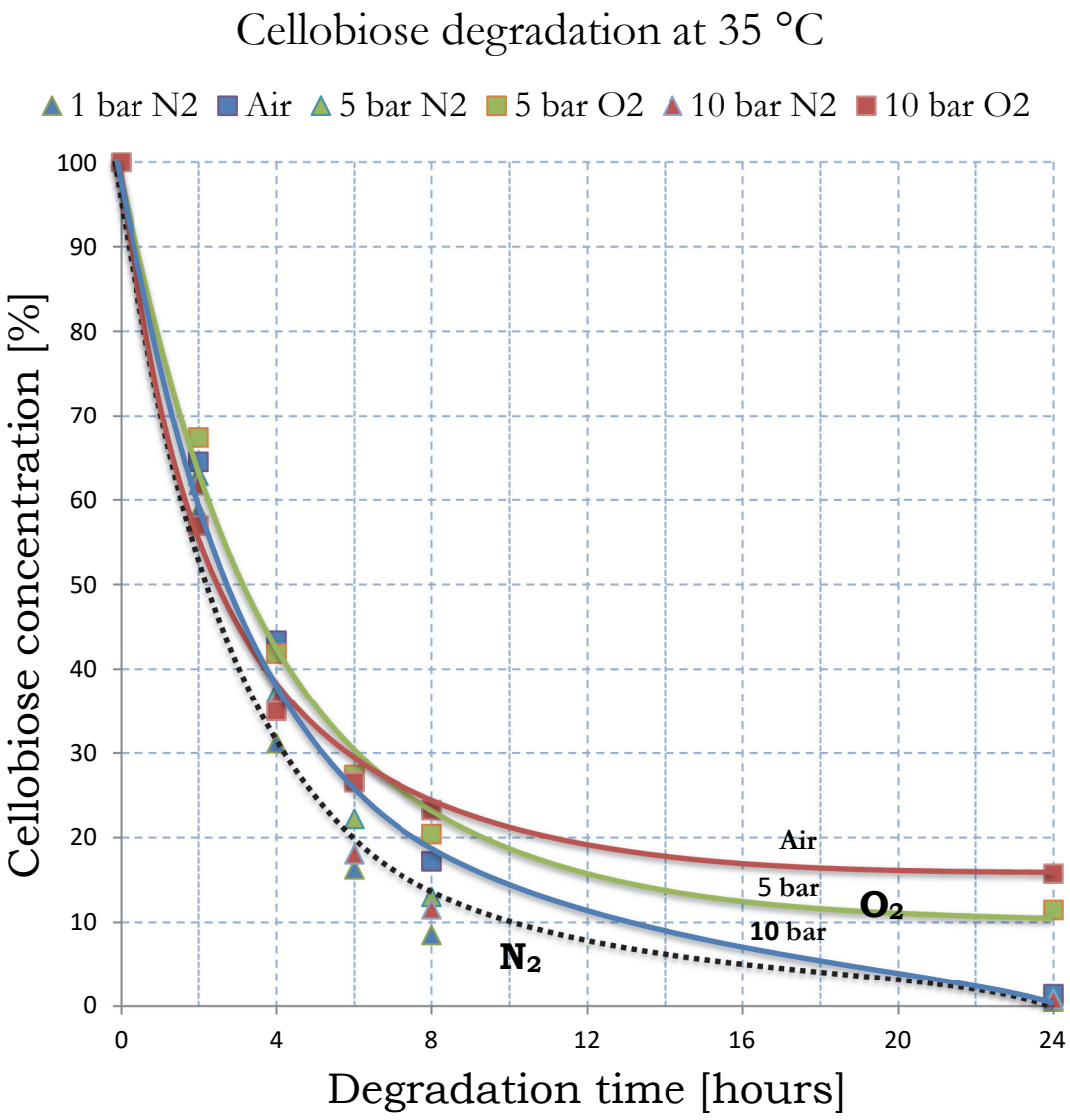

FIGURE 49. Cellobiose degradation at 35 °C in nitrogen (black dotted line) and oxygen atmosphere (full lines).

TABLE 14. A_0, k, and $t_{1/2}$ values at 35 °C

	Pressure [bar]	A_0 [ppm]	k [h^{-1}]	k/k_{AIR}	$t_{1/2}$
Nitrogen	1	3800	0.2894	1.3	2 h 24 min
	5	3800	0.2460	1.1	2 h 49 min
	10	3950	0.2607	1.2	2 h 40 min
Oxygen	0.2 (air)	3633	0.2161	1	3 h 12 min
	5	3282	0.2073	1.0	3 h 21 min
	10	3250	0.2338	1.1	2 h 58 min

In both, nitrogen and oxygen, the degradation of cellobiose proceeded quickly at 50 °C, with half-lives between 10 minutes to 30 minutes. Cellobiose was found in trace amounts after two hours of degradation time.

Table 15 illustrates A_0, k, and $t_{1/2}$ values of the six degradation curves that are depicted in Figure 50.

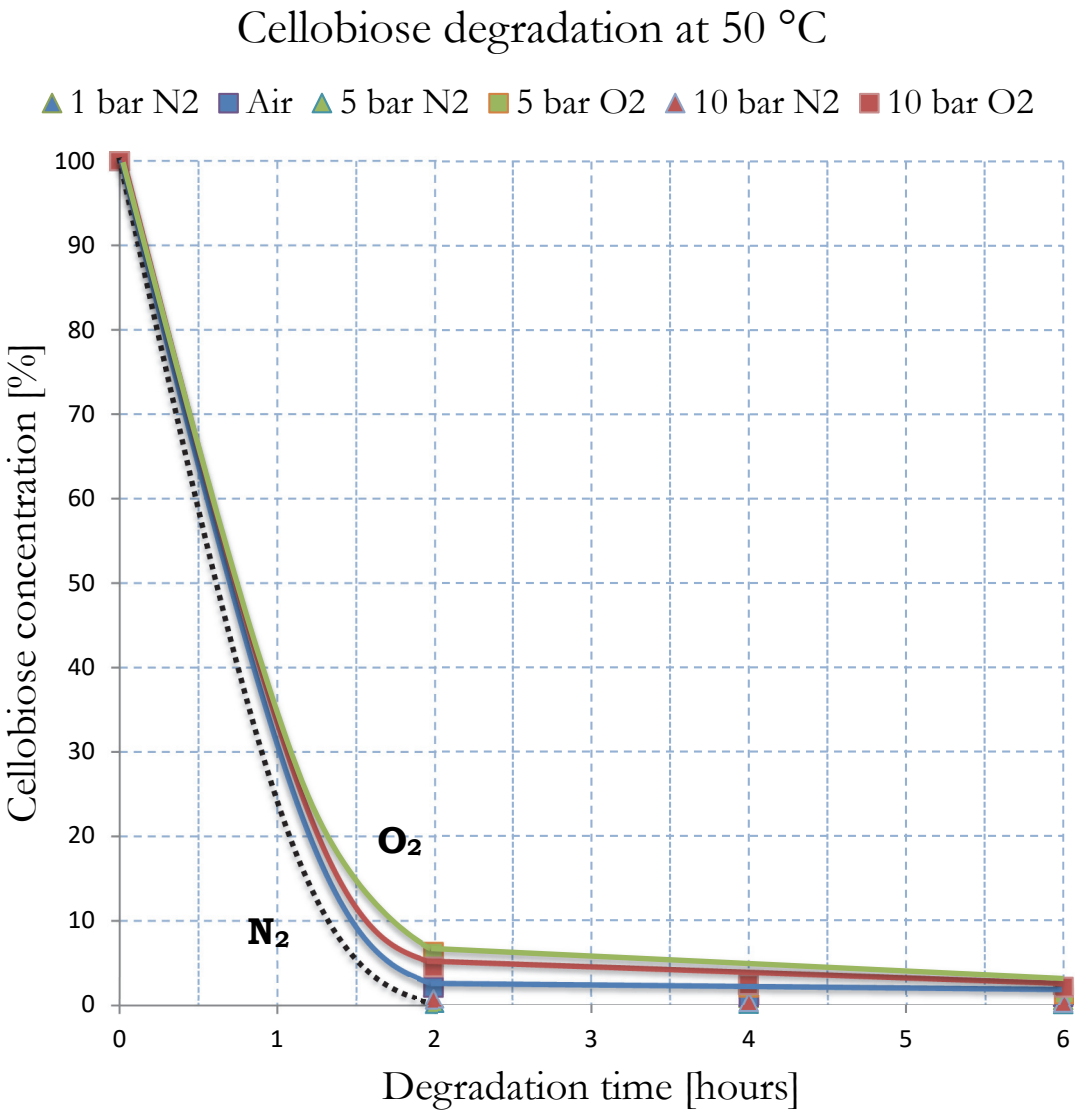

FIGURE 50. Cellobiose degradation at 50 °C in nitrogen (black dotted line) and oxygen atmosphere (full lines).

TABLE 15. A_0, k, and $t_{1/2}$ values at 50 °C

	Pressure [bar]	A_0 [ppm]	k [h^{-1}]	k/k_{AIR}	$t_{1/2}$
Nitrogen	1	3,600	1.4291	0.7	29 min
	5	3,400	3.0674	1.6	14 min
	10	3,400	2.4637	1.3	17 min
Oxygen	0.2 (air)	3,500	1.9116	1	22 min
	5	3,400	1.3685	0.7	30 min
	10	3,210	1.5231	0.8	27 min

Rowell and Green [87] degraded several cellulose model substances in 10 % NaOH, at 170 °C, and in the presence and absence of oxygen. They could show that the addition of oxygen into the system increased the degradation rate of all model substances in comparison to oxygen free nitrogen atmosphere. In our investigation, the introduction of oxygen showed a decrease of degradation rate. However, the degradation rate approximated the nitrogen rate constants with increasing temperature.

It could be assumed that at low temperatures, the oxygen presence had inhibiting influence upon the degradation of cellulose and its model substances and above a critical temperature, however, accelerated their degradation.

8.3 Activation energies and A-factors

By applying the Arrhenius equation (8) and written equivalently as (9), both the activation energy and A-factor values were determined (Table 16):

$$k = Ae^{-E_a/RT} \tag{8}$$

$$\ln(k) = -\frac{E_a}{R}\frac{1}{T} + \ln(A) \tag{9}$$

The factor k represents the rate constant of the reaction. A is the A-factor, E_a the activation energy, R the gas constant, and T the absolute temperature in Kelvin.

The results in Table 16 indicated similar activation energies around 100 kJ/mol in both nitrogen and oxygen atmospheres and at 5 bar and 10 bar pressures. In air and at 1 bar nitrogen pressure the activation energy was 122 kJ/mol and 79 kJ/mol, respectively. Figures 51 and 52 illustrate the Arrhenius plots in nitrogen and oxygen, respectively.

TABLE 16. Activation energies and A-factors

OXYGEN	NITROGEN
E_a (Air) = 122 ± 5 kJ/mol	E_a (1bar) = 79 ± 3 kJ/mol
A (Air) = 3 $\cdot 10^{17}$ s^{-1}	A (1 bar) = 2 $\cdot 10^{10}$ s^{-1}
E_a (5 bar) = 103 ± 3 kJ/mol	E_a (5 bar) = 103 ± 16 kJ/mol
A (5 bar) = 2 $\cdot 10^{14}$ s^{-1}	A (5 bar) = 3 $\cdot 10^{14}$ s^{-1}
E_a (10 bar) = 101 ± 2 kJ/mol	E_a (10 bar) = 97 ± 11 kJ/mol
A (10 bar) = 3 $\cdot 10^{13}$ s^{-1}	A (10 bar) = 3 $\cdot 10^{13}$ s^{-1}

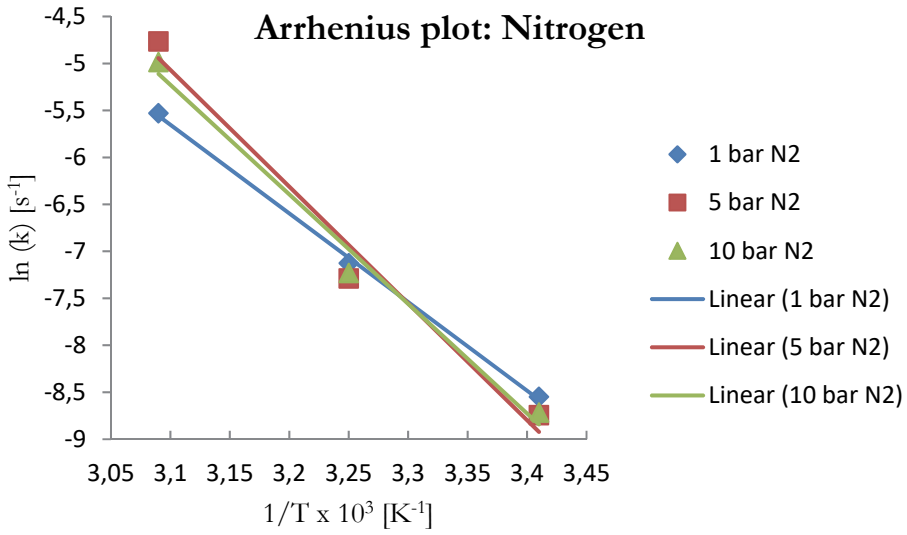

FIGURE 51. Arrhenius plot for nitrogen atmosphere.

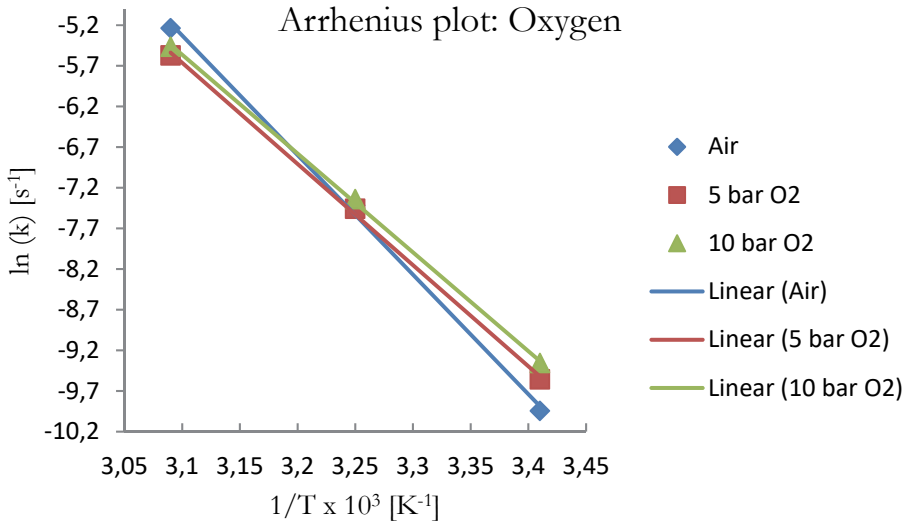

FIGURE 52. Arrhenius plot for oxygen atmosphere.

Other researchers have investigated the degradation kinetics of cellulose and carbohydrates and determined the activation energy for the applied process. Bamford and Collins [77] could determine an activation energy of 108 kJ/mol for the alkaline degradation of fructose and glucose. Van Loon and Glaus [88] determined an activation energy of 101 kJ/mol for the degradation of cellulose. Extensive study on the kinetics of cellulose degradation under various conditions was executed by Emsley and Stevens [89] who concluded that independently of the reaction conditions and degradation method the activation energy for different cellulose and cellulosic materials was about 111 kJ/mol at temperatures below 140 °C. The research of Bigger *et al.* [90] about the kinetics of cellulose degradation

referred to the conclusion made by Emsley and Stevens [89] as the "universal" activation energy. With our research on the degradation of cellobiose we could provide supporting evidence for the universal activation energy theory.

9 DISCUSSION AND CONCLUDING REMARKS

The results and made observations from this work together with the considerations of other researchers have allowed a new reaction mechanism for the alkaline oxidative degradation of cellobiose, cellulose, and cellulosic materials to be postulated.

As discussed above, cellobiose degrades at room temperature at a noticeably higher rate in nitrogen than in oxygen with glucose, lactic acid, and glucoisosaccharinic acid as main degradation products. In air the concentration of these degradation products declined. Oxidatives were formed in trace amounts. Oxygen interacted as an inhibitor. The highest inhibiting effect was observed in air. Higher oxygen pressures increased the degradation rate of cellobiose.

The inhibiting effect of oxygen could be described as follows. The C-2 deprotonation of the glucose end-group in cellobiose by a hydroxyl ion leads to the formation of a mesomeric-stabilized enediolate. The enediolate reacts with molecular oxygen *via* the nucleophilic addition at either the C-1 or the C-2 position, adding to the carbon atom that holds the hydroxyl group. The presence of a reducing aldehyde group is required for the enediolate reaction and subsequent degradation to occur. Entwistle *et al.* [41] could show a linear proportionality between the copper number which is sensitive to reducing aldehyde groups and the initial autoxidation rate. The attempts of Lee [91] to degrade methyl-β-D-glucoside in a pressurized oxygen system under alkaline conditions remained unsuccessful, due to the lack of aldehyde groups.

Molecular oxygen in its ground state is a diradical, having two unpaired electrons in two degenerate antibonding molecular orbitals. Hence, it would stand to reason that molecular oxygen reacts *via* the radical one-electron transfer oxidation reactions as suggested by Entwistle *et al.*[41,42] The presence of radicals in alkaline oxidative degradation of cellulose could not be proven to this day and other researchers like Mattor [43] proposed ionic two-electron transfer oxidation reactions with oxygen. This means that molecular oxygen would need to be present in the alkaline medium as singlet oxygen, having the two electrons paired in one antibonding molecular orbital. Singlet oxygen would therefore react as a Lewis acid and interact with a nucleophile, such as a dienolate as described above.

The disagreement, whether the autoxidation reaction mechanism would be ionic or radical, is most likely a matter of the overall reaction conditions, largely the degradation temperature. Relatively low temperatures were utilized in this research to degrade cellobiose and the obtained results and observations point to an ionic reaction mechanism. However, due to the fact that molecular oxygen is a diradical in its ground state, it is possible that the ionic reaction mechanism gradually turns into a radical reaction mechanism, caused by temperature increase. Degradation temperatures of at least 100 °C have been suggested to be necessary for radical autoxidation reactions to be favored.[84]

However, the formed hydroperoxide in the suggested reaction mechanism was an unstable intermediate, thus existing for a very short time period. That would explain why the existence of hydroperoxides in alkaline oxidative degradation of aldoses and cellulosic materials have been controversially discussed in literature, either suggesting [41,42] or denying [84] their existence.

At lower temperatures, like at room temperature, the enthalpy is insufficient for the formed hydroperoxide intermediates to react further and oxidize into the glucosone moiety and hydrogen peroxide. Henceforth, under low-enthalpy alkali-oxidative degradation conditions the equilibrium between enediolate and hydroperoxide was shifted toward the enediolate intermediate. The hydroperoxide formation was kinetically and fructose transformation reaction was thermodynamically favored, and therefore, the latter reaction occurred to a much lower rate than under oxygen-free conditions. This characteristic finding explained why cellobiose degrades four times slower at room temperature when 20 % of 1 bar nitrogen was exchanged by 20 % oxygen (atmospheric pressure, air). The oxygen presence seemingly inhibited cellobiose degradation. Interestingly though, the activation energy of cellobiose degradation in air was 50 % higher than in 1 bar nitrogen.

By increasing the oxygen pressure the equilibrium shifts toward the hydroperoxide intermediate and therefore, the concentration of glucosone and its subsequent oxidative degradation products increased progressively. In the current research, the main oxidative degradation products were formed in trace or small amounts at all three investigated degradation temperatures when the reactions were performed in air. The increased oxygen gas pressures enhanced oxidative fragmentation or oxidation reactions of degradation products formed by other intermediates and decreased the formation of non-oxidative degradation products. Thus, an oxygen partial pressure of 0.2 bar in air was sufficient to inhibit the Lobry-de-Bruyn-van Ekenstein transformation of the enediolate form into fructose but it was not sufficient enough to shift the equilibrium adequately towards oxidation and oxidative fragmentation reactions.

As anticipated, by the higher enthalpy at 35 °C degradation temperature the overall degradation rate increased in all oxygen gas pressures. However, in air the oxygen content was not sufficient and therefore, non-oxidative degradation products were mainly formed and oxidatives were formed in trace amounts. Applied oxygen pressures of 5 bar and 10 bar resulted in a drastic reduction of non-

oxidatives in favor of oxidative degradation products. This indicated that in contrast to room temperature, at 35 °C the enthalpy was sufficient to cause a shift towards oxidation reactions. The beneficial influences of the temperature increase upon oxidation reactions could be explained by an increase in the rate of oxygen absorption in NaOH.[92] Hence, mainly oxidation and related fragmentation reactions are observed.

With further temperature rise to 50 °C the enthalpy was large enough to cause thermodynamically favored, *i.e.*, non-oxidative degradation products to be mainly formed, even under high oxygen pressures.

Noteworthy and supportive observations to this reaction mechanism were made by Onda *et al.* [93] who degraded *i.a.* glucose under alkaline conditions in air into gluconic acid, lactic acid, and to some minor extend into other degradation products by using Pt/C catalysts. The temperature range in their set of experiments was between 30 °C and 90 °C. The observations made by the authors could be interpreted in the following way. The presence of the Pt/C catalyst noticeably enhanced the oxidation reaction as illustrated in Figure 53 and the yield of gluconic acid was almost 100 % at 30 °C. At 90 °C the concentrations of both, lactic acid and gluconic acid were around 50 %. The Pt/C catalysts reduced the activation energies of oxidation reactions and the equilibriums shifted to the right, causing gluconic acid to be formed quantitatively at 30 °C from glucosone *via* the benzilic acid rearrangement.

Figure 53 illustrates the above described reaction mechanism.

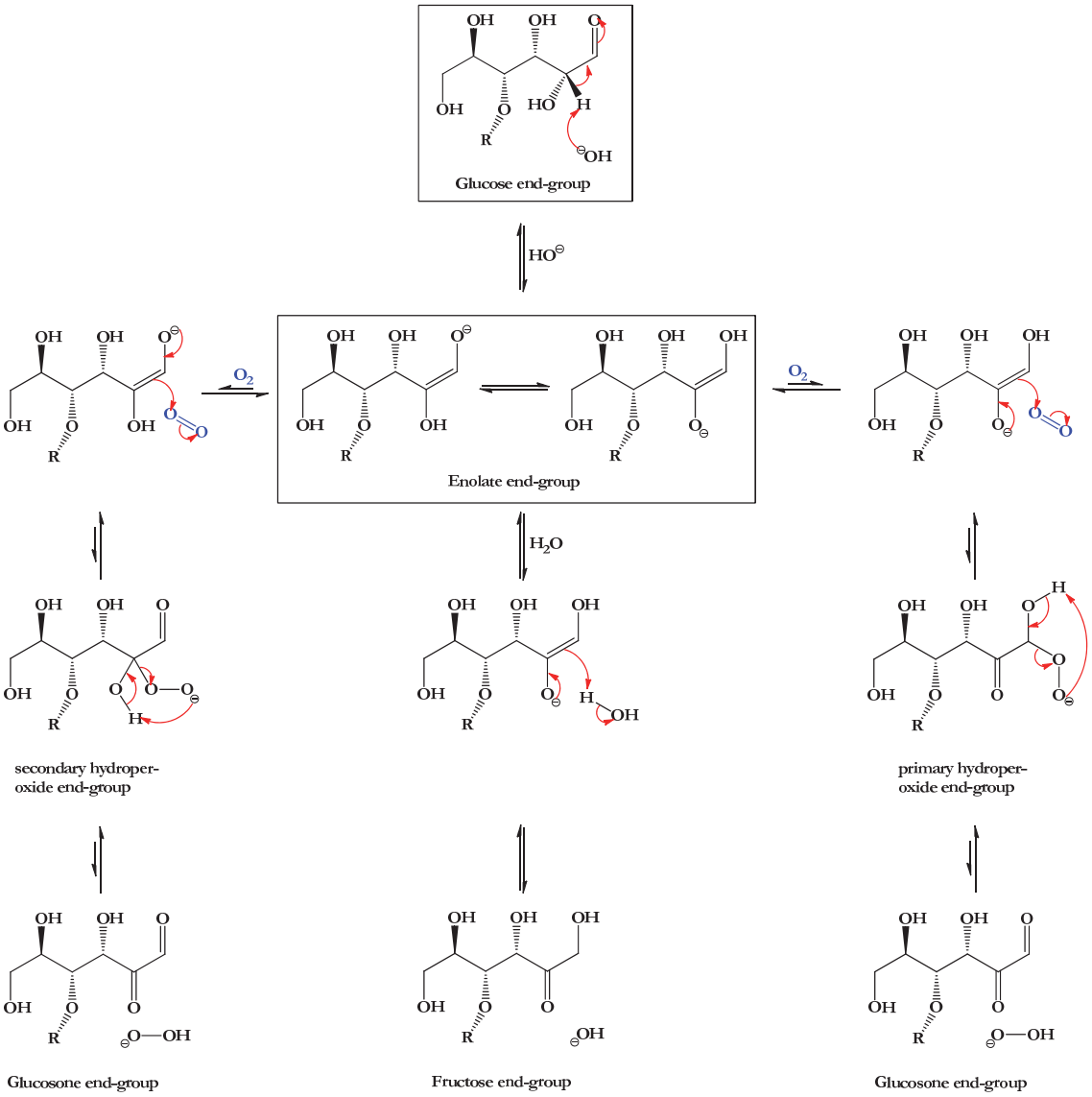

FIGURE 53. Postulated oxidation reaction mechanism for the formation of glucosone end-groups.

REFERENCES

1. Nishiyama, Y., Chanzy, H., Wada, M., Sugiyama, J., Mazeau, K., Forsyth, T., Riekel, C., Mueller, M., Rasmussen, B., and Langan, P., Synchrotron X-ray and neutron fiber diffraction studies of cellulose polymorphs, *Int. Centre for Diffraction Data 2002, Adv. in X-ray Anal.*, 45(2002)385-390.
2. Nishiyama, Y., Sugiyama, J., Chanzy, H., and Langan, P., Crystal structure and hydrogen bonding system in cellulose Iα from synchrotron X-ray and neutron fiber diffraction, *J. Am. Chem. Soc.*, 125(47)(2003)14300-14306.
3. Richmond, P.A., Occurrence and functions in native cellulose. In: Haigler, C.H. and Weimer, P.J. (Eds.), *Biosynthesis and Biodegradation of Cellulose*, Marcel Dekker, New York, NY, USA, 1991, pp. 5-23.
4. Emons, A.M.C., Role of particle rosettes and terminal globules in cellulose synthesis. In: Haigler, C.H. and Weimer, P.J. (Eds.), *Biosynthesis and Biodegradation of Cellulose*, Marcel Dekker, New York, NY, USA, 1991, pp. 71-98.
5. Van der Hart, D.L. and Atalla, R.H., Studies of microstructure in native celluloses using solid-state carbon-13 NMR, *Macromolecules*, 17(8)(1984)1465-1472.
6. Qian, X., Ding, S.-Y., Nimlos, M.R., Johnson, D.K., and Himmel, M.E., Atomic and electronic structures of molecular crystalline cellulose Iβ: A first-principles investigation, *Macromolecules*, 38(25)(2005)10580-10589.
7. Speakman, P., Shirts and shish-kebabs; John Mercer and mercerization, *Biochem. Educ.*, 19(4)(1991)200-203.
8. Klemm, D., Philipp, B., Heinze, T., Heinze, U., and Wagenknecht, W., *Comprehensive Cellulose Chemistry: Functionalization of Cellulose, Vol. 2*, Wiley-VCH, Weinheim, Germany, 1998, pp. 31-69.
9. Lee, M.H., Park, H.S., Yoon, K.J., and Hauser, P.J., Enhancing the durability of linen-like properties of low temperature mercerized cotton, *Text. Res. J.*, 74(2)(2004)146-154.
10. Peters, R.H., *Textile Chemistry, Vol. 2*, Elsevier, New York, NY, USA, 1967, pp. 328-365.
11. Philipp, B., Kunze, J., and Fink, H.-P., Solid-state carbon-13 NMR and wide-angle X-ray scattering study of cellulose disordering by alkali treatment. In: Atalla, R.H., (Ed.), *The Structures of Cellulose – Characterization of the Solid States, ACS Symposium Series, Vol. 340*, American Chemical Society, Washington DC, USA, 1987, pp. 178-188.
12. Ibanescu, C., Schimper, C., and Bechtold, T., Alkaline treatment of cotton in different reagent mixtures with reduced water content. I. Influence of alkali type and additives, *J. Appl. Polym. Sci.*, 99(5)(2006)2848-2855.
13. Baker, A.A., Helbert, W., Sugiyama, J., and Miles, M.J., High-resolution atomic force microscopy of native valonia cellulose I microcrystals, *J. Struct. Biol.*, 119(2)(1997)129-138.
14. South Pacific Viscose (Lenzing AG), How Viscose is Made, http://pt-spv.com/english/viscose/how.asp (read on 27.09.2011).

15. Klemm, D., Philipp, B., Heinze, T., Heinze, U., and Wagenknecht, W., *Comprehensive Cellulose Chemistry: Functionalization of Cellulose, Vol. 2*, Wiley-VCH, Weinheim, Germany, 1998, pp. 147-161.
16. Sakurada, I. and Okamura, S., Untersuchung der Molekülverbindungen der Zellulose durch Bestimmung des scheinbaren spezifischen Volumens und röntgenographische Ermittlung des kristallographischen Elementarkörpers der gequollenen Zellulose, *Colloid Polym. Sci.*, 81(2)(1937)199-208.
17. Porro, F., Bédué, O., Chanzy, H., and Heux, L., Solid-state ^{13}C NMR study of Na-cellulose complexes, *Biomacromolecules*, 8(8)(2007)2586-2593.
18. Okano, T. and Sarko, A., Mercerization of cellulose. I. X-ray diffraction evidence for intermediate structures, *J. Appl. Polym. Sci.*, 29(12)(1984)4175-4182.
19. Nishimura, H., Okano, T., and Sarko, A., Mercerization of cellulose. 5. Crystal and molecular structure of Na-cellulose I, *Macromolecules*, 24(3)(1991)759-770.
20. Okano, T. and Sarko, A., Mercerization of cellulose. II. Alkali-cellulose intermediates and a possible mercerization mechanism, *J. Appl. Polym. Sci.*, 30(1)(1985)325-332.
21. Nishimura, H. and Sarko, A., Mercerization of cellulose. III. Changes in crystallite sizes, *J. Appl. Polym. Sci.*, 33(3)(1987)855-866.
22. Revol, J.F., Dietrich, A., and Goring, D.A.I., Effect of mercerization on the crystallite size and crystallinity index in cellulose from different sources, *Can. J. Chem.*, 65(8)(1987)1724-1725.
23. Revol, J.-F. and Goring, D.A.I., Directionality of the fibre c-axis of cellulose crystallites in microfibrils of *Valonia ventricosa*, *Polymer*, 24(12)(1983)1547-1550.
24. Simon, I., Glasser, L., Scheraga, H.A., and John Manley, R.S., Structure of cellulose. 2. Low-energy crystalline arrangements, *Macromolecules*, 21(4)(1988)990-998.
25. Kroon-Batenburg, L.M.J., Bouma, B., and Kroon, J., Stability of cellulose structures studied by MD simulations. Could mercerized cellulose II be parallel?, *Macromolecules*, 29(17)(1996)5695-5699.
26. Dinand, E., Vignon, M., Chanzy, H., and Heux, L., Mercerization of primary wall cellulose and its implication for the conversion of cellulose I → cellulose II, *Cellulose*, 9(1)(2002)7-18.
27. Crawshaw, J., Bras, W., Mant, G.R., and Cameron, R.E., Simultaneous SAXS and WAXS investigations of changes in native cellulose fiber microstructure on swelling in aqueous sodium hydroxide, *J. Appl. Polym. Sci.*, 83(6)(2002)1209-1218.
28. El Seoud, O.A., Fidale, L.C., Ruiz, N., D'Almeida, M.L.O., and Frollini, E., Cellulose swelling by protic solvents: Which properties of the biopolymer and the solvent matter?, *Cellulose*, 15(3)(2008)371-392.
29. Le Moigne, N. and Navard, P., Dissolution mechanisms of wood cellulose fibres in NaOH-water, *Cellulose*, 17(1)(2010)31-45.

30. Isogai, A. and Atalla, R.H., Dissolution of cellulose in aqueous NaOH solutions, *Cellulose*, 5(4)(1998)309-319.
31. Kubo, T., Untersuchungen über die Umwandlung von Hydratzellulose in natürliche Zellulose, V. Der Mechanismus der Umwandlung und die Stabilität von natürlicher Zellulose sowie Hydratzellulose, *Colloid Polym. Sci.*, 93(3)(1940)338-345.
32. Kubo, T., Untersuchungen über die Umwandlung von Hydratzellulose in natürliche Zellulose, VIII. Über die Umwandlung der mit verschiedenen Verbindungen behandelten Hydratzellulose in natürliche Zellulose, *Colloid Polym. Sci.*, 96(1)(1941)41-47.
33. Philipp, B., Fink, H.-P., Kunze, J., and Frigge, K., NMR-spektroskopische und Röntgen-diffraktometrische Untersuchungen zur Wechselwirkung zwischen Zellulose und Natronlauge, *Ann. Phys.*, 497(4-6)(1985)507-523.
34. Hayashi, J., Recent development in the studies on crystal structure of cellulose, *Sen'I Gakkaishi*, 32(2)(1976)37-45.
35. Liu, Y. and Hu, H., X-ray diffraction study of bamboo fibers treated with NaOH, *Fibers Polym.*, 9(6)(2008)735-739.
36. Schenzel, K., Almlöf, H., and Germgård, U., Quantitative analysis of the transformation process of cellulose I → cellulose II using NIR FT Raman spectroscopy and chemometric methods, *Cellulose*, 16(3)(2009)407-415.
37. Kolpak, F.J. and Blackwell, J., Determination of the structure of cellulose II, *Macromolecules*, 9(2)(1976)273-278.
38. Langan, P., Nishiyama, Y., and Chanzy, H., X-ray structure of mercerized cellulose II at 1 Å resolution, *Biomacromolecules*, 2(2)(2001)410-416.
39. Raymond, S., Kvick, Å., and Chanzy, H., The structure of cellulose II: A revisit, *Macromolecules*, 28(24)(1995)8422-8425.
40. Sjöström, E., *Wood Chemistry – Fundamentals and Applications*, 2. Edn., Academic Press, San Diego, CA, USA, 1993.
41. Entwistle, D., Cole, E.H., and Wooding, N.S., The autoxidation of alkali cellulose. Part I: An experimental study of the kinetics of the reaction, *Text. Res. J.*, 19(9)(1949)527-546.
42. Entwistle, D., Cole, E.H., and Wooding, N.S., The autoxidation of alkali cellulose. Part II, *Text. Res. J.*, 19(10)(1949)609-624.
43. Mattor, J.A., A study of the mechanism of alkali cellulose autoxidation, PhD Thesis, Georgia Institute of Technology, Institute of Paper Science and Technology, Appleton, WI, USA, 1963.
44. Nonhebel, D.C., Tedder, J.M., and Walton, J.C., *Radicals*, Cambridge University Press, Cambridge, Great Britain, 1979, pp. 150-157.
45. Dyumaev, K.M., Nikiforov, G.A., and Silaev, Y.V., Inhibitors of free-radical reactions, *Russ. Chem. Bull.*, 10(1)(1961)151-153.
46. Kadla, J.F. and Chang, H.-m., The reactions of peroxides with lignin and lignin model compounds. In: Argyropoulos, D.S. (Ed.), *Oxidative Delignification Chemistry: Fundamentals and Catalysis*, *ACS Symposium Series Vol. 785*, American Chemical Society, MI, USA, 2001.

47. Bamford, C.H. and Collins, J.R., Kinetic studies on carbohydrates in alkaline conditions. III. Interconversion of D-glucose, D-fructose and D-mannose in feebly alkaline solution, *Proc. R. Soc. London, Ser. A*, 228(1172)(1955)100-119.
48. Sinkey, J.D., The function of magnesium compounds in an oxygen-alkali-carbohydrate system, PhD Thesis, Georgia Institute of Technology, Institute of Paper Science and Technology, Appleton, WI, USA, 1973.
49. Green, J.W., Thompson, N.S., Pearl, I.A., and Swanson, J.W., Study of the carbohydrate peeling and stopping reactions under the conditions of oxygen-alkali pulping. Project 3265, report one: A progress report to members of the institute of paper chemistry, Project Report, Georgia Institute of Technology, Institute of Paper Science and Technology, Appleton, WI, USA, 1976.
50. Kharasch, M.S. and Fono, A., Metal salt-induced hemolytic reactions. I. A new method of introducing peroxy groups into organic molecules, *J. Org. Chem.*, 24(1)(1959)72-78.
51. Kuptsan, N.A., Makarova, T.P., and Meos, A.I., Catalyst-assisted oxidative cellulose degradation in an alkaline medium, *Fibre Chem.*, 5(5)(1974)517-520.
52. McCloskey, J.T., The degradation of methyl-β-D-glucopyranoside by oxygen in alkaline solution, PhD Thesis, Georgia Institute of Technology, Institute of Paper Science and Technology, Appleton, WI, USA, 1971.
53. Weaver, J.W., The alkaline hydrogen peroxide reaction of methyl β-D-glucopyranoside and methyl 4-O-methyl-β-D-glucopyranoside, PhD Thesis, Georgia Institute of Technology, Institute of Paper Science and Technology, Appleton, WI, USA, 1976.
54. Haber, F. and Weiss, J., The catalytic decomposition of hydrogen peroxide by iron salts, *Proc. R. Soc. London, Ser. A*, 147(1934)332-351.
55. Robertson, A. and Waters, W.A., Some features of the autoxidation of tetralin, *Trans. Faraday Soc.*, 42(1946)201-210.
56. Chen, S.-L. and Lucia, L.A., Improved method for evaluation of cellulose degradation, *J. Wood Sci.*, 49(3)(2003)285-288.
57. Waters, W.A., *The Chemistry of Free Radicals*, Clarendon Press, Michigan, USA, 1948, pp. 232.
58. Militzer, W.E., The inhibition of carbohydrate oxidations by borate, *J. Biol. Chem.*, 158(1945)247-253.
59. Yang, B.Y. and Montgomery, R., Alkaline degradation of glucose: Effect of initial concentration of reactants, *Carbohydr. Res.*, 280(1)(1996)27-45.
60. Nef, J.U., Hedenburg, O.F., and Glattfeld, J.W.E., The method of oxidation and the oxidation products of L-arabinose and of L-xylose in alkaline solutions with air and with cupric hydroxide, *J. Am. Chem. Soc.*, 39(8)(1917)1638-1652.
61. Isbell, H.S., Interpretation of some reactions in the carbohydrate field in terms of consecutive electron displacement, *J. Res. Natl. Bur. Stand. (U.S.)*, 32(1944)45-59.
62. Knill, C.J. and Kennedy, J.F., Degradation of cellulose under alkaline conditions, *Carbohydr. Polym.*, 51(3)(2003)281-300.

63. Fargher, R.G. and Higginbotham, L., Chemical analysis of cotton: Micro-analytical methods for the examination of small quantities of waxes, in particular cotton wax, *J. Text. Inst.*, 15(1924)T75-T80.
64. Johansson, M.H. and Samuelson, O., End-wise degradation of hydrocellulose during hot alkali treatment, *J. Appl. Polym. Sci.*, 19(11)(1975)3007-3013.
65. Davidson, G.F., The solution of chemically modified cotton cellulose in alkaline solutions, I: In solutions of sodium hydroxide particularly at temperatures below the normal, *J. Text. Inst.*, 25(1934)T174-T196.
66. Malinen, R. and Sjöström, E., Studies on the reactions of carbohydrates during oxygen bleaching, *Pap. Puu*, 54(1972)451-468.
67. Greenfield, B.F., Hurdus, M.H., Pilkington, N.J., Spindler, M.W., and Williams, S.J., The degradation of cellulose in the near field of a radioactive waste repository, In: Barkatt, A. and Konynenburg, R.A. (Eds.), *Scientific Basis for Nuclear Waste Management XVII, Vol. 333*, Materials Research Society Symposium Series, Pittsburgh, PA, USA, 1994, pp. 705-710.
68. Kaylor, R.M., Dimmel, D.R., Ragauskas, A.J., and Liotta, C.L., A new model compound for studying alkaline cellulose chain cleavage reactions, Technical Paper, Georgia Institute of Technology, Institute of Paper Science and Technology, Appleton, WI, USA, 1994.
69. Yang, B.Y. and Montgomery, R., Alkaline degradation of fructofuranosides, *Carbohydr. Res.*, 280(1)(1996)47-57.
70. Atalla, R.H., Gentile, V.M., and Schroeder, L.R., Effects of physical structure on the alkaline degradation of hydrocellulose, Technical Paper, Georgia Institute of Technology, Institute of Paper Science and Technology, Appleton, WI, USA, 1987.
71. Alén, R., Basic chemistry of wood delignification. In: Stenius, P. (Ed.), *Forest Products Chemistry*, Fapet Oy, Helsinki, Finland, 2000, p. 91.
72. Clayden, J., Greeves, N., Warren, S. and Wothers, P., Organic *Organic Chemistry*, Oxford University Press, Oxford, Great Britain, 2009.
73. Evans, W.L, Some less familiar aspects of carbohydrate chemistry, *Chem. Rev.*, 31(3)(1942)537-560.
74. Schmidt, O., The mechanism of some important organic reactions, *Chem. Rev.*, 17(2)(1935)137-154.
75. Warshowsky, B. and Sandstrom, W.M., The action of oxygen on glucose in the presence of potassium hydroxide, *Arch. Biochem. Biophys.*, 37(1)(1952)46-55.
76. Bamford, C.H. and Collins, J.R., Kinetic studies on carbohydrates in alkaline conditions. I. The kinetics of the autoxidation of glucose, *Proc. R. Soc. Lond. A.*, 204(1076)(1950)62-84.
77. Bamford, C.H. and Collins, J.R., Kinetic studies on carbohydrates on alkaline conditions. II. The kinetics of the rearrangements of glucose and fructose in alkaline solution, *Proc. R. Soc. Lond. A.*, 204(1076)(1950)85-98.

78. Ackman, R.G., Fundamental groups in the response of flame ionization detectors to oxygenated aliphatic hydrocarbons, *J. Gas Chromatogr.*, 2(6)(1964)173-179.
79. Verhaar, L.A.T. and de Wilt, H.G.J., The gas chromatographic determination of polyhydroxy monocarbonic acids obtained by oxygenation of hexoses in aqueous alkaline solutions, *J. Chromatogr. A*, 41(2)(1969)168-179.
80. Petersson, G., Gas-chromatographic analysis of sugars and related hydroxy acids as acyclic oxime and ester trimethylsilyl derivatives, *Carbohydr. Res.*, 33(1974)47-61.
81. Hyppänen, T., Sjöström, E., and Vuorinen, T., Gas-liquid chromatographic determination of hydroxy carboxylic acids on a fused-silica capillary column, *J. Chromatogr.*, 261(1983)320-323.
82. Parr Instrument Company, Series 4590 Micro Stirred Reactors, https://www.parrinst.com/products/stirred-reactors/series-4590-micro-stirred-reactors/ (read on 31.07.2019).
83. Niemelä, K., *Mass Spectra of Organic Bayer Process Compounds*, Alcoa of Australia Ltd, Booragoon, WA, Australia, 1995.
84. Malinen, R., *Behavior of Wood Polysaccharides during Oxygen-alkali Delignification*, PhD Thesis, Helsinki University of Technology, Laboratory of Wood Chemistry, Otaniemi, Finland, 1974.
85. Microsoft, About Solver – Microsoft Excel, http://office.microsoft.com/en-us/excel-help/about-solver-HP005198368.aspx (read on 26.3.2012).
86. Microsoft, About Solver GRG2 Algorithm, http://support.microsoft.com/kb/82890/en-us (read on 26.3.2012).
87. Rowell, R.M. and Green, J., Kinetics of oxidative alkaline degradation of end group stabilized cellulose models, *Tappi*, 55(9)(1972)1326-1327.
88. Van Loon, L.R. and Glaus, M.A., Review of the kinetics of alkaline degradation of cellulose in view of its relevance for safety assessment of radioactive waste repositories, *J. Polym. Environ.*, 5(2)(1997)97-109.
89. Emsley, A.M. and Stevens, G.C., Kinetics and mechanisms of the low-temperature degradation of cellulose, *Cellulose*, 1(1)(1994)26-56.
90. Bigger, S.W., Scheirs, J., and Camino, G., An investigation of the kinetics of cellulose degradation under non-isothermal conditions, *Polym. Degrad. Stab.*, 62(1)(1998)33-40.
91. Lee, O.-K., *Mechanistic Studies of the Oxidation of Lignin and Cellulose Models*, PhD Thesis, The University of Maine, Orono, ME, USA, 2002.
92. Golova, O.P. and Nosova, N.I., Degradation of cellulose by alkaline oxidation, *Russian Chemical Reviews*, 42(4)(1973)327f.
93. Onda, A. Ochi, T., Kajiyoshi, K., and Yanagisawa, K., A new chemical process for catalytic conversion of D-glucose into lactic acid and gluconic acid, *Applied Catalysis A: General*, 343(1-2)(2008)49-54.

DEPARTMENT OF CHEMISTRY, UNIVERSITY OF JYVÄSKYLÄ
RESEARCH REPORT SERIES

1. Vuolle, Mikko: Electron paramagnetic resonance and molecular orbital study of radical ions generated from (2.2)metacyclophane, pyrene and its hydrogenated compounds by alkali metal reduction and by thallium(III)trifluoroacetate oxidation. (99 pp.) 1976
2. Pasanen, Kaija: Electron paramagnetic resonance study of cation radical generated from various chlorinated biphenyls. (66 pp.) 1977
3. Carbon-13 Workshop, September 6-8, 1977. (91 pp.) 1977
4. Laihia, Katri: On the structure determination of norbornane polyols by NMR spectroscopy. (111 pp.) 1979
5. Nyrönen, Timo: On the EPR, ENDOR and visible absorption spectra of some nitrogen containing heterocyclic compounds in liquid ammonia. (76 pp.) 1978
6. Talvitie, Antti: Structure determination of some sesquiterpenoids by shift reagent NMR. (54 pp.) 1979
7. Häkli, Harri: Structure analysis and molecular dynamics of cyclic compounds by shift reagent NMR. (48 pp.) 1979
8. Pitkänen, Ilkka: Thermodynamics of complexation of 1,2,4-triazole with divalent manganese, cobalt, nickel, copper, zinc, cadmium and lead ions in aqueous sodium perchlorate solutions. (89 pp.) 1980
9. Asunta, Tuula: Preparation and characterization of new organometallic compounds synthesized by using metal vapours. (91 pp.) 1980
10. Sattar, Mohammad Abdus: Analyses of MCPA and its metabolites in soil. (57 pp.) 1980
11. Bibliography 1980. (31 pp.) 1981
12. Knuuttila, Pekka: X-Ray structural studies on some divalent 3d metal compounds of picolinic and isonicotinic acid N-oxides. (77 pp.) 1981
13. Bibliography 1981. (33 pp.) 1982
14. 6^{th} National NMR Symposium, September 9-10, 1982, Abstracts. (49 pp.) 1982
15. Bibliography 1982. (38 pp.) 1983
16. Knuuttila, Hilkka: X-Ray structural studies on some Cu(II), Co(II) and Ni(II) complexes with nicotinic and isonicotinic acid N-oxides. (54 pp.) 1983
17. Symposium on inorganic and analytical chemistry May 18, 1984, Program and Abstracts. (100 pp.) 1984
18. Knuutinen, Juha: On the synthesis, structure verification and gas chromatographic determination of chlorinated catechols and guaiacols occuring in spent bleach liquors of kraft pulp mill. (30 pp.) 1984
19. Bibliography 1983. (47 pp.) 1984
20. Pitkänen, Maija: Addition of BrCl, B_2 and Cl_2 to methyl esters of propenoic and 2-butenoic acid derivatives and ^{13}C NMR studies on methyl esters of saturated aliphatic mono- and dichlorocarboxylic acids. (56 pp.) 1985
21. Bibliography 1984. (39 pp.) 1985
22. Salo, Esa: EPR, ENDOR and TRIPLE spectroscopy of some nitrogen heteroaromatics in liquid ammonia. (111 pp.) 1985

23. Humppi, Tarmo: Synthesis, identification and analysis of dimeric impurities of chlorophenols. (39 pp.) 1985
24. Aho, Martti: The ion exchange and adsorption properties of sphagnum peat under acid conditions. (90 pp.) 1985
25. Bibliography 1985 (61 pp.) 1986
26. Bibliography 1986. (23 pp.) 1987
27. Bibliography 1987. (26 pp.) 1988
28. Paasivirta, Jaakko (Ed.): Structures of organic environmental chemicals. (67 pp.) 1988
29. Paasivirta, Jaakko (Ed.): Chemistry and ecology of organo-element compounds. (93 pp.) 1989
30. Sinkkonen, Seija: Determination of crude oil alkylated dibenzothiophenes in environment. (35 pp.) 1989
31. Kolehmainen, Erkki (Ed.): XII National NMR Symposium Program and Abstracts. (75 pp.) 1989
32. Kuokkanen, Tauno: Chlorocymenes and Chlorocymenenes: Persistent chlorocompounds in spent bleach liquors of kraft pulp mills. (40 pp.) 1989
33. Mäkelä, Reijo: ESR, ENDOR and TRIPLE resonance study on substituted 9,10-anthraquinone radicals in solution. (35 pp.) 1990
34. Veijanen, Anja: An integrated sensory and analytical method for identification of off-flavour compounds. (70 pp.) 1990
35. Kasa, Seppo: EPR, ENDOR and TRIPLE resonance and molecular orbital studies on a substitution reaction of anthracene induced by thallium(III) in two fluorinated carboxylic acids. (114 pp.) 1990
36. Herve, Sirpa: Mussel incubation method for monitoring organochlorine compounds in freshwater recipients of pulp and paper industry. (145 pp.) 1991
37. Pohjola, Pekka: The electron paramagnetic resonance method for characterization of Finnish peat types and iron (III) complexes in the process of peat decomposition. (77 pp.) 1991
38. Paasivirta, Jaakko (Ed.): Organochlorines from pulp mills and other sources. Research methodology studies 1988-91. (120 pp.) 1992
39. Veijanen, Anja (Ed.): VI National Symposium on Mass Spectrometry, May 13-15, 1992, Abstracts. (55 pp.) 1992
40. Rissanen, Kari (Ed.): The 7. National Symposium on Inorganic and Analytical Chemistry, May 22, 1992, Abstracts and Program. (153 pp.) 1992
41. Paasivirta, Jaakko (Ed.): CEOEC'92, Second Finnish-Russian Seminar: Chemistry and Ecology of Organo-Element Compounds. (93 pp.) 1992
42. Koistinen, Jaana: Persistent polychloroaromatic compounds in the environment: structure-specific analyses. (50 pp.) 1993
43. Virkki, Liisa: Structural characterization of chlorolignins by spectroscopic and liquid chromatographic methods and a comparison with humic substances. (62 pp.) 1993
44. Helenius, Vesa: Electronic and vibrational excitations in some

biologically relevant molecules. (30 pp.) 1993

45. Leppä-aho, Jaakko: Thermal behaviour, infrared spectra and x-ray structures of some new rare earth chromates(VI). (64 pp.) 1994
46. Kotila, Sirpa: Synthesis, structure and thermal behavior of solid copper(II) complexes of 2-amino-2- hydroxymethyl-1,3-propanediol. (111 pp.) 1994
47. Mikkonen, Anneli: Retention of molybdenum(VI), vanadium(V) and tungsten(VI) by kaolin and three Finnish mineral soils. (90 pp.) 1995
48. Suontamo, Reijo: Molecular orbital studies of small molecules containing sulfur and selenium. (42 pp.) 1995
49. Hämäläinen, Jouni: Effect of fuel composition on the conversion of fuel-N to nitrogen oxides in the combustion of small single particles. (50 pp.) 1995
50. Nevalainen, Tapio: Polychlorinated diphenyl ethers: synthesis, NMR spectroscopy, structural properties, and estimated toxicity. (76 pp.) 1995
51. Aittola, Jussi-Pekka: Organochloro compounds in the stack emission. (35 pp.) 1995
52. Harju, Timo: Ultrafast polar molecular photophysics of (dibenzylmethine)borondifluoride and 4-aminophthalimide in solution. (61 pp.) 1995
53. Maatela, Paula: Determination of organically bound chlorine in industrial and environmental samples. (83 pp.) 1995
54. Paasivirta, Jaakko (Ed.): CEOEC'95, Third Finnish-Russian Seminar: Chemistry and Ecology of Organo-Element Compounds. (109 pp.) 1995
55. Huuskonen, Juhani: Synthesis and structural studies of some supramolecular compounds. (54 pp.) 1995
56. Palm, Helena: Fate of chlorophenols and their derivatives in sawmill soil and pulp mill recipient environments. (52 pp.) 1995
57. Rantio, Tiina: Chlorohydrocarbons in pulp mill effluents and their fate in the environment. (89 pp.) 1997
58. Ratilainen, Jari: Covalent and non-covalent interactions in molecular recognition. (37 pp.) 1997
59. Kolehmainen, Erkki (Ed.): XIX National NMR Symposium, June 4-6, 1997, Abstracts. (89 pp.) 1997
60. Matilainen, Rose: Development of methods for fertilizer analysis by inductively coupled plasma atomic emission spectrometry. (41 pp.) 1997
61. Koistinen, Jari (Ed.): Spring Meeting on the Division of Synthetic Chemistry, May 15-16, 1997, Program and Abstracts. (36 pp.) 1997
62. Lappalainen, Kari: Monomeric and cyclic bile acid derivatives: syntheses, NMR spectroscopy and molecular recognition properties. (50 pp.) 1997
63. Laitinen, Eira: Molecular dynamics of cyanine dyes and phthalimides in solution: picosecond laser studies. (62 pp.) 1997
64. Eloranta, Jussi: Experimental and theoretical studies on some

quinone and quinol radicals. (40 pp.) 1997

65. Oksanen, Jari: Spectroscopic characterization of some monomeric and aggregated chlorophylls. (43 pp.) 1998
66. Häkkänen, Heikki: Development of a method based on laser-induced plasma spectrometry for rapid spatial analysis of material distributions in paper coatings. (60 pp.) 1998
67. Virtapohja, Janne: Fate of chelating agents used in the pulp and paper industries. (58 pp.) 1998
68. Airola, Karri: X-ray structural studies of supramolecular and organic compounds. (39 pp.) 1998
69. Hyötyläinen, Juha: Transport of lignin–type compounds in the receiving waters of pulp mills. (40 pp.) 1999
70. Ristolainen, Matti: Analysis of the organic material dissolved during totally chlorine-free bleaching. (40 pp.) 1999
71. Eklin, Tero: Development of analytical procedures with industrial samples for atomic emission and atomic absorption spectrometry. (43 pp.) 1999
72. Välisaari, Jouni: Hygiene properties of resol-type phenolic resin laminates. (129 pp.) 1999
73. Hu, Jiwei: Persistent polyhalogenated diphenyl ethers: model compounds syntheses, characterization and molecular orbital studies. (59 pp.) 1999
74. Malkavaara, Petteri: Chemometric adaptations in wood processing chemistry. (56 pp.) 2000
75. Kujala Elena, Laihia Katri, Nieminen Kari (Eds.): NBC 2000, Symposium on Nuclear, Biological and Chemical Threats in the 21st Century. (299 pp.) 2000
76. Rantalainen, Anna-Lea: Semipermeable membrane devices in monitoring persistent organic pollutants in the environment. (58 pp.) 2000
77. Lahtinen, Manu: *In situ* X-ray powder diffraction studies of Pt/C, CuCl/C and Cu_2O/C catalysts at elevated temperatures in various reaction conditions. (92 pp.) 2000
78. Tamminen, Jari: Syntheses, empirical and theoretical characterization, and metal cation complexation of bile acid-based monomers and open/closed dimers. (54 pp.) 2000
79. Vatanen, Virpi: Experimental studies by EPR and theoretical studies by DFT calculations of α-amino-9,10-anthraquinone radical anions and cations in solution. (37 pp.) 2000
80. Kotilainen, Risto: Chemical changes in wood during heating at 150-260 °C. (57 pp.) 2000
81. Nissinen, Maija: X-ray structural studies on weak, non-covalent interactions in supramolecular compounds. (69 pp.) 2001
82. Wegelius, Elina: X-ray structural studies on self-assembled hydrogen-bonded networks and metallosupramolecular complexes. (84 pp.) 2001
83. Paasivirta, Jaakko (Ed.): CEOEC'2001, Fifth Finnish-Russian Seminar: Chemistry and Ecology of Organo-Element Compounds. (163 pp.) 2001
84. Kiljunen, Toni: Theoretical studies on spectroscopy and

atomic dynamics in rare gas solids. (56 pp.) 2001

85. Du, Jin: Derivatives of dextran: synthesis and applications in oncology. (48 pp.) 2001
86. Koivisto, Jari: Structural analysis of selected polychlorinated persistent organic pollutants (POPs) and related compounds. (88 pp.) 2001
87. Feng, Zhinan: Alkaline pulping of non-wood feedstocks and characterization of black liquors. (54 pp.) 2001
88. Halonen, Markku: Lahon havupuun käyttö sulfaattiprosessin raaka-aineena sekä havupuun lahontorjunta. (90 pp.) 2002
89. Falábu, Dezsö: Synthesis, conformational analysis and complexation studies of resorcarene derivatives. (212 pp.) 2001
90. Lehtovuori, Pekka: EMR spectroscopic studies on radicals of ubiquinones Q-*n*, vitamin K_3 and vitamine E in liquid solution. (40 pp.) 2002
91. Perkkalainen, Paula: Polymorphism of sugar alcohols and effect of grinding on thermal behavior on binary sugar alcohol mixtures. (53 pp.) 2002
92. Ihalainen, Janne: Spectroscopic studies on light-harvesting complexes of green plants and purple bacteria. (42 pp.) 2002
93. Kunttu, Henrik, Kiljunen, Toni (Eds.): 4th International Conference on Low Temperature Chemistry. (159 pp.) 2002
94. Väisänen, Ari: Development of methods for toxic element analysis in samples with environmental concern by ICP-AES and ETAAS. (54 pp.) 2002
95. Luostarinen, Minna: Synthesis and characterisation of novel resorcarene derivatives. (200 pp.) 2002
96. Louhelainen, Jarmo: Changes in the chemical composition and physical properties of wood and nonwood black liquors during heating. (68 pp.) 2003
97. Lahtinen, Tanja: Concave hydrocarbon cyclophane π-prismands. (65 pp.) 2003
98. Laihia, Katri (Ed.): NBC 2003, Symposium on Nuclear, Biological and Chemical Threats – A Crisis Management Challenge. (245 pp.) 2003
99. Oasmaa, Anja: Fuel oil quality properties of wood-based pyrolysis liquids. (32 pp.) 2003
100. Virtanen, Elina: Syntheses, structural characterisation, and cation/anion recognition properties of nano-sized bile acid-based host molecules and their precursors. (123 pp.) 2003
101. Nättinen, Kalle: Synthesis and X-ray structural studies of organic and metallo-organic supramolecular systems. (79 pp.) 2003
102. Lampiselkä, Jarkko: Demonstraatio lukion kemian opetuksessa. (285 pp.) 2003
103. Kallioinen, Jani: Photoinduced dynamics of $Ru(dcbpy)_2(NCS)_2$ – in solution and on nanocrystalline titanium dioxide thin films. (47 pp.) 2004
104. Valkonen, Arto (Ed.): VII Synthetic Chemistry Meeting and XXVI Finnish NMR Symposium. (103 pp.) 2004

105. Vaskonen, Kari: Spectroscopic studies on atoms and small molecules isolated in low temperature rare gas matrices. (65 pp.) 2004
106. Lehtovuori, Viivi: Ultrafast light induced dissociation of $Ru(dcbpy)(CO)_2I_2$ in solution. (49 pp.) 2004
107. Saarenketo, Pauli: Structural studies of metal complexing Schiff bases, Schiff base derived *N*-glycosides and cyclophane π-prismands. (95 pp.) 2004
108. Paasivirta, Jaakko (Ed.): CEOEC'2004, Sixth Finnish-Russian Seminar: Chemistry and Ecology of Organo-Element Compounds. (147 pp.) 2004
109. Suontamo, Tuula: Development of a test method for evaluating the cleaning efficiency of hard-surface cleaning agents. (96 pp.) 2004
110. Güneş, Minna: Studies of thiocyanates of silver for nonlinear optics. (48 pp.) 2004
111. Ropponen, Jarmo: Aliphatic polyester dendrimers and dendrons. (81 pp.) 2004
112. Vu, Mân Thi Hong: Alkaline pulping and the subsequent elemental chlorine-free bleaching of bamboo (*Bambusa procera*). (69 pp.) 2004
113. Mansikkamäki, Heidi: Self-assembly of resorcinarenes. (77 pp.) 2006
114. Tuononen, Heikki M.: EPR spectroscopic and quantum chemical studies of some inorganic main group radicals. (79 pp.) 2005
115. Kaski, Saara: Development of methods and applications of laser-induced plasma spectroscopy in vacuum ultraviolet. (44 pp.) 2005
116. Mäkinen, Riika-Mari: Synthesis, crystal structure and thermal decomposition of certain metal thiocyanates and organic thiocyanates. (119 pp.) 2006
117. Ahokas, Jussi: Spectroscopic studies of atoms and small molecules isolated in rare gas solids: photodissociation and thermal reactions. (53 pp.) 2006
118. Busi, Sara: Synthesis, characterization and thermal properties of new quaternary ammonium compounds: new materials for electrolytes, ionic liquids and complexation studies. (102 pp.) 2006
119. Mäntykoski, Keijo: PCBs in processes, products and environment of paper mills using wastepaper as their raw material. (73 pp.) 2006
120. Laamanen, Pirkko-Leena: Simultaneous determination of industrially and environmentally relevant aminopolycarboxylic and hydroxycarboxylic acids by capillary zone electrophoresis. (54 pp.) 2007
121. Salmela, Maria: Description of oxygen-alkali delignification of kraft pulp using analysis of dissolved material. (71 pp.) 2007
122. Lehtovaara, Lauri: Theoretical studies of atomic scale impurities in superfluid ^{4}He. (87 pp.) 2007
123. Rautiainen, J. Mikko: Quantum chemical calculations of structures, bonding, and spectroscopic properties of some sulphur and selenium iodine cations. (71 pp.) 2007
124. Nummelin, Sami: Synthesis, characterization, structural and

retrostructural analysis of self-assembling pore forming dendrimers. (286 pp.) 2008

125. Sopo, Harri: Uranyl(VI) ion complexes of some organic aminobisphenolate ligands: syntheses, structures and extraction studies. (57 pp.) 2008
126. Valkonen, Arto: Structural characteristics and properties of substituted cholanoates and *N*-substituted cholanamides. (80 pp.) 2008
127. Lähde, Anna: Production and surface modification of pharmaceutical nano- and microparticles with the aerosol flow reactor. (43 pp.) 2008
128. Beyeh, Ngong Kodiah: Resorcinarenes and their derivatives: synthesis, characterization and complexation in gas phase and in solution. (75 pp.) 2008
129. Välisaari, Jouni, Lundell, Jan (Eds.): Kemian opetuksen päivät 2008: uusia oppimisympäristöjä ja ongelmalähtöistä opetusta. (118 pp.) 2008
130. Myllyperkiö, Pasi: Ultrafast electron transfer from potential organic and metal containing solar cell sensitizers. (69 pp.) 2009
131. Käkölä, Jaana: Fast chromatographic methods for determining aliphatic carboxylic acids in black liquors. (82 pp.) 2009
132. Koivukorpi, Juha: Bile acid-arene conjugates: from photoswitchability to cancer cell detection. (67 pp.) 2009
133. Tuuttila, Tero: Functional dendritic polyester compounds: synthesis and characterization of small bifunctional dendrimers and dyes. (74 pp.) 2009
134. Salorinne, Kirsi: Tetramethoxy resorcinarene based cation and anion receptors: synthesis, characterization and binding properties. (79 pp.) 2009
135. Rautiainen, Riikka: The use of first-thinning Scots pine (*Pinus sylvestris*) as fiber raw material for the kraft pulp and paper industry. (73 pp.) 2010
136. Ilander, Laura: Uranyl salophens: synthesis and use as ditopic receptors. (199 pp.) 2010
137. Kiviniemi, Tiina: Vibrational dynamics of iodine molecule and its complexes in solid krypton - Towards coherent control of bimolecular reactions? (73 pp.) 2010
138. Ikonen, Satu: Synthesis, characterization and structural properties of various covalent and non-covalent bile acid derivatives of N/O-heterocycles and their precursors. (105 pp.) 2010
139. Siitonen, Anni: Spectroscopic studies of semiconducting single-walled carbon nanotubes. (56 pp.) 2010
140. Raatikainen, Kari: Synthesis and structural studies of piperazine cyclophanes – Supramolecular systems through Halogen and Hydrogen bonding and metal ion coordination. (69 pp.) 2010
141. Leivo, Kimmo: Gelation and gel properties of two- and three-component Pyrene based low molecular weight organogelators. (116 pp.) 2011
142. Martiskainen, Jari: Electronic energy transfer in light-harvesting complexes isolated from *Spinacia oleracea* and from three

photosynthetic green bacteria *Chloroflexus aurantiacus*, *Chlorobium tepidum*, and *Prosthecochloris aestuarii*. (55 pp.) 2011

143. Wichmann, Oula: Syntheses, characterization and structural properties of [O,N,O,X´] aminobisphenolate metal complexes. (101 pp.) 2011
144. Ilander, Aki: Development of ultrasound-assisted digestion methods for the determination of toxic element concentrations in ash samples by ICP-OES. (58 pp.) 2011
145. The Combined XII Spring Meeting of the Division of Synthetic Chemistry and XXXIII Finnish NMR Symposium. Book of Abstracts. (90 pp.) 2011
146. Valto, Piia: Development of fast analysis methods for extractives in papermaking process waters. (73 pp.) 2011
147. Andersin, Jenni: Catalytic activity of palladium-based nanostructures in the conversion of simple olefinic hydro- and chlorohydrocarbons from first principles. (78 pp.) 2011
148. Aumanen, Jukka: Photophysical properties of dansylated poly(propylene amine) dendrimers. (55 pp.) 2011
149. Kärnä, Minna: Ether-functionalized quaternary ammonium ionic liquids – synthesis, characterization and physicochemical properties. (76 pp.) 2011
150. Jurček, Ondřej: Steroid conjugates for applications in pharmacology and biology. (57 pp.) 2011
151. Nauha, Elisa: Crystalline forms of selected Agrochemical actives: design and synthesis of cocrystals. (77 pp.) 2012
152. Ahkola, Heidi: Passive sampling in monitoring of nonylphenol ethoxylates and nonylphenol in aquatic environments. (92 pp.) 2012
153. Helttunen, Kaisa: Exploring the self-assembly of resorcinarenes: from molecular level interactions to mesoscopic structures. (78 pp.) 2012
154. Linnanto, Juha: Light excitation transfer in photosynthesis revealed by quantum chemical calculations and exiton theory. (179 pp.) 2012
155. Roiko-Jokela, Veikko: Digital imaging and infrared measurements of soil adhesion and cleanability of semihard and hard surfaces. (122 pp.) 2012
156. Noponen, Virpi: Amides of bile acids and biologically important small molecules: properties and applications. (85 pp.) 2012
157. Hulkko, Eero: Spectroscopic signatures as a probe of structure and dynamics in condensed-phase systems – studies of iodine and gold ranging from isolated molecules to nanoclusters. (69 pp.) 2012
158. Lappi, Hanna: Production of Hydrocarbon-rich biofuels from extractives-derived materials. (95 pp.) 2012
159. Nykänen, Lauri: Computational studies of Carbon chemistry on transition metal surfaces. (76 pp.) 2012
160. Ahonen, Kari: Solid state studies of pharmaceutically important molecules and their derivatives. (65 pp.) 2012

161. Pakkanen, Hannu: Characterization of organic material dissolved during alkaline pulping of wood and non-wood feedstocks. (76 pp.) 2012
162. Moilanen, Jani: Theoretical and experimental studies of some main group compounds: from closed shell interactions to singlet diradicals and stable radicals. (80 pp.) 2012
163. Himanen, Jatta: Stereoselective synthesis of Oligosaccharides by *De Novo* Saccharide welding. (133 pp.) 2012
164. Bunzen, Hana: Steroidal derivatives of nitrogen containing compounds as potential gelators. (76 pp.) 2013
165. Seppälä, Petri: Structural diversity of copper(II) amino alcohol complexes. Syntheses, structural and magnetic properties of bidentate amino alcohol copper(II) complexes. (67 pp.) 2013
166. Lindgren, Johan: Computational investigations on rotational and vibrational spectroscopies of some diatomics in solid environment. (77 pp.) 2013
167. Giri, Chandan: Sub-component self-assembly of linear and non-linear diamines and diacylhydrazines, formulpyridine and transition metal cations. (145 pp.) 2013
168. Riisiö, Antti: Synthesis, Characterization and Properties of Cu(II)-, Mo(VI)- and U(VI) Complexes With Diaminotetraphenolate Ligands. (51 pp.) 2013
169. Kiljunen, Toni (Ed.): Chemistry and Physics at Low Temperatures. Book of Abstracts. (103 pp.) 2013
170. Hänninen, Mikko: Experimental and Computational Studies of Transition Metal Complexes with Polydentate Amino- and Aminophenolate Ligands: Synthesis, Structure, Reactivity and Magnetic Properties. (66 pp.) 2013
171. Antila, Liisa: Spectroscopic studies of electron transfer reactions at the photoactive electrode of dye-sensitized solar cells. (53 pp.) 2013
172. Kemppainen, Eeva: Mukaiyama-Michael reactions with α-substituted acroleins – a useful tool for the synthesis of the pectenotoxins and other natural product targets. (190 pp.) 2013
173. Virtanen, Suvi: Structural Studies of Dielectric Polymer Nanocomposites. (49 pp.) 2013
174. Yliniemelä-Sipari, Sanna: Understanding The Structural Requirements for Optimal Hydrogen Bond Catalyzed Enolization – A Biomimetic Approach.(160 pp.) 2013
175. Leskinen, Mikko V: Remote β-functionalization of β'-keto esters. (105 pp.) 2014
176. 12th European Conference on Research in Chemistry Education (ECRICE2014). Book of Abstracts. (166 pp.) 2014
177. Peuronen, Anssi: N-Monoalkylated DABCO-Based N-Donors as Versatile Building Blocks in Crystal Engineering and Supramolecular Chemistry. (54 pp.) 2014
178. Perämäki, Siiri: Method development for determination and recovery of rare earth elements from industrial fly ash. (88 pp.) 2014

179. Chernyshev, Alexander, N.: Nitrogen-containing ligands and their platinum(IV) and gold(III) complexes: investigation and basicity and nucleophilicity, luminescence, and aurophilic interactions. (64 pp.) 2014
180. Lehto, Joni: Advanced Biorefinery Concepts Integrated to Chemical Pulping. (142 pp.) 2015
181. Tero, Tiia-Riikka: Tetramethoxy resorcinarenes as platforms for fluorescent and halogen bonding systems. (61 pp.) 2015
182. Löfman, Miika: Bile acid amides as components of microcrystalline organogels. (62 pp.) 2015
183. Selin, Jukka: Adsorption of softwood-derived organic material onto various fillers during papermaking. (169 pp.) 2015
184. Piisola, Antti: Challenges in the stereoselective synthesis of allylic alcohols. (210 pp.) 2015
185. Bonakdarzadeh, Pia: Supramolecular coordination polyhedra based on achiral and chiral pyridyl ligands: design, preparation, and characterization. (65 pp.) 2015
186. Vasko, Petra: Synthesis, characterization, and reactivity of heavier group 13 and 14 metallylenes and metalloid clusters: small molecule activation and more. (66 pp.) 2015
187. Topić, Filip: Structural Studies of Nano-sized Supramolecular Assemblies. (79 pp.) 2015
188. Mustalahti, Satu: Photodynamics Studies of Ligand-Protected Gold Nanoclusters by using Ultrafast Transient Infrared Spectroscopy. (58 pp.) 2015
189. Koivisto, Jaakko: Electronic and vibrational spectroscopic studies of gold-nanoclusters. (63 pp.) 2015
190. Suhonen, Aku: Solid state conformational behavior and interactions of series of aromatis oligoamide foldamers. (68 pp.) 2016
191. Soikkeli, Ville: Hydrometallurgical recovery and leaching studies for selected valuable metals from fly ash samples by ultrasound-assisted extraction followed by ICP-OES determination. (107 pp.) 2016
192. XXXVIII Finnish NMR Symposium. Book of Abstracts. (51 pp.) 2016
193. Mäkelä, Toni: Ion Pair Recognition by Ditopic Crown Ether Based bis-Urea and Uranyl Salophen Receptors. (75 pp.) 2016
194. Lindholm-Lehto, Petra: Occurrence of pharmaceuticals in municipal wastewater treatment plants and receiving surface waters in Central and Southern Finland. (98 pp.) 2016
195. Härkönen, Ville: Computational and Theoretical studies on Lattice Thermal conductivity and Thermal properties of Silicon Clathrates. (89 pp.) 2016
196. Tuokko, Sakari: Understanding selective reduction reactions with heterogeneous Pd and Pt: climbing out of the black box. (85 pp.) 2016
197. Nuora, Piia: Monitapaustutkimus LUMA-Toimintaan liittyvissä oppimisympäristöissä tapahtuvista kemian oppimiskokemuksista. (171 pp.) 2016

198. Kumar, Hemanathan: Novel Concepts on The Recovery of By-Products from Alkaline Pulping. (61 pp.) 2016
199. Arnedo-Sánchez, Leticia: Lanthanide and Transition Metal Complexes as Building Blocks for Supramolecular Functional Materials. (227 pp.) 2016
200. Gell, Lars: Theoretical Investigations of Ligand Protected Silver Nanoclusters. (134 pp.) 2016
201. Vaskuri, Juhani: Oppiennätyksistä opetussuunnitelman perusteisiin - lukion kemian kansallisen opetussuunnitelman kehittyminen Suomessa vuosina 1918-2016. (314 pp.) 2017
202. Lundell Jan, Kiljunen Toni (Eds.): 22nd Horizons in Hydrogen Bond Research. Book of Abstracts. 2017
203. Turunen, Lotta: Design and construction of halogen-bonded capsules and cages. (61 pp.) 2017
204. Hurmalainen, Juha: Experimental and computational studies of unconventional main group compounds: stable radicals and reactive intermediates. (88 pp.) 2017
205. Koivistoinen Juha: Non-linear interactions of femtosecond laser pulses with graphene: photo-oxidation, imaging and photodynamics. (68 pp.) 2017
206. Chen, Chengcong: Combustion behavior of black liquors: droplet swelling and influence of liquor composition. (39 pp.) 2017
207. Mansikkamäki, Akseli: Theoretical and Computational Studies of Magnetic Anisotropy and Exchange Coupling in Molecular Systems. (190 p. + included articles) 2018.
208. Tatikonda, Rajendhraprasad: Multivalent N-donor ligands for the construction of coordination polymers and coordination polymer gels. (62 pp.) 2018
209. Budhathoki, Roshan: Beneficiation, desilication and selective precipitation techniques for phosphorus refining from biomass derived fly ash. (64 pp.) 2018
210. Siitonen, Juha: Synthetic Studies on 1-azabicyclo[5.3.0]decane Alkaloids. (140 pp.) 2018
211. Ullah, Saleem: Advanced Biorefinery Concepts Related to Non-wood Feedstocks. (57 pp.) 2018
212. Ghalibaf, Maryam: Analytical Pyrolysis of Wood and Non-Wood Materials from Integrated Biorefinery Concepts. (106 pp.) 2018

DEPARTMENT OF CHEMISTRY, UNIVERSITY OF JYVÄSKYLÄ
DISSERTATIONS PUBLISHED IN THE JYU DISSERTATIONS RESEARCH SERIES

1. Bulatov, Evgeny: Synthetic and structural studies of covalent and non-covalent interactions of ligands and metal center in platinum(II) complexes containing 2,2′-dipyridylamine or oxime ligands. (58 pp.) 2019. JYU Dissertations 70.
2. Annala, Riia: Conformational Properties and Anion Complexes of Aromatic Oligoamide Foldamers. (80 pp.) 2019. JYU Dissertations 84.
3. Isoaho, Jukka Pekka: Dithionite Bleaching of Thermomechanical Pulp - Chemistry and Optimal Conditions. (73 pp.) 2019. JYU Dissertations 85.
4. Nygrén, Enni: Recovery of rubidium from power plant fly ash. (98 pp.) 2019. JYU Dissertations 136.
5. Kiesilä, Anniina: Supramolecular chemistry of anion-binding receptors based on concave macromolecules. (68 pp.) 2019. JYU Dissertations 137.
6. Sokolowska, Karolina: Study of water-soluble p-MBA-protected gold nanoclusters and their superstructures. (60 pp.) 2019. JYU Dissertations 167.
7. Lahtinen, Elmeri: Chemically Functional 3D Printing: Selective Laser Sintering of Customizable Metal Scavengers. (71 pp.) 2019. JYU Dissertations 175.